Vacuum Steam Technology for Rapid Plasticization and Bending of Maple

Robert S. Wright

Thesis submitted to the faculty of the Virginia Polytechnic Institute and State University
in partial fulfillment of the requirements for the degree of

Master of Science
In
Wood Science and Forest Products

Brian H. Bond, Chairman
Zhangjing Chen
Richard M. Goff
D. Earl Kline
Alan A. Kornhauser

May 12, 2011
Blacksburg, VA

Keywords: vacuum, steam, VST, plasticization, bending, wood

Vacuum Steam Technology for Rapid Plasticization and Bending of Maple

Robert S. Wright

ABSTRACT

Bending wood dates back to antiquity in the form of baskets from willow branches and when boats were no longer made of hollowed out logs. Fresh growth willow twigs are readily bent into practically any shape; however, when wood has been separated from the tree and dried it is more rigid, difficult to bend, and breakable. Steamed wood is less rigid since adding moisture and heat to wood results in plasticization. Steaming at atmospheric pressure is the common technique for wood bending where diffusion prevails as the predominant mechanism governing moisture movement. Applications using conventional atmospheric steaming are time consuming and can result in failed bends. While other wood plasticization methods exist, Vacuum Steam Technology offers a promising method that utilizes pressure differentials to accelerate the addition of steam to wood due to water vapor bulk flow and subsequently an accelerated temperature rise and moisture addition.

The objectives of this work were: (1) determine whether cycles of vacuum and steaming could significantly improve the plastic-deformable state relative to the classic process of atmospheric steaming given equivalent treatment times when beginning with low moisture content (<10%) maple, and (2) compare the work required to bend to form between Vacuum Steam Technology treated maple and atmospheric-steamed maple when beginning with low moisture content (<10%) specimens.

A procedure for Vacuum Steam Technology to enable rapid plasticization of maple specimens from a kiln-dried state was developed. Kiln dried maple specimens were either treated according to the Vacuum Steam Technology procedure or were atmospherically steamed for a time equivalent to the Vacuum Steam Technology treatment and then bent into a 180° semi-circular form. Vacuum Steam Technology treated specimens had 0 failed bends whereas the atmospheric steamed specimens resulted in 39% failed bends. Vacuum Steam Technology treated specimens resulted in 17% less work to bend. The results clearly indicate that Vacuum Steam Technology is a superior technique for attaining a plastic deformable state prior to bending when beginning with low moisture content maple. Additional results included time to temperature, rate of moisture content change, final moisture contents, specific gravity influence.

Acknowledgements

Work toward this degree began in 1997 inspired by my desire to develop as a more beneficial employee to the department and ultimately secure a better financial future for my relatively young family. As I write this now, 14 years later, a tremendous amount of life has transpired. My daughters are grown and virtually on their own. I find myself an 'empty-nester' and no longer work in the career which I had attempted to improve upon.

On such a long degree path succinct acknowledgements are a challenge. Positive and negative experiences mingle, making resolution into which was the most influential quite grey. It is equally beneficial to have witnessed what not to become as it is to become. It is most important to be able to simply observe and develop the wisdom to know your own path.

I am grateful to my daughters Chelsea and Brianna because as I have observed them grow into their paths, I have grown in mine. I am grateful to my former wife Barbara who perhaps more than any other individual has challenged me with finding my own path. I am grateful for the support from my friends always, who in the moments when a kind word was critical shared their kind words freely. I am grateful to Paul Winistorfer who had it not been for his necessary and difficult task to eliminate a position, I might never have made time to complete this project and thesis. I am grateful to my friend Greg Galbreath for talking about banjo building; inspiring this project. I am grateful to Lauren Jones for space to stay on my path.

The project and thesis are a step on the path, and I am grateful to friends who comprise my committee. We began and we complete the process as friends. I am grateful for their support, their attentive, critical thinking, their gracious, precise, and gentle feedback. The thesis would not exist without having the support and the patient, critical attention from Brian Bond.

Table of Contents

List of Figures

List of Graphs

List of Tables

List of Abbreviations and Symbols; UPPERCASE

A	Area
ANSI	American National Standards Institute
ASME	American Society of Mechanical Engineers
C	Concentration
°C	Celsius degrees
CV	Control Volume
D	Diffusion Coefficient
DB	Dry Bulb
E	Elastic Modulus
G	Specific Gravity
Hg	Mercury element
Hz	Hertz
I	Area Moment of Inertia
J	Diffusion Flux
K	Kelvin or thermocouple type; context definitive
M	Moment (bending)
MC	Moisture Content, dry basis
MPa	Mega Pascal
MTS	Machine Testing Systems
N.A.	Neutral Axis
P	Pressure

Q	Heat
$\overline{R}$	Universal Gas Constant
RA	Research Area
Sp	Specimen
T	Temperature
TC	Thermocouple
Tg	Glass Transition
UK-FPL	United Kingdom-Forest Products Laboratory
USDA-FPL	United States Department of Agriculture-Forest Products Laboratory
USUF	Uniform State Uniform Flow
V	Volume or Velocity; context definitive
VAC	Vacuum
VST	Vacuum Steam Technology
WB	Wet Bulb
Wcv	Work, control volume
WVBF	Water Vapor Bulk Flow
X	Quality; steam

List of Abbreviations and Symbols; lowercase

b	base dimension of rectangular cross section
c	distance from neutral axis to extreme outer fiber
fs	fiber saturation
g	acceleration of gravity or gram; context definitive
h	height dimension or specific enthalpy; context definitive
k	thermal conductivity or ratio of specific heats; context specific
k_g	superficial gas permeability
kPa	kilopascal
kW	kilowatt
l_m	liquid mass
m	meter or mass; context definitive
mm	millimeter
n	number of moles
psig	pounds per square inch gauge
s	second
t	time
u	specific internal energy
v_m	vapor mass
w_o	oven dry mass of wood
x	length

List of Abbreviations and Symbols; Greek lowercase

ε	strain
π	pi
ρ	density
σ	stress

Chapter 1: Introduction

1.1 Problem Statement

Bending wood exists alongside cutting or carving of wood as a method to form curved shapes. Curved wood is used in the mass production furniture industry, the boat building industry, the mass production musical instrument industry, in the manufacture of sport equipment and agricultural or gardening hand tools, in the specialty architectural wood working and instrument luthier private studios. Bending wood along the grain enables the strongest direction of wood to remain intact and consistent throughout the bend, and when properly selected and steamed, it can be bent into fairly small radii (Peck 1957, Stevens and Turner 2008, Benson 2008). There are several methods which may be used on wood to produce a curved shape, these include: cutting wood in a curved shape, glulam beams, chemical softening, microwave softening and steam bending.

To cut a radius and produce an arc from solid wood requires that at some point the saw must cut across the grain of the wood and that portion where the grain direction shifts will be considerably weaker. There is waste associated with the removed portion following a cut and avoiding this waste is another benefit of bending solid wood (Stevens and Turner 2008).

Another technique for creating curved wooden members is the technique of gluing and laminating thin, dry veneers that can be bent using forms rather than steaming. This method produces large amounts of wood waste when cutting the individual strips and leaves glue-lines within the lamination. Other specialized wood bending techniques include chemical softening and microwave softening of moist wood but are not considered in this thesis.

Steaming wood results in it becoming more plastic, this enables large amounts of strain to occur in compression when undergoing a bending force relative to un-steamed wood. The increased capability for wood to sustain large compressive strains without visible wood failure allows for the fairly small bend radii. The literature suggests that 25% moisture content is optimal for common steam bending techniques (Stevens and Turner 2008); however, the Storage of moist wood requires sub-ambient temperatures to slow microbial activity (molds and fungi) and staining. Air drying to 25% moisture content (MC) requires additional space and time and does not entirely rule out mold or fungi growth or staining. Using kiln dried wood for steam bending currently requires one or both of the following: soaking the wood in water for extended periods of time, or steaming in excess of 30 minutes/centimeter (75 minutes/inch) (Peck 1957). The soaking approach requires time to soak the wood and the energy expense to raise the temperature of the water in the wood up to the steaming temperature. If the wood becomes too wet from soaking excessively, it is susceptible to checking or splitting upon drying after bending (Peck 1957). Extended steaming consumes a great deal of time, energy and may lead to weakened wood that can fail in compression during bending (Wengert 1988). The implication for anyone interested in steam bending but not capable of sub-ambient storage of moist wood, or without sufficient space to permit a supply for air drying, is that they are left with the choice to purchase the material kiln dried (Galbreath 2010).

This study proposes a new technique; Vacuum Steam Technology (VST) to plasticize wood. In what is tantamount to the reverse process of cyclic vacuum drying of wood, as a cyclic technique VST can result in uniform moisture and heat regain suitable for the needs of plasticization of wood at significantly faster rates when compared to atmospheric steaming. This

new technique will be compared to traditional steaming for treatment times and the work to bend for small maple specimens. Computing the work required to bend specimens will determine which technique better plasticized the wood as the work will diminish with better plasticization (Rice and Lucas, 2003).

1.2 Objectives

(1) Determine whether cycles of vacuum and steaming could significantly improve the plastic-deformable state relative to the classic process of atmospheric steaming given equivalent treatment times when beginning with low moisture content (<10%) maple.

(2) Compare the work required to bend to form between VST treated maple and atmospheric-steamed maple given equivalent treatment times when beginning with low moisture content (<10%) specimens.

1.3 Hypotheses

Accomplishment of the objectives was based on the following generalized hypothesis. When a vacuum is initially applied to wood there is a lowering of the internal pressure and temperature due to the resident gas (air) expanding and exiting under reduced pressure. A subsequent steam cycle would rapidly move steam to the interior of the wood due to Water Vapor Bulk Flow (WVBF) (Chen 1997, Chen and White 2009). Upon condensation of the steam within the wood, maximum heat transfer and maximum moisture addition to the interior of the wood would occur. At low moisture contents, such as kiln dried wood, this initial moisture addition would quickly become bound water within the cell wall. By introducing a low pressure

state again (vacuum) there would be a repeat of internal wood temperature depression, follow that by another subsequent higher pressure steam cycle and the fast heat gain / moisture gain repeats. A sequence of these stages would result in rapid, uniform moisture re-gain up to the fiber saturation point if desired and rapid internal heat gains due to the latent heat of vaporization from steam condensing inside the wood, yielding plasticized wood in reduced time.

To demonstrate the generalized hypothesis and accomplish the research objectives two research null hypotheses were proposed:

1) There is not a difference in the time required (elapsed time) to attain the goal internal wood temperature due to a preliminary vacuum cycle relative to the classic process of atmospheric steaming when beginning with low moisture content (<10%) maple.

Alternate Hypothesis: There is one technique which is faster than the other.

2) There is not a difference in total work required to bend maple due to the VST treatment relative to the classic process of atmospheric steaming when beginning with low moisture content (<10%) maple.

Alternate Hypothesis: There is one treatment method which requires less work to bend maple than the other.

1.4 Significance

A positive outcome of this research would advance the state of the art for steam bending of wood. Successful experimentation would demonstrate that plasticization of kiln dried maple for bending applications due to the VST process was accomplished within a shorter time, with increased uniformity of both moisture re-distribution and heat regain ultimately evidenced by reduced work to bend, an increased percentage of successful bends, and *perhaps* at a lower energy cost relative to the existing state of the art for steaming and bending solid maple to form.

The potential energy savings due to the decreased time for attaining a plastic deformable state with VST may be somewhat offset by the requirement of operating both a steam generator and a vacuum system. Successful treatment with VST might indicate a very large improvement in a uniform plastic state of the wood, due to more uniform moisture and heat re-distribution within the wood, which could enable the use of lower grades of wood or species currently considered difficult to bend.

Chapter 2: Literature Review

2.1 Brief History

The technology of steam or hot water based bending of solid wood to form has its earliest beginnings before recorded history. Rowell et al. (2002) describes: “Early Native Americans in the Pacific Northwest made fish hooks of wood using steam” where small sticks of green wood were cut and sharpened and placed in tubes of kelp, filled with water, plugged with moss and placed under the ashes of a dying fire for the night. In the morning the sticks were shaped into hooks and held in place for cooling. Benson (2008) cites evidence of Egyptian tomb paintings portraying images of chairs with bent wood. Ancient Greece in the 5th century B.C. produced the Klismos chair with bent wooden legs, Figure 2.1.

Bending wood dates back to antiquity in baskets from osier branches and when boats were no longer made of hollowed out logs (Stevens and Turner 2008). Other methods for acquiring bent wood included the collection of tree or limbs already curved in the approximate proportions, bending wood in its green state which required being held in that position by other structural members and dry bending of thin sections where the shape is retained by fastening the bent wood to fixed framework (Stevens and Turner 2008). By the mid-fifteenth century instrument Luthiers were using steam bent wood to substitute for carved wood and by the early eighteenth century steam bending of solid wood was a well known technique (Benson 2008).

Examples of the applications for steam bent wood include; boat hull structural members and planking for the skin of the hull, agricultural and gardening tool handles, furniture, sporting goods, musical instruments, works of art, sled runners, and wooden wheels built with spokes.

Figure 2.1 Klismos chair on the Tombstone of the shoemaker Xanthippos.

Greek marble artwork, ca. 430-420 BC. British Museum, London, United Kingdom; Townley Collection. Photographer: © Marie-Lan Nguyen (2007), Wikimedia Creative Commons; fair use determination attached.

2.2 Background for the Current State of the Art

Two literature contributions; Bending Solid Wood to Form (USDA-FPL R1764 1950); as precursor to *Bending Solid Wood to Form* by Edward Peck 1957) and *Solid and Laminated Wood Bending* by Stevens and Turner (1948; as precursor to the republished *Wood Bending Handbook* 2008) offer extremely thorough information for selection, preparation, bending and setting of wood. Literature published since the 1950's essentially re-describes Peck (1957) and Stevens and Turner (1948) with regard to the use of steam for wood bending. The Wood Bending Handbook (2008) is the most recent republication of Stevens and Turner (1948). By customary citation rules the 2008 edition of Stevens and Turner will be cited because it is the most recent. However, relative to the contribution to the state of the art that the author's research can provide it is prudent to realize the current technology is *at least* 60 years old.

The traditional practice of bending wood so that an individual piece of solid wood retains the bent shape has evolved along essentially one single process; softening and bending the wood followed by a setting period (Stevens and Turner 2008). There are several contemporary techniques for achieving bent wood forms. Among these are: laminating thin sections of dry wood bent and held in place to a form and then gluing the laminations together, chemical softening, radio wave softening, pre-compressed wood, and steam bending (Stevens and Turner 2008).

Stevens and Turner (2008) recognized "obvious shortcomings" to the technique of selective harvesting for curved shapes as mentioned in the early history, Section 2.1. This approach will not be addressed any further except to mention the technique still exists and fills the niche of artistry; see Figure 2.2.

Figure 2.2 “Atlantis”; by sculptor Heather Jansch (copyright 2009); using selected driftwood
Fair use determination at http://www.heatherjansch.com/index.php

Dry bending of wood is a viable technique for many applications; however, bending dry wood will only retain the desired shape if it is securely fixed to other adjacent structural elements. It is very difficult, almost impossible, to bend thick dry wood to a small radius. Stevens and Turner (2008) provide data (Table 2.1, in part) relating the ratio of the radius of curvature to the thickness for “structural laminations” (thickness not mentioned) at approximately 12% moisture content. As an example, ash at a thickness of 19mm (0.75inch) bent dry (12%MC) would have a minimum radius of 1.62m (5ft., 4in.). Such a long radius is acceptable for certain applications such as architectural / structural.

Table 2.1 Ratio of radius of curvature to thickness for structural laminations bent dry at approximately 12% moisture content. Stevens and Turner, ©1970

Standard Name	Botanical Name	Radius/Thickness
Douglas Fir	*Pseudotsuga menziesii*	125
Larch, European	*Larix decidua*	110
Scots pine	*Pinus sylvestris*	85
Sitka spruce	*Picea Sitchensis*	115
Western hemlock	*Tsuga heterophylla*	120
Ash	*Fraximus excelsior*	85
Beech	*Fagus sylvatica*	80
Danta	*Nesogordonia papaverifera*	95
Elm, rock	*Ulmus thomasii*	70
Greenheart	*Ocotea rodiaei*	130
Gurjan	*Dipterocarpus spp.*	135
Idigbo	*Terminalia ivorensis*	135
Iroko	*Chlorophora excelsa*	150
Mahogany, African	*Khaya ivorensis*	110
Makore	*Tieghemella heckelii*	110
Oak, European	*Quercus robur*	100
Opepe	*Nauclea diderrichii*	195
Ramin	*Gonystylus bancanus*	160
Teak	*Tectona grandis*	110

(From “Wood Bending Handbook”, Table 6 (in part), Stevens and Turner ©1970, Fox Chapel Publishing, 1970 Broad St., East Petersburg, PA 17520, used with permission)
http://www.foxchapelpublishing.com/default.aspx

The thickness of the cross section undergoing bending has a strong influence on the minimum radius. Experiments for Table 2.2 were done at 12% MC like Table 2.1, but the thickness decreased from an unknown 'structural thickness' to 3.2mm.

Table 2.2 Minimum radius for 3.2mm thick pieces at 12% MC, and ratio of radius/thickness

Standard Name	*Botanical Name*	Radius, mm	Radius/Thickness
Walnut, European (home-grown)	*Juglans regia*	91	29
Elm, Dutch (home-grown)	*Ulmus hollandica*	99	31
Cypress, European (home-grown)	*Cupressocyparis leylandii*	102	32
Sycamore (home-grown)	*Acer pseudoplatanus*	102	32
Elm, White	*Ulmus americana*	109	34
Beech, European (home-grown)	*Fagus sylvatica*	112	35
Oak, Red (home-grown)	*Quercus rubra*	112	35
Beech, European (Rumanian)	*Fagus sylvatica*	114	36
Oak, Turkey (home-grown)	*Quercus cerris*	114	36
Elm, Wych	*Ulmus glabra*	117	37
Ash, European (home-grown)	*Fraxinus excelsior*	122	38
Horse-chestnut, European	*Aesculus hippocastanum*	127	40
Ebony, African	*Diospyros crassiflora*	130	41
Beech, European (Danish)	*Fagus sylvatica*	135	42
Plane, European	*Platunus acerfolia*	135	42
Oak, American White	*Quercus alba.*	137	43
Spruce, Sitka (home-grown)	*Picea Sitchensis*	137	43
Elm, English	*Ulmus procera*	147	46
Hickory	*Carya sp.*	147	46
Oak, European (home-grown)	*Quercus robur*	147	46
Cherry, European (home-grown)	*Prunus avium*	150	47
'Douglas Fir' (imported)	*Pseudotsuga menziesii*	150	47
Pine, Corsican (home-grown)	*Pinus nigra* var. *calabrica*	150	47
Larch, European (home-grown)	*Larix decidua*	152	48
Poplar (French)	*Populus sp.*	160	50
Maple, Field	*Acer campestre*	163	51
Teak (N. Nigeria)	*Tectona grandis*	165	52
Yew	*Taxus baccata*	173	54
Redwood, Baltic	*Pinus sylvestris*	175	55
Chestnut, Sweet	*Castanea sativa*	191	60
'Douglas Fir' (home-grown)	*Pseudotsuga menziesii*	198	62
Spruce European (home-grown)	*Picea abies*	198	62
Larch, Japanese (home-grown)	*Larix leptolepis*	201	63
'Western Red Cedar' (home-grown)	*Thuja plicata*	203	64
Mahogany, African	*Khaya grandifoliola*	216	68
Hemlock, Western (home-grown)	*Tsuga heterophylla*	223	70
	Average Values (n=129)	169.7	53.3

(From "Wood Bending Handbook", Table 2 (in part), Stevens and Turner ©1970, Fox Chapel Publishing, 1970 Broad St., East Petersburg, PA 17520, used with permission)
http://www.foxchapelpublishing.com/default.aspx

The complete table from the cited reference had 129 entries; only selected species similar to North American species plus a few tropical woods were included here. The average values at the bottom of Table 2.2 reflect the data of the full 129 specimen table. In comparing Tables 2.1 and 2.2 it should be recognizable that the benefit of plasticizing wood for bending begins at some minimum thickness and that thickness is species dependent. The maple genus (*Acer campestre*) mentioned in Table 2.2 had a minimum bend radius was 163mm and the ratio of radius / thickness was 51 for a 3.2mm thick section at 12% MC. For comparison, this research used steamed maple (*Acer spp*) bent to a radius of 152 mm and the ratio of radius / thickness was 32 for a 4.7mm thickness.

Other techniques exist for forming bent wood pieces. The process of dry forming and gluing laminations together (glulam beams) dates to 19th century England (Müller 2000). It is a very common, current industrial practice, but as an engineered wood product which does not involve steam bending, it falls outside of the purview of this research. Similarly; microwave and chemical softening are outside of the scope of the current thesis research effort. The Wood Handbook (2010), chapter 19 “Specialty Treatments” provides a comparative overview and chapter 11 “Glued Structural Members” provides specific design criteria.

Bending of green wood can be accomplished with little or no heat addition (Stevens and Turner 2008). There are potential complications: excessive moisture in the green state can result in wood vessels rupturing from excessive hydraulic pressure due to *in situ* water, the setting time for the bend is dependent upon the green wood air drying which might occur over weeks of time, the air dry process can result in shrinkage, warp, splits, checks and other complications. Green stock is not suitable for many bent items (Peck 1957).

Bending stock should be air dried to the desired moisture content, generally 12 to 20 percent, and stored under controlled conditions (Peck 1957). The Wood Handbook (2010) states 25% MC. Stevens and Turner (2008) state that bending wood at 25% is essentially equal in effort to bending in the green state and the setting time from 25% MC is reduced from the green state. Air drying of green wood requires it be properly stacked, protected from weather, and permitted to air dry to 25% moisture content. Moist wood at 25% MC can be problematic for long-term storage under practically any conditions other than significantly sub-ambient temperatures to slow microbial attack.

Within the niche of luthiers; individual artisans handcrafting stringed musical instruments, beginning with kiln dried wood is essentially the most pragmatic option (Galbreath 2010). Luthiers are able to machine it to the precise standards necessary for fine musical instruments and carefully permit only the amount of moisture regain essential to their particular need. Luthiers that work with very thin sections such as the curved sides of guitars, the curved backs of fiddles, or the curved side of a bouzouki do not necessarily require steam for bending due to the thin section. A spray application of moisture followed by an application of heat via a flexible high temperature silicone heat blanket can accomplish the softening step (Hall 2010, Jones 2010). Thicker sections, such as the hoop for a banjo or the side pieces for an autoharp require steaming of kiln dried wood to create the instrument parts as shown in Figures 2.3 and 2.4 (Galbreath 2010, Hollandsworth 2010).

Figure 2.3 Greg Galbreath, luthier and “Buckeye Banjos” owner bends steamed curly maple around hoop mould. Photograph by author, 2008

Figure 2.4 Galbreath attaches bent banjo hoop to cooling form. Photograph by author, 2008

2.3 Bending Wood

Wood is an orthotropic material, having unique material properties in each of the three primary directions: longitudinal or along the grain direction, radial or from the center of the tree out, and tangential to the growth rings (Wood Handbook 2010). The longitudinal direction has by far the greatest modulus of elasticity relative to the other two directions. The Wood Handbook (2010) reports values for the ratio of longitudinal to tangential modulus of elasticity from 12 times to 23 times as great, and the ratio of longitudinal to radial from 5 to 22 times as great for various hardwood species. Bending wood along the grain enables retention of the continuity of this strongest direction, which in turn results in the completed bent product being as strong as possible.

The bending of any material that behaves elastically involves the displacement of some of the material within the zone of bending. In 1773 Charles-Augustin de Coulomb published a paper describing the correct, ideal distribution of forces within a mechanical member undergoing bending (Onouye and Kane 2007). Since recognition of the correct model, the classic presentation for a uniform beam with uniform rectangular cross section undergoing pure bending (without other torsion stresses or direct shear stresses across the beam section) as shown in Figure 2.5. The theory of bending as described below pertains to elastic bending only. It is meant to serve as an introductory illustration of bending theory to aid in visualization of the more complex issues involved in plastic bending. Steam bending of wood involves plastic bending; i.e. permanent deformation.

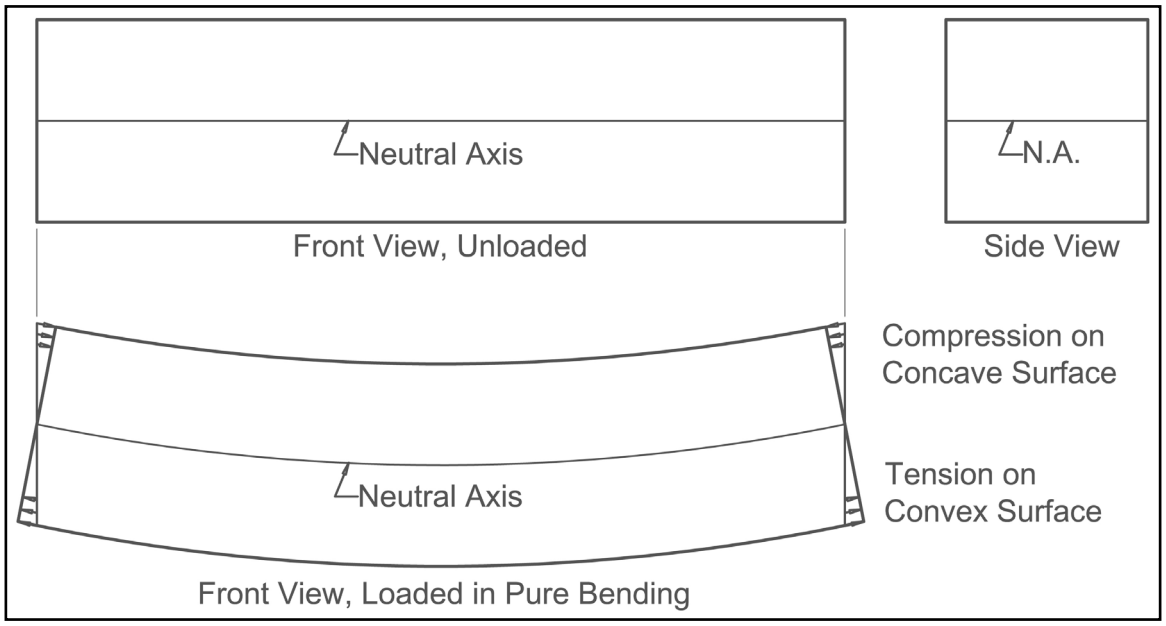

Figure 2.5 Horizontal strain induced in a beam from bending (equilibrium vertical strain not depicted). Sketch by author, 2011.

In Figure 2.5 the top two images depict a beam of uniform material and uniform cross section; the cross section shown as the square image to the right. The classic model of bending also assumes that parallel cross sections before bending remain parallel after bending (Onouye and Kane 2007). In Figure 2.5 the two images of the longer beam portion are positioned such that the vertical end lines of the un-bent beam are precisely above the vertical lines shown at the end of the bent beam. The slightly angled end lines of the bent beam represent the parallel section assumption of the bending model. The line through the middle of all three images is called the “neutral axis” and as can be seen in the bent beam the neutral axis retains its original length because it remains in contact with the vertical end lines. Portions of the beam above the neutral axis, on the concave side of the curve, must shorten in order for transverse sections to remain parallel; the arrows indicate compression above the neutral axis. Portions of the beam

below the neutral axis, on the convex side of the curve, must lengthen in order for parallel sections to remain parallel; the arrows indicate tension below the neutral axis.

The modulus of elasticity (E) is the ratio of stress to strain (Onouye and Kane 2007).

$$E = \frac{\sigma}{\varepsilon} \qquad \text{Equation 2.1}$$

Where: E = modulus of elasticity, Pascals or pounds per square inch
σ = stress, Pascals or pounds per square inch
ε = strain, mm/mm or inch/inch

The interpretation is that any elastic material when subjected to a stress, or force, or load of some sort will strain against the stress and deflect or deform. The elastic quality of the material will force the original shape of the material to resume when the load is removed, provided the load did not go beyond the elastic limit of the material. In Figure 2.5 the strain is represented by the arrows of compression on the concave side and tension on the convex side. The strain manifests as shear parallel and perpendicular to the grain for infinitesimal segments of the beam to remain in force equilibrium. Note that the strain is greatest at the extreme outer surfaces in both compression and tension, and zero at the neutral axis.

Bending stress is a function of the amount of force required on a beam to cause bending to occur, which is directly related to the bending moment applied. In the case of a luthier, this force would be in the form of individual arm strength. Bending stress is given in Equation 2.2 (Onouye and Kane 2007).

$$\sigma = \frac{Mc}{I} \qquad \text{Equation 2.2}$$

Where: σ = bending stress, Pascals or pounds per square inch

M = bending moment, N-m or pound-feet (maintain unit consistency)

c = distance from neutral axis to extreme outer fibers

I = area moment of inertia, mm^4 or $inch^4$

Bending stress from Equation 2.2 can be the stress value used in Equation 2.1 and then the outcome becomes the modulus of elasticity in bending which is the predominant form of E in wood science. The area moment of inertia is a property of the cross sectional area and for a rectangular cross section, as Figure 2.5, is given by Equation 2.3 (Onouye and Kane 2007).

$$I = \frac{bh^3}{12} \qquad \text{Equation 2.3}$$

Where: I = area moment of inertia, mm^4 on $inch^4$

b = base length of cross section, mm or inch

h = height of cross section, mm or inch

12 = constant; function of the cross section

To support the following derivation, set an assumption that the neutral axis is in the geometric center of the beam cross section (as in Figure 2.5) and in that case, c = h/2. Insertion of Equation 2.3 into Equation 2.2 and simplification yields:

$$\sigma = \frac{6M}{bh^2} \qquad \text{Equation 2.4}$$

Rearrangement of Equation 2.4, solved in terms of M gives:

$$M = \frac{\sigma bh^2}{6} \qquad \text{Equation 2.5}$$

Rearrangement of Equation 2.1 and solved in terms of σ and then substituted into Equation 2.5 gives:

$$M = \frac{E\varepsilon\, bh^2}{6} \qquad \text{Equation 2.6}$$

Equation 2.6 describes the material properties that affect the bending moment which any person's strength or machine capability would have to exert to cause a bend to occur. From Equation 2.6 it can be seen that the moment is a function of the square of the height of the bending specimen. This explains why thinner pieces of wood are bent more easily. "E" is a material property which averages approximately 7,000 - 9,000 MPa for green hardwoods (1.0 – 1.3 million psi) to 11,000 – 13, 000 MPa for 12% MC hardwoods (1.6 – 1.9 million psi). The E is responsible for the great difficulty in bending dry wood and also the wood springing back. To alleviate those challenges steam is added to temporarily modify the elastic property of wood, enabling the bending of solid wood to form.

2.4 Wood and Steam

Wood is an intricate, complex, heterogeneous, anisotropic composite material comprised of a mixed polymer matrix and a reinforcing material that is both amorphous as well as crystalline (Back and Salmen 1982). The mechanical behavior includes the qualities of elasticity, plasticity, viscoelasticity and mechano-sorptive creep (Remond and Passard 2007). The potential for bending solid wood and for wood to retain the bent shape is dependant upon all aforementioned characteristics as well as hindered by a few of them.

Steaming wood results in the wood becoming more plastic and successful plasticization of wood requires water and elevated temperature (Back and Salmon 1982, Irvine 1984, Kelley

et al. 1987). The process of steaming wood involves three discrete steps: softening, bending, and setting the bend. Stevens and Turner (2008) detail the various procedures and related information for each of these three steps. Historically each of the steps had been developed through trial and error. Stevens and Turner (2008) stressed: “Success in bending depends as much upon the skill and experience of the operators as upon any theoretical knowledge acquired from books.”

More recent research has investigated the intricacies of the mechanisms of wood softening. According to Ward (1983) the viscoelastic behavior of a material, such as the amorphous polymers in wood, is due to the characteristics they can exhibit in a range from viscous fluid-like behavior to linearly elastic solids as a function of temperature, loading rate, and moisture content. In the spectrum of material properties between the extremes of viscous fluid-like behavior and elastic solid behavior lies a broad range of material property transition wherein small changes in the aforementioned independent properties (moisture content, temperature, loading rate) have a strong affect.

Within the range of elastic behavior, stress and strain occur precisely at the same time during the application of a force. It is said that stress and strain are in phase. This characteristic of the material results in the modulus of elasticity or E as described in Section 2.3. On a typical plot of stress vs. strain, the E is the slope of the straight line segment of the curve. Within the range of purely viscous behavior the strain resulting from the stress of an applied force does not occur immediately. There exists a maximum phase difference of 90^{o} ($\pi/2$ radians) between the stress from an applied load and the strain associated with that stress (Meyers and Chawla

1999). However, wood does not possess nor exhibit any purely viscous behavior (Wolcott et al. 1990).

A viscoelastic material does have time-dependent strain variations when a load is applied (Meyers and Chawla 1999) and wood exhibits creep (Figure 2.6) and relaxation (Figure 2.7), both qualities of a viscoelastic material.

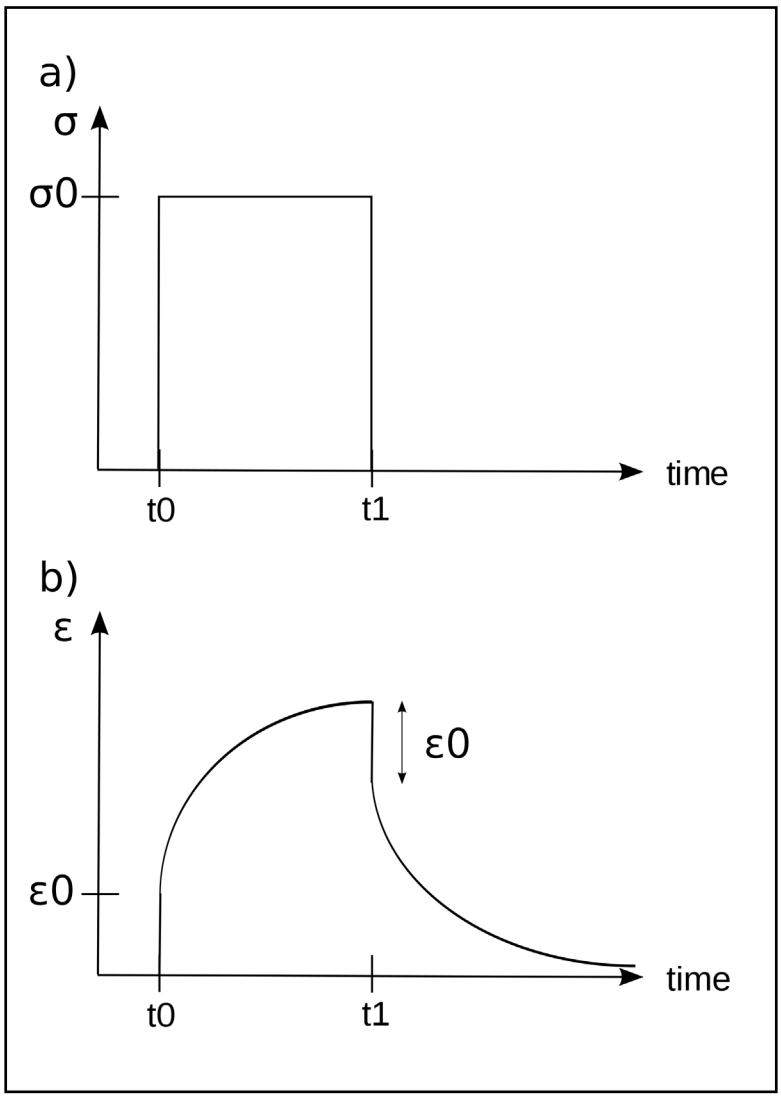

Figure 2.6 Time dependent stress (a) and strain (b) curves for the condition of creep. From "Creep (deformation)"; http://en.wikipedia.org/wiki/Creep_%28deformation%29 fair use; http://en.wikipedia.org/wiki/Wikipedia:Text_of_Creative_Commons_Attribution-ShareAlike_3.0_Unported_License

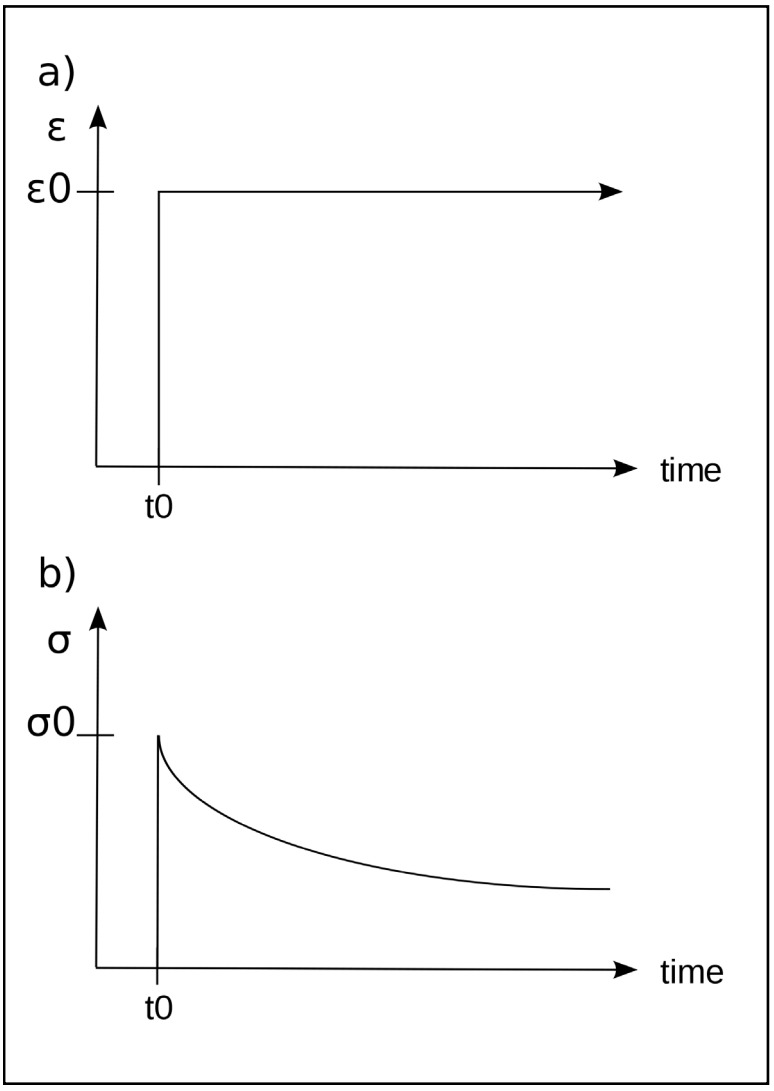

Figure 2.7 Time dependent strain (a) and stress (b) curves for the condition of relaxation From "Stress Relaxation"; http://en.wikipedia.org/wiki/Stress_relaxation fair use; http://en.wikipedia.org/wiki/Wikipedia:Text_of_Creative_Commons_Attribution-ShareAlike_3.0_Unported_License

Creep occurs when a stress (load) is held constant as shown in figure (a) of Figure 2.6 and the strain (deflection) continues to occur as shown in figure (b). Note that both stress and strain are time dependent. The continued deflection as in (b) is a result of the viscous properties of wood, which are due to the amorphous components of wood, the lignin, the hemicellulose and the amorphous cellulose (Back and Salmen 1982, Irvine 1984)

Stress relaxation occurs when a strain (deformation) is held constant as shown in figure (a) of Figure 2.7 and the stress is reduced over time as in figure (b). This too results from the amorphous components in wood.

Bending wood involves both material properties creep and stress relaxation; whether steam is involved or not. However, when steam is utilized the heat from the steam and the moisture from the steam work together to modify the viscoelastic properties and therefore the modulus of elasticity (Back and Salmen 1982, Irvine 1984, Kelley et al. 1987).

The viscoelastic nature of wood enabling a change in the elastic property due to an influence of heat or steam is referred to as the glass transition (Back and Salmen 1982, Irvine 1984, Kelley et al. 1987). Figure 2.8 depicts a plot of instantaneous modulus of elasticity (E) vs. temperature (T) for an amorphous, glassy material where time is progressing as temperature changes. E_1 represents the initial modulus of elasticity. The illustration of how the elastic behavior is altered and becomes less glassy over a range of temperature is similar to the interpretation of the amorphous components of wood (Irvine 1984). E is approximately constant within the glassy region. This corresponds to the E value for wood within the linear portion of a typical stress/strain curve i.e. the `elastic´ region previously referred to. The glass transition temperature, also referred to as $T_{g,}$ is a derived point based on tangents drawn to the curve from the glassy region and the transition region, but it is important to realize the curve is continuous and actually a range of temperature is more appropriate (Irvine 1984). The “Transition” of Figure 2.8 is the region within which steam plasticizing of wood occurs. Softening of wood must occur for successful permanent bending of wood, which retains the bent shape after cooling, setting, and any restraint has been removed (Stevens and Turner 2008).

An introduction to the theory describing viscoelastic behavior and plastic deformation within the transition zone as shown in Figure 2.8 is appropriate since these are the phenomena that occur within wood during steam bending. The term 'Viscoelasticity' implies a combination of the properties of viscous and elastic behavior. Pure elastic behavior is the ideal stress/strain relationship wherein stress and strain are directly, immediately, linearly proportional to one another via Young's Modulus, or E (see Equation 2.1). In viscous materials the strain or deformation of the material does not occur immediately when a stress is applied but lags behind the stress in measurable amounts of time and in the case of vibratory dynamic mechanical analysis, in a measurable phase angle. Purely viscous materials exhibit a phase shift of 90°or π/2 radians. Viscoelastic materials have properties in a spectrum between the extremes (Meyers and Chawla 1999).

Viscoelasticity permits rearrangement of the molecules; plastic deformation, via creep. Creep (see Figure 2.6) enables plastic deformation and is dependent upon an instantaneous value for E during creep. This instantaneous value for E would be positioned somewhere along the curve in the transition zone of Figure 2.8. As shown in Figure 2.6 there is an initial level of strain at t_0, called ε_0, and when stress is relieved at t_1 the initial strain is recovered as seen in Figure 2.6 b). This strain is proportional to what is referred to as the "storage modulus". Stress relaxation also occurs within viscoelastic materials and is one of the processes occurring when steam bent wood is taking the "set" of the finished form (see Figure 2.7). As the strain is constant, i.e. when the bent wood is positioned in the finished form, the stresses within the wood relax to minimize spring back. This stress relaxation is proportional to the "loss modulus" and is indicative of the viscous aspects of the material in the plasticized state; energy lost in

heat due to molecular motion. A complex variable relationship exists between the storage modulus and the loss modulus reconciling them to the theoretical original modulus E but further pursuit of the theory and explaining specifically what transpires within the complex process of steam bending of wood is beyond the scope of this research.

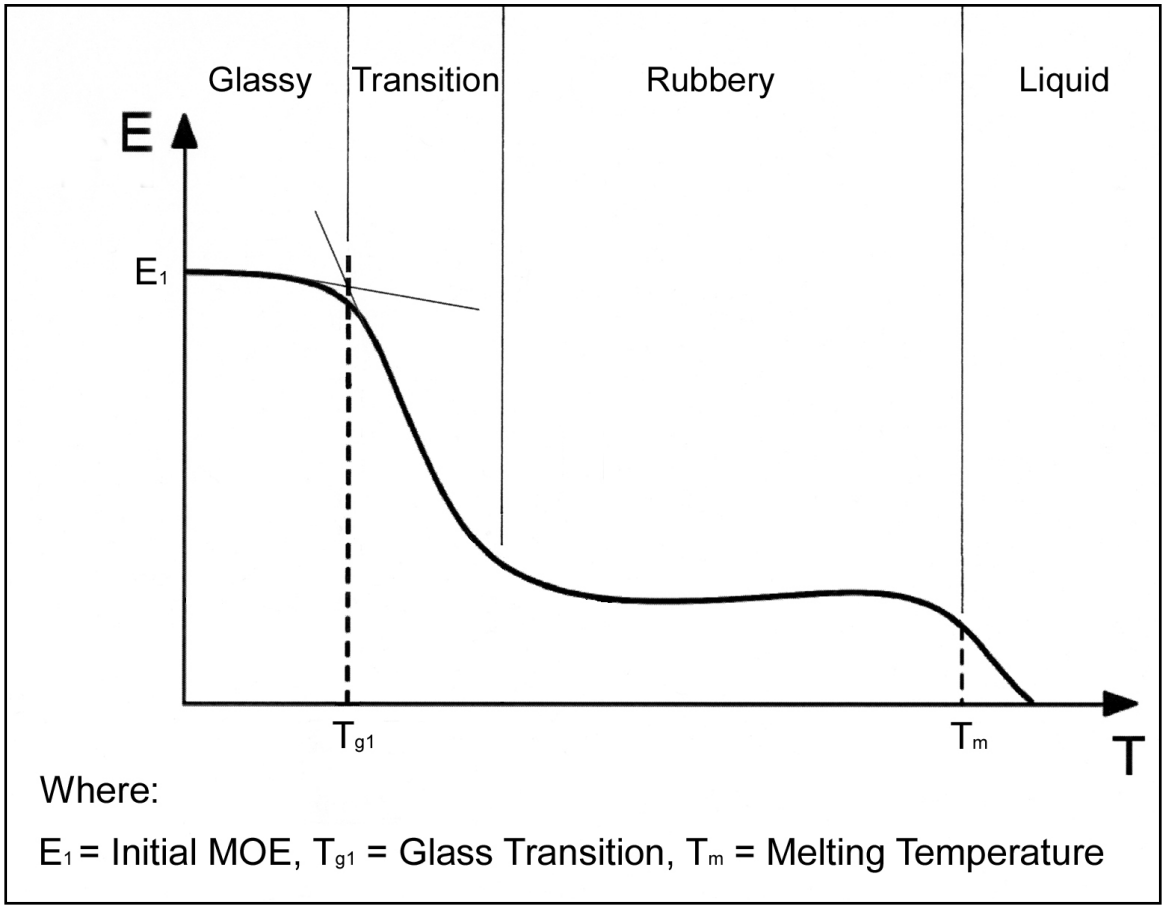

Figure 2.8 Model curve for the changes in modulus of elasticity with temperature for an amorphous, glass material. Adapted by author, 2011, from "Glass Transition"; http://en.wikipedia.org/wiki/Glass_transition fair use; http://en.wikipedia.org/wiki/Wikipedia:Text_of_Creative_Commons_Attribution-ShareAlike_3.0_Unported_License

The softening of wood within the transition region has been studied extensively as a critical aspect of pulping in the manufacture of paper; particularly mechanical and chemi-

mechanical pulping due to the reduction of energy requirements for mechanically breaking down the structure of wood (Back and Salmen 1982, Irvine 1984). The strength or stiffness of wood is dependant upon the glass transitions of the amorphous constituents and the relative amounts of those constituents. The hemicellulose, lignin, and non-crystalline cellulose constituents are each capable of absorbing water, and water is a known plasticizer for these components (Back and Salmon 1982, Irvine 1984, Kelley et. al. 1987, Rowell et al. 2002, Karenlampi et al. 2003).

The polymer groups which make up the solid wood; hemicellulose, lignin and cellulose possess hydroxyl functional groups. In a process which is believed to be reversible with some hysteresis effect, the polymeric molecules when exposed to water tend to replace the intermolecular hydrogen bonds with hydrogen-bonded water linkages. This is referred to as the "bound water". It is the process of water linkage addition which tends to serve as the plasticizer to the polymers of wood. As the water content increases toward the fiber saturation point, the available hydrogen bonding sites for water linkage addition are minimized, and the effects of plasticization due to water reach a maximum and the Tg reaches a minimum (Reimschuessel 1978, Back and Salmen 1982, Kelley et al.1987)

The effect of plasticization of wood by water is manifest by a significant lowering of the glass transition temperature. Back and Salmen (1982) compiled published Tg values for the individual components of wood in a completely dry state. For cellulose the temperature range was 200 - 250˚C; the upper limit is above the open air ignition temperature of paper. For hemicellulose the range was 150 - 220˚C, and for lignin the range was 125 - 205˚C. Back and Salmen (1982) used the Kaelble (1971) modeling equation to estimate the influence of moisture on Tg. This equation is based on the dry matter glass transitions incorporating a solubility

parameter and an energy parameter describing intermolecular attraction. From this modeling work they concluded: (a) The Tg of cellulose was shown to be affected by both the MC and the percent crystallinity. Completely amorphous cellulose was shown to behave like the hemicellulose, but 80% crystalline cellulose was calculated to exhibit a rapid lowering of Tg with increasing MC to below ambient room temperature at about 7% MC. (b) The hemicelluloses exhibited a continual lowering of the Tg with increasing moisture content to a point below ambient room temperature around 30% MC. (c) The Tg of lignin leveled off around 115˚C at a moisture content of about 3%.

Irvine (1984) worked with eucalypt and pine woods (*E. regnans and E. marginata, P. radiata and P. elliotti)* as solid, untreated wood. The Tg lowering effect due to water leveled off around 20 – 23% MC at about 60˚C for solid, unmodified *E. regnans*. Irvine used differential thermal analysis to detect the Tg. Kelley et al. (1987) state all work involving the individual constituents of wood suffer from the unavoidable fact that the process of isolating the polymer either modifies it or at least does not permit complete representation of the polymer *in situ* . The intimate association of wood polymers and the subsequent secondary interactions influence the composite's viscoelastic response, and that cannot be captured via individual component analysis. Their results for solid maple at 10%MC show two transitions. One at about 100˚C and another of about 60˚C; the higher temperature transition was associated with lignin and the lower temperature transition was associated with hemicellulose. Spruce was investigated from 5% to 30%MC and it was found that at 5% there was not a glass transition to well above 100˚C, and at about 10%MC the glass transition for lignin reached a plateau at about 70˚C and did not decrease in temperature at higher MC. The Tg for spruce hemicellulose continued to drop until

at about 30%MC where it was around -20˚C (Kelley et al.1987). These results demonstrate that the constituent polymers of wood behave differently according to species, and that the different polymers within the same wood respond differently to moisture content.

In a series of articles Ishimaru and Iida (2001, 2002) demonstrated that mechanical properties of wood in a transient state while achieving equilibrium during a temperature or moisture reduction period were affected in a manner that decreased the E and the coefficient of viscosity of the amorphous components. The process of change effectively increased the fluidity of the hemicellulose and lignin matrix material. A similar effect was observed by Armstrong and Christensen (1961). This is important because after wood is removed from a steaming chamber for the bending operation both the temperature and moisture content will be in a transient, reduction mode. Moreover, during diffusion-based atmospheric steaming of wood the generation of moisture gradients within the wood is a highly probable outcome within the allotted conditioning period of a production environment. The instability and weak state of wood in this condition (Ishimaru and Iida 2001, 2002) might lead to unexpected bend failures.

The process of steam treating wood results in cleavage of the lignin-carbohydrate complex as a result of organic acid production when steam condenses within the wood with sufficient activation energy (i.e. temperature) to combine with the hemicellulose (Yilgor et al. 2001). Skaar (1976) demonstrated the increased damage due to the combination of heat and steam where approximately 53 days at 100˚C dry heat was necessary to reduce the modulus of rupture of dry wood by 5% compared to only 16 hours for steaming at 100˚C, and only 5 hours for steaming at 120˚C. Clearly, reducing the amount of time required during the steaming process in preparing wood for bending is beneficial to retaining strength in the bent product,

which is important because the novel technique presented in this research has strong potential to reduce overall time at 100˚C steaming temperatures.

Superficial gas permeability of wood is affected by steaming treatments. In an unpublished research paper by Wright (1999) ramin wood (Gonystylus bancanus), a diffuse porous tropical hardwood, was exposed to various temperature steam cooks of 30 minutes duration (80˚C, 100˚C, 150˚C and 175˚C). The superficial gas permeability was tested and results were normalized to the control group average permeability. At 80˚C a 2600% increase, at 100˚C a 3200% increase, at 150˚C a 3900% increase and at 175˚C a 13,300% increase. Increased permeability can be exploited for moisture movement if there is a pressure differential through the wood such as the VST process developed in the current research (Wright 1999).

Other research indicated mixed results. Alexiou et al. (1990) found no significant increase in longitudinal permeability of *Eucalyptus piluluris* when steamed at atmospheric pressure. Morris et al. (1997) reported approximately doubled uptake of borate treatment solution in western hemlock following a steam treatment of 82˚C for four hours compared to end matched un-steamed specimens. The longitudinal air permeability of an evergreen, southeastern Asia oak (*Quercus Cyclobalanopsis* spp.) was found to double following a five hour steam treatment (TaiAn et al. 2003). Narayanappa (2005) found an increase in axial permeability with steaming when working with babul (*Acacia nilotic*).

Increased axial permeability due to steaming would have a cumulative effect on moisture regain in a cyclic process of vacuum and steam. After each steam cycle the permeability of the wood may increase, permitting a greater moisture gain in the subsequent steam cycle thus increasing the rate of plasticization in a non-linear fashion.

2.5 Atmospheric Steaming and Bending of Wood

Stevens and Turner (1948, historical reference) and Peck (1957) established the empirical guidelines for the atmospheric steaming and plasticization of wood. From these guidelines essentially all steam treatment for bending has occurred at about 100^{o}C and atmospheric pressure. Traditional steaming is dependant upon steam temperature, wood species, original wood moisture content, and the dimensions. Thickness and the original moisture content of the wood have a dominant effect on the steaming time. Wetter wood required approximately 15 min/cm (38 min/inch) of wood thickness and drier wood required about 30 min/cm (75 min/inch). Bending the steamed wood is dependant upon; wood species, original location of the wood within the tree, original moisture content, defects existing in the wood, slope of grain, the thickness of the wood section, the length prior to bending, the desired radius of the finished bend, and the ratio between section thickness and radius of curvature (Stevens and Turner 2008, Peck 1957).

The process of selecting wood for bending has a collection of recommendations in various books on the topic (Peck 1957, Stevens and Turner 2008). The recommendations include: straight, clear grained wood, slope of grain on any face limited to 1:15 (4° angle). Defects to be avoided include; knots and associated grain distortion, in-grown bark, surface checks, shake (separation in wood parallel to annual rings), pith, decayed wood and saw tooth marks. Experiments at the USDA-FPL were conducted in an effort to correlate bending quality with specific gravity and rate of growth (number of annual rings per unit length). White oak from 20 trees and four different locations in Kentucky and Ohio were tested and no correlation was

found. The wood of highest bending quality was almost identical to the wood of lowest bending quality in terms of specific gravity and rate of growth (Peck 1957).

Wood is bent while in the plastic state, or in the transition zone below Tg_1 as shown in Figure 2.8. The model of bending (flexure), as shown in Figure 2.5 wherein the neutral axis of bending stress remains at the centroid of the cross section of the beam undergoing flexure, may not be applicable to flexure in the plastic region. The neutral axis will only remain at the centroid in plastic flexure if the cross sectional area has two axes of symmetry and the stress-strain diagram is identical for the material in compression and tension (Popov 1976). The second condition is never true when wood is the material. Stevens and Turner (2008) prepared figures from their data on ash, including a diagram of the neutral axis shift which occurs during the flexure of a plastic material. The figures are reproduced on the next page in their entirety from the 1970 edition of their book.

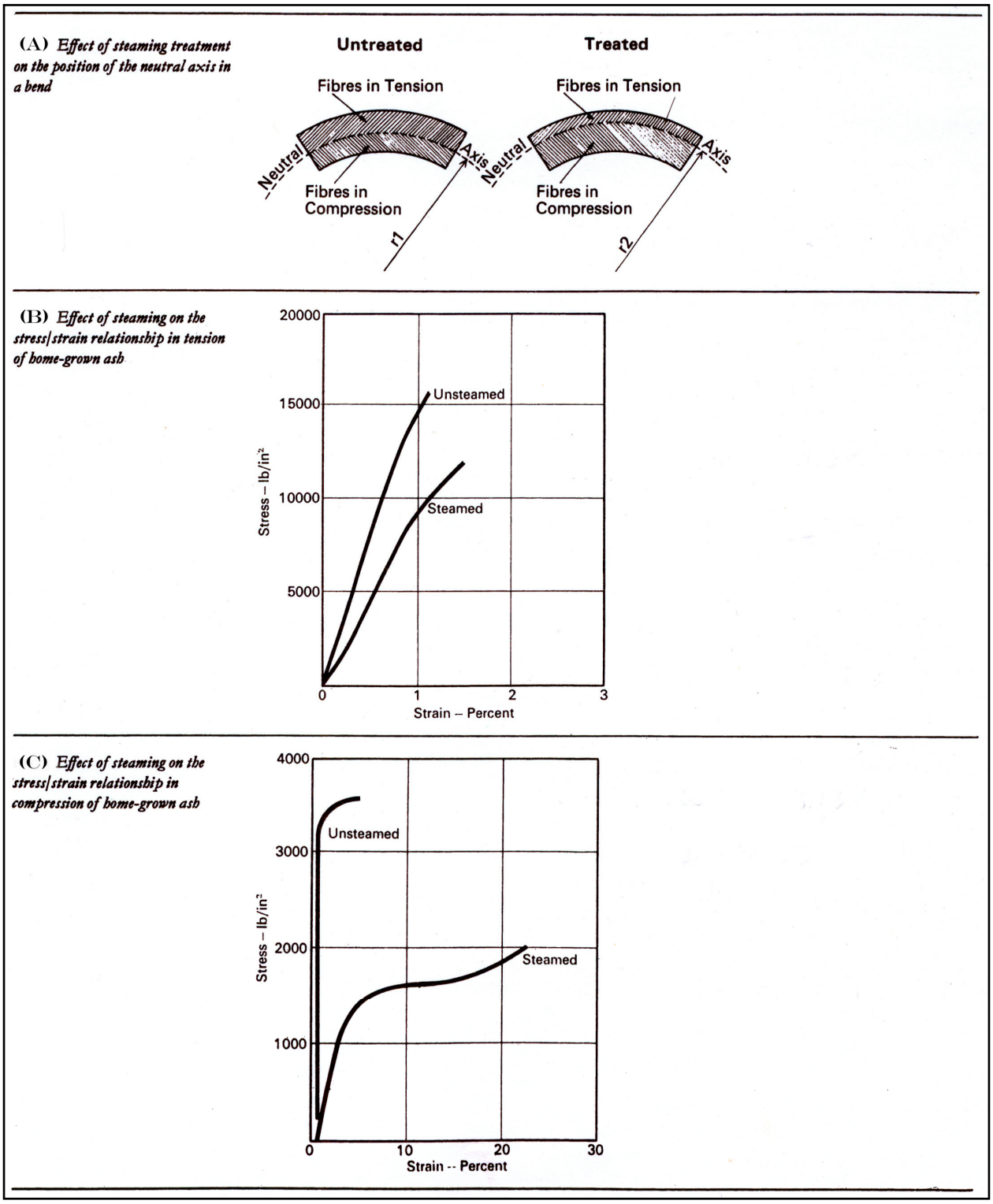

Figure 2.9 Effect on mechanical properties of steamed wood due to plasticization of the viscoelastic amorphous constituents. Reproduced from “Wood Bending Handbook” by W.C. Stevens and N. Turner, ©1970, Fox Chapel Publishing, Broad St., East Petersburg, PA 17520, used with permission. http://www.foxchapelpublishing.com/default.aspx

In Figure 2.9 (A) the ‘untreated’ image shows the neutral axis remaining on the centroid of a vertically symmetrical cross section during elastic bending. After the wood is steamed and has become plastic, the ‘‘treated’ image shows a shift of the neutral axis toward the convex face; this is the tension face. The result is that plasticized wood undergoing a bending operation is preferentially strained in compression considerably more than in tension. Wengert (1988) estimated the additional capacity of compressive strain for plasticized wood to be 10 times that of dry wood. However plasticized wood does not exhibit a similar increase in tensile strain capacity and Wengert estimated that increase to be about 3%. The precise solution is beyond the scope of this work, but Popov (1976) states force equilibrium remains consistent despite the disproportionate strains and the force on the compression side of the beam must equal the force on the tension side.

Figure 2.9 (B) provides a quantitative illustration of material property changes in ash stressed in tension due to steaming. The increased capacity for tensile strain due to steam treatment is less than one-half of one percent; failure at about 1.5% strain. The accompanying reduction in the stress at failure was about 16.5%. Fig 2.9 (C) is a quantitative illustration of material property changes in ash stressed in compression due to steaming. The increased capacity for compression strain went from about 5% strain for un-steamed and up to about 23% strain for steamed, with an accompanying reduction in stress of about 43%.

Due to the vast differential in strain capacities and the shift in the neutral axis, stress concentration on the tensile side of steamed wood undergoing bending is significant and is the limiting factor for small radius of curvature (Stevens and Turner 2008). Clever end-clamping devices attached to flexible flat steel straps were devised to essentially pre-compress the tensile

side of an intended severe bend of wood, offering support. The pre-compression minimizes tensile stress development until near the end of the bend, thereby reducing the tensile strain and avoiding failure. When end-compression and support are used in bending it becomes important that the length of the wood very closely matches the distance between the end supports. Matched length is critical when bending more than one piece in the same support fixture at the same time (Wengert 1988). The bend radius used in this research was not severe enough to require protection of the tensile face. The reader is directed to the references listed for detailed descriptions of end-pressure devices for severe bending of steamed wood.

After steaming and bending, wood must be held in the desired bent shape until it cools to leave it 'set' in the bent shape and excess introduced moisture gradually diffuses out and evaporates. If steaming is excessive, the bent wood must then be held in place longer to permit time for the 'set' to occur. Therefore attaining an optimum amount of moisture and heat regain in the wood to be bent is the goal.

2.5.1 Impact of Wood Anatomy on Bending

During the review of two independent studies involving steam bending various species of wood the author noticed a predominance of ring porous species among the top-ranked woods for bending. Stevens and Turner (2008) reported on extensive testing performed by the (UK) Forest Products Laboratory on 149 species of wood. All were air dried and machined to 25.4mm x 25.4mm square dimensions. After the steaming operation they were bent without support to determine the minimum radius attainable by species with only 5% failed bends. The U.S. Forest Products Laboratory ranked 25 hardwood species on the basis of percentage of breakage

sustained during uniform bending made without end pressure (Peck 1957). A failed bend would be any fracture of the wood in the bend zone or buckling and other visible structural damage in the wood. Alternatively, a successful bend is any bend that sustains a permanent deformation without any visually obvious wood failure (Rice and Lucas 2003).

Table 2.3 lists the top 25 woods from the 149 reported on by the UK-FPL and the 25 woods reported by the USDA-FPL, with a column added by the author stating the anatomical feature of ring porous or diffuse porous where known.

Table 2.3 Experimentally determined woods exhibiting optimal steam bending properties without end pressure; includes author's note regarding the macro-anatomical features of ring porous or diffuse porous where known.

Wood Bending Handbook, Table 1; W. Stevens and N. Turner ©1970, Fox Chapel Publishing					USDA Forest Products Laboratory		
Minimum Radius for Best 25 Species in Steam Bending; Without End Pressure					Agricultural Handbook #125; Edward C. Peck, 1957		
air-dried material 25.4mm square, steamed, 5% maximum failed bends				Author's Note	Uniform Bending Test Without End Pressure		Author's Note
Standard Name	*Botanical Name*	Radius (mm)	Radius/ Thickness	Macro Anatomy	Standard Name	*Botanical Name*	Macro Anatomy
Elm, Dutch (home-grown)	*Ulmus hollandica*	240	9.4	ring porous	Hackberry	*Celtis occidentalis*	ring porous
Walnut, European (home-grown)	*Juglans regia*	280	11.0	ring porous	White Oak	*Quercus alba*	ring porous
Robinia (home-grown)	*Robinia pseudoacacia*	280	11.0	ring porous	Red Oak	*Quercus rubra*	ring porous
Oak, Turkey (home-grown)	*Quercus cerris*	280	11.0	ring porous	Chestnut Oak	*Quercus prinus*	ring porous
Oak, Red (home-grown)	*Quercus rubra*	290	11.4	ring porous	Magnolia	*Magnolia grandiflora*	diffuse porous
Ash, European (home-grown)	*Fraxinus excelsior*	300	11.8	ring porous	Pecan	*Carya illinoinensis*	ring porous
Oak, Japanese	*Quercus spp.*	320	12.6	ring porous	Black Walnut	*Juglans nigra*	ring porous
Elm, Wych	*Ulmus glabra*	320	12.6	ring porous	Hickory	*Carya sp*	ring porous
Karri (South African)	*Eucalyptus diversicolor*	320	12.6		Beech	*Fagus sp*	diffuse porous
Oak, American White	*Quercus alba.*	330	13.0	ring porous	American Elm	*Ulmus americana*	ring porous
Oak, European (home-grown)	*Quercus robur*	330	13.0	ring porous	Willow	*Salix sp*	diffuse porous
Beech, European (home-grown)	*Fagus sylvatica*	330	13.0	diffuse porous	Birch	*Betula sp*	diffuse porous
Ash, American	*Fraxinus sp.*	330	13.0	ring porous	Ash	*Fraxinus sp.*	ring porous
Pillarwood	*Cassipourea malosana*	330	13.0		Sweetgum	*Liquidambar styraciflua*	diffuse porous
Elm, English	*Ulmus procera*	340	13.4	ring porous	Soft Maple	*Acer spp.*	diffuse porous
Elm, White	*Ulmus americana*	340	13.4	ring porous	Yellow Poplar	*Liriodendron tulipifera*	diffuse porous
Ash, European (French)	*Fraxinus sp.*	340	13.4	ring porous	Hard Maple	*Acer spp.*	diffuse porous
Elm, Rock	*Ulmus thomasii*	360	14.2	ring porous	Chestnut	*Castanea sp*	ring porous
Afzelia (mbembakoti)	*Afzelia quanzensis*	360	14.2		Water Tupelo	*Nyssa aquatica*	diffuse porous
Sterculia, Brown	*Sterculia rhinopetala*	360	14.2		Cottonwood	*Populus deltoides*	diffuse porous
Sycamore (home-grown)	*Acer pseudoplatanus*	370	14.6	diffuse porous	Black Tupelo	*Nyssa sylvatica*	diffuse porous
Beech, European (Danish)	*Fagus sylvatica*	370	14.6	diffuse porous	Mahagany	*Swietenia mahagoni*	diffuse porous
Hickory	*Carya sp.*	380	15.0	ring porous	American Sycamore	*Platinus occidentalis*	diffuse porous
Chestnut, Sweet	*Castanea sativa*	380	15.0	ring porous	Buckeye	*Aesculus sp*	diffuse porous
Ebony, African	*Diospyros crassiflora*	380	15.0	diffuse porous	Basswood	*Tilia americana*	diffuse porous

Left table section from "Wood Bending Handbook", Table 1 (in part), Stevens and Turner ©1970, Fox Chapel Publishing, 1970 Broad St., East Petersburg, PA 17520, used with permission) http://www.foxchapelpublishing.com/default.aspx

Right table section from USDA Forest Products Laboratory (US Government laboratory).

Superficial gas permeability of wood is affected by wood anatomy (Siau 1995). The observation that ring porous woods tend to perform better may indicate that the anatomy of the wood, perhaps the vessel size, has an important influence upon the ability of traditional steaming to adequately plasticize the wood for bending success.

However, Sorz and Hietz (2005) tested radial and axial diffusion of gas in different species of wood using oxygen gas. Wood specimens from coniferous, ring-porous and diffuse-porous species specimens were precision machined and sealed into a special flow testing apparatus with an oxygen concentration sensor at one end. Oxygen gas was supplied at various flow rates and the diffusion coefficient D (m2/s) was determined. As the gas flow increased from 15% maximum flow to 40% maximum flow, the diffusion coefficient in the radial direction increased 5-13 times in the coniferous and ring porous, but 1000 times greater in the diffuse porous. Results in the axial direction were proportionally similar but 1-2 orders of magnitude higher overall. The diffuse porous woods had significantly higher gas diffusion rates than the ring porous. This was suspected to be due to vessel blockage by tyloses in the ring porous. The result strongly suggests larger vessel size may not aid steam dispersal during the steaming process for bending.

Another possibility for an anatomical influence may be the ability of larger vessels in ring porous woods to accept the extensive compression deformation that occurs during steam bending; i.e. displacement of the solid wood component into the vessel. Karenlampi et al. (2003) cites that in particular radial and tangential compression display a plateau region in the stress strain curve where strain can occur without a major change in stress and the plateau region is

likely to be due to the buckling of cell walls into cell lumen. Once the lumen fill with displaced cell wall material, compressive stress continues to rise (2003).

The force equilibrium discussed by Popov (1976) dictates that as compressive stress resumes its increase, the tensile stress must also resume its increase. Due to plastic deformation and shift in the neutral axis the available area for tensile stress decreases and estimated tensile strain limits are 1.5 to 3%. It is conceivable that ring porous woods perform better in bending in part because there is more physical space for compression induced cell wall displacement after plasticization and not due to certain wood species plasticizing better than other species.

The potential correlation between anatomy and better steam bending performance had not been revealed in any other literature. An in-depth, quantitative endeavor to perform an anatomical comparison relative to steamed wood bending is beyond the scope of this work. However the cyclic vacuum and steam combination developed in this research may expand the number of wood species suitable for bending due to a different method of moisture movement within the wood relative to atmospheric steaming as the UK-FPL and the USDA-FPL studies were based upon.

2.5.2 Influence of Steam Temperature on Bending

The influence of steam temperature on bending was demonstrated by Peck (1957) who tested steamed specimens of clear, straight-grain white oak with an initial moisture content of 25% at various pressures and time durations; then bent them. The results were reported as numbers of successful and failed bends. At 100˚C and 20, 40, or 60 minutes of steam time, an

average of 6.5% of the boards failed. At 123˚C and 20 minutes 18% of the boards failed. At 138˚C and 10 or 20 minutes, about 38% of the boards failed (Peck 1957). Wood at 120°C rapidly lost strength compared to wood steamed at 100°C (Skaar 1976). This information is important because the upper limit of steam temperature for bending had been established to be approximately at 100°C.

2.5.3 Influence of Moisture Content on Bending Wood

It is known from previous discussion that the moisture content of wood must be at a minimum level to soften wood effectively and reduce the modulus of elasticity. Rice and Lucas (2003) provided data quantifying a relationship between moisture and the work effort to bend red oak. Their bending apparatus involved a matched set of convex and concave forms that permitted specimens 11.9mm (15/32 inches) thick with a centerline radius of 178 mm (7 inches) and vertical displacement of 88.9mm (3.5 inches). This provided repeatable force/displacement data for identical displacement. Work is defined as the action of a force through a distance (Onouye and Kane 2007). Fixing displacement leaves force as the variable and if the modulus decreases the force decreases and subsequently the work to bend decreases. Their work to bend analysis was based on the calculating the area beneath the load vs. deflection curve for each specimen after Bodig and Jayne (1982). Rice and Lucas (2003) state the work levels should be sensitive to changes in independent variables given identical deformation. Their results showed that work to bend decreased by 32% between 12%MC specimens and 15%MC specimens. This is important because a 3%MC change resulted in a 32% decrease in work demonstrating a strong moisture content influence, and the author utilized a similar approach to

this demonstrated one for quantifying a relationship between moisture content and work to bend for maple.

2.6 Vacuum Applied to Wood

Vacuum is currently applied to wood within a few common production technologies; the preservative industry, the cabinet and furniture industry, and the lumber industry (Hiziroglu 1996, Serrano and Cassens 2000). Knowledge about how wood behaves at different moisture contents while under vacuum will aid in understanding how wood in a cyclic vacuum and steam system might behave.

Evacuation of wood prior to impregnation with liquid-based anti-microbial preservatives is commonplace. For commercial applications in timber and wood preservation the “full cell” process for impregnation of wood utilizes a vacuum cycle of approximately 30-60 minutes to remove air and free water from the cell lumen. That step is followed by a 1.14– 1.48 MPa (150-200 psig) pressure cycle for several hours with preservative (Hiziroglu 1996). The preservative fills the empty, evacuated spaces first and then diffuses into the cell wall. Following the high pressure treatment the wood is evacuated again to recover the residual free liquid preservative within the cell lumen. The process is also known as the Bethell process and has been in use since 1838 (Richardson 1953). Both vacuum steps in the Bethell process are utilized to remove liquid from wood with extended 60 minute vacuum periods. This is opposite of the desire in this research, but helpful in establishing approximate process boundaries.

Furniture, cabinet manufacturers use vacuum drying of wood for moisture reductions without material degrade. Serrano and Cassens (2000) attribute economically viable recovery of

clear component parts from top logs and small diameter red oak to the vacuum drying of the parts at about 45°C. This was helpful in understanding that moisture is readily removed from wood under vacuum at very mild temperatures; a detail to avoid during moisture regain.

In drying of thick section (260mm x 260mm) western hemlock (*Tsuga heterophylla*) radio frequency combined with vacuum was used to reduce degrade to the wood. Radio frequency electromagnetic waves were used to heat the moist wood via molecular excitation to lower temperatures than a conventional dry kiln and vacuum is used in combination with that mild heat to remove moisture as vapor. This offers insight for a cyclic vacuum and steam process to add moisture to wood via antithetic thinking.

According to Chen (1997) the current technological approach to vacuum drying of wood began in 1962. Standard steam tables show that a chamber pressure of 7.75kPa will result in water changing state to steam at a temperature just in excess of 40°C. Cyclic vacuum drying occurs with intermittent heating of the wood up to about 40°C followed by evacuation of the chamber containing the heated wood to the low pressure of 7.75kPa whereupon water in the wood changes state to steam vapor and migrates out of the wood as a gas/vapor. The change of state requires energy which is gained from the wood. When the wood temperature is reduced and the rate of water loss diminishes the vacuum is interrupted, the wood is heated again and the cycle repeats.

An ideal model of wood vacuum drying with pure water has two readily measured independent properties; pressure and temperature. If the model has no air to function as a diluent and contribute partial pressure components, the total system pressure represents pressure due to water vapor only (Chen et.al. 2009). At low pressure water vapor will exist as

superheated steam and has temperature and pressure as independent properties (VanWylen and Sonntag 1976). This provides important information about the atmosphere surrounding wood under vacuum; to readily interpret it from steam tables it should be free of diluent air.

Chen (1997) concluded that in vacuum drying the primary driving force for moisture movement is the pressure differential between the lower chamber atmosphere and the higher internal wood pressure. The reason for higher pressure inside the wood is a combination of 'pressure drop' through the anatomical voids (permeability of wood), the vapor pressure of the water within the wood and the boiling of the water within the wood. 'Pressure drop' was the author's choice of words but is a slight misnomer because the pressure gradient actually increases from the outside of the wood toward the center of the wood, but is consistent with discussions of fluid mechanics.

Water vapor bulk flow (WVBF) is the primary mechanism of moving moisture from wood during vacuum drying. In vacuum drying the moisture movement is largely a longitudinal migration. Migration in the transverse direction is non-dominant in vacuum drying in contrast to conventional atmospheric pressure kiln drying. Under vacuum, water within the wood actually boils to vapor. Water vapor quickly responds to the total pressure differential and follows the path of least resistance in the longitudinal direction of the wood. The performance of cyclic vacuum drying was not affected by the specimen thickness, but the specimen length (Chen 1997). Figure 2.10 is reproduced from Chen's dissertation and shows curves of moisture movement calculated from Chen's (1997) model of moisture movement. It predicts WVBF to be two orders of magnitude greater than diffusion based moisture movement (0.001 to 0.1). The two curves per mechanism represent calculated maximum and minimum flow rates.

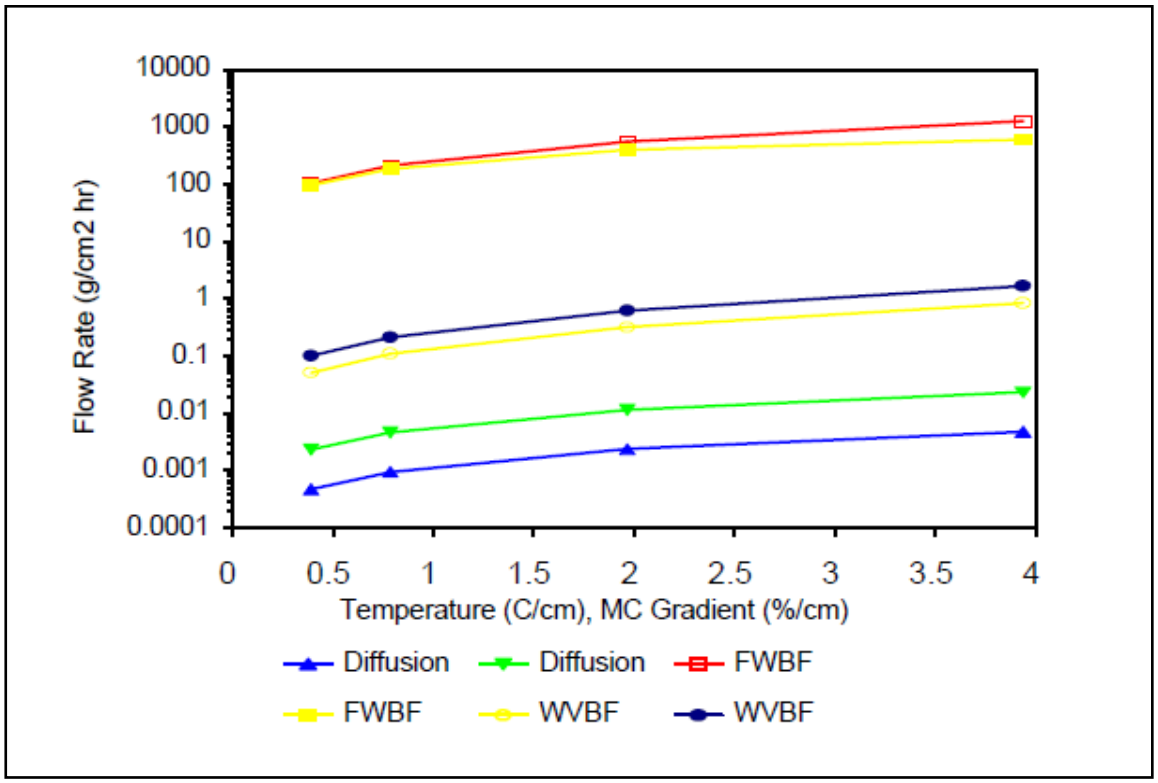

Figure 2.10 Calculated flow rates through red oak via various mechanisms.
(Chen 1997: "Primary driving force in wood vacuum drying" used with permission)
Note: free water bulk flow (FWBF) in the figure is not particularly applicable to the cyclic vacuum and steam technique developed in this research work

Chen (1997) provided experimental evidence for the rate of evacuation of wood. A performance curve for pressure distribution through the length of a 10"L X 2" X 2" red oak specimen during a vacuum cycle was produced. Pressure signals from capillary tubes sealed in the wood had been fit through the chamber to a recorder and data for the pressure inside of the wood was recorded. The author was struck by a similarity between the performance curve for the pressure reduction within red oak generated from experimental data and the vacuum pump performance curve Chen published as used for his experimentation. The scales on the axes did not match between the two curves but the author used a graphic software package to approximately match and overlay the two curves. The time scale matched at 10 minutes but the

pressure scale is off a small amount. However, both traces would have begun at atmospheric pressure (760mm Hg at sea level). The inference from Figure 2.11 being that given wood with gas permeability at least as good as red oak, the atmosphere is removed from the wood at almost the same rate as the vacuum pump can work. The time required to attain a stabile minimum pressure was about 12 minutes. This was important because it helped define a beginning point for the vacuum cycle in cyclic vacuum and steam moisture regain. The 12 minute time period is greatly reduced from the 60 minute period used in the Bethell process.

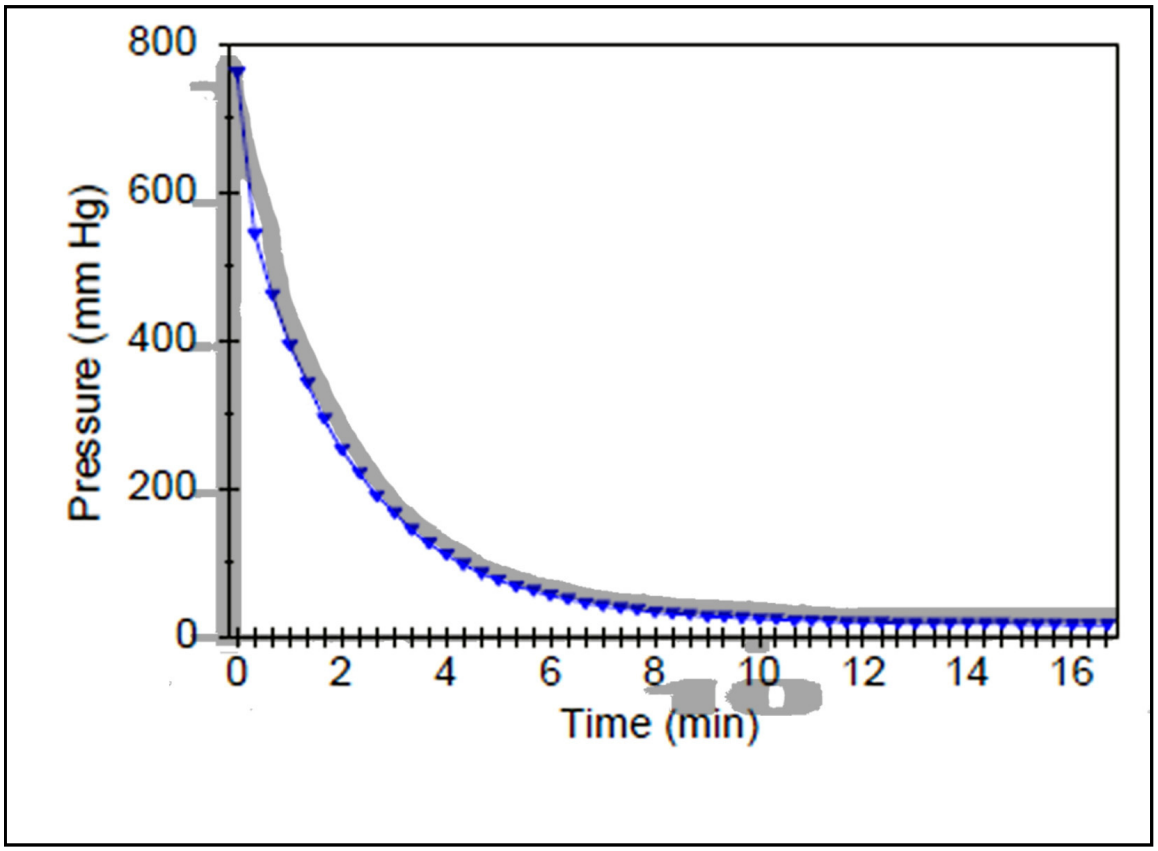

Figure 2.11 Overlay of vacuum pump performance in blue and internal wood pressure for red oak in gray. (From Chen; 1997, figures 9.2 and 10.4 respectively, used with permission).

2.7 Vacuum and Steam Applied to Wood

Wood that is air dried or kiln dried and cooled to ambient temperature has the remaining gases (primarily air) within the void spaces of the wood at essentially one atmosphere of pressure in equilibrium with the surroundings. In traditional steaming (and in the control for this experiment) as wood at atmospheric pressure is placed into a conventional steaming chamber using 100°C steam, also at one atmosphere of pressure, there is a stalemate as far as any moisture movement due to pressure differential. From a macroscopic perspective both air and steam are at equivalent pressures and neither has any significant motive force to move.

The Ideal Gas Law provides an introduction to the complex combination of factors that affect moisture movement in wood. Water vapor (steam) is considered the ideal gas in motion relative to the wood. The ideal gas law on a molar basis (moles of gas) is (VanWylan and Sonntag 1976):

$$PV = n\bar{R}T \qquad \text{Equation 2.7}$$

Where: P = pressure (Pa)
V = volume (m^3)
n = number of moles of gas
$\bar{R}$ = universal gas law constant (J / mol. K)
T = temperature (K).

Consider a system comprised of a pressure-tight chamber into which steam can be introduced and/or a vacuum can be sustained. A piece of wood is placed Inside of the chamber. The following schematic, Figure 2.12, illustrates:

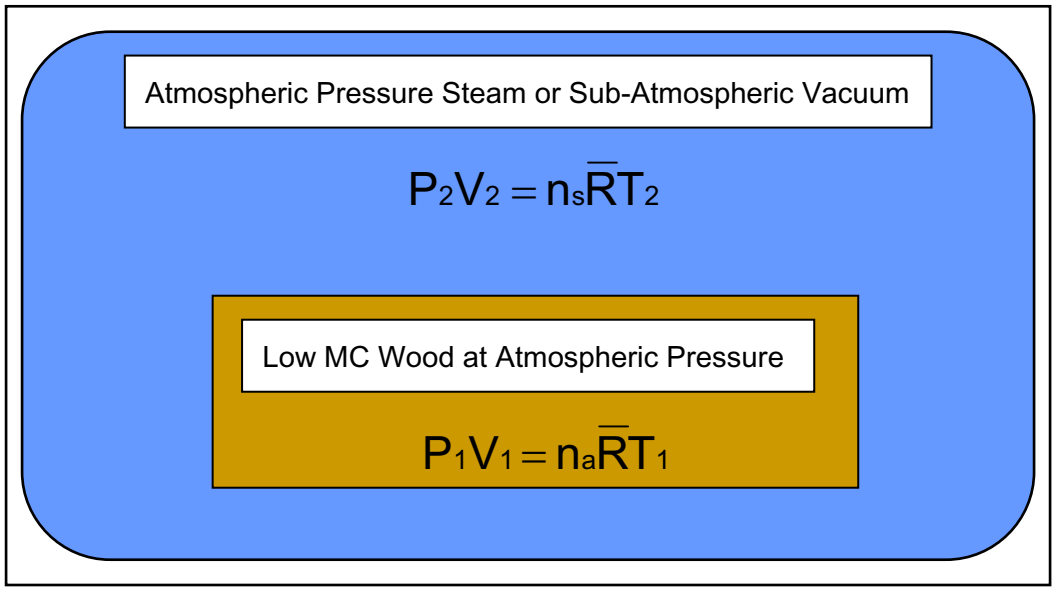

Figure 2.12 Schematic of low moisture content (MC) wood in variable atmosphere Image produced by author, 2010.

As mentioned above in the case of atmospheric steaming; $P_1 = P_2$ = atmospheric pressure, and in the molar form the universal gas constant is the same and therefore cancels. By solving each state equation for pressure (P) and setting them equal the ideal gas law model simplifies to:

$$\frac{n_a T_1}{V_1} = \frac{n_s T_2}{V_2}$$ Equation 2.8

In the case where the pressures are equal the mechanism of gas movement due to a pressure differential has been removed from possibility. The remaining influences for moisture movement are due to temperature differences and diffusion. Temperature differences fall into the realm of conductive heat transfer when the piece of wood is considered as the thermodynamic control volume and Fourier's Law of Conduction states that (Arpaci 1979, Siau 1995):

$$\frac{\Delta Q}{\Delta t} = -kA\left[\frac{T_2 - T_1}{\Delta x}\right] \qquad \text{Equation 2.9}$$

Where: $\Delta Q / \Delta t$ = rate of heat flow (W)

k = thermal conductivity (material property) [W / (m $^{\circ}$K)]

T = temperature (K)

A = area through which heat is conducted (m^2)

Δx = length of heat transfer path in one dimension (m)

The negative sign corresponds to the fact that heat flows from a higher temperature source to a lower temperature source. Thermal conductivity (k) is a material property, but in the case of anisotropic wood, it is greater for the longitudinal direction (parallel to the grain) than the transverse direction (perpendicular to the grain) by a factor of about 2.5. Thermal conductivity also changes with specific gravity and moisture content of the wood (Siau 1995). Values of thermal conductivities are shown in Table 2.4.

Table 2.4 Thermal Conductivity Values (k), (Siau 1995)

Material	k, [W / (m K)]
Wood, G = 0.45, MC = 12%, ⊥	0.13
Wood, G = 0.45, MC = 12%, ‖	0.31
Wood, G = 0.70, MC = 12%, ⊥	0.18
Wood, G = 0.70, MC = 12%, ‖	0.44
Water, free	0.59
Air, still	0.024
Concrete	0.93
Glass	1.05
Fiberglass	0.039
Copper	396
Stainless Steel	16.3

The thermal conductivity values for wood indicate it is a reasonable thermal insulator, particularly perpendicular to the grain. The rate of heat flow into the wood when the pressure inside of the wood is identical to the pressure of the steam (as was the case in the control for this experiment) is limited by the thermal resistive quality of the wood as outlined in Figure 2.12.

Diffusion involves volumetric differences and the number of moles of air (subscript ‘a’) and number of moles of steam (subscript ‘s’).The number of moles of gas divided by the volume they occupy is equivalent to the concentration (mass per unit volume) gradient existing between two different states or locations and diffusion governs the molecular mass flow below the fiber saturation point; i.e. bound water diffusion. Diffusion of moisture in wood is variable and is

affected by specific gravity, wood moisture content, temperature, and the moisture concentration difference or gradient (Siau 1995, Skaar 1988).

The diffusion phenomenon is a flux or transfer of molecules from an area of high concentration to an area of low concentration over time. In simple one-dimensional, isothermal flow Fick's equation for diffusion is (Siau 1995):

$$J = -D\frac{\partial C}{\partial x} \qquad \text{Equation 2.10}$$

Where: J = diffusion flux [mol / (m^2s)]
D = diffusion coefficient (m^2 / s)
C = concentration of molecules in flux (mol / m^3)
x = length in the flow direction

The negative sign corresponds to the fact that molecules flow from an area of higher concentration to an area of lower concentration.

The diffusion coefficient for wood is described by Siau (1995) as:

$$D = \frac{w/t}{\Delta C/L}A \qquad \text{Equation 2.11}$$

Where: w / t = rate of water vapor transport (kg / s)
$\Delta C / L$ = water concentration difference / length, in flow direction [(kg / m^3) / m]
A = cross-section area perpendicular to flow (m^2)

Values for the diffusion coefficient of water in wood up to the fiber saturation point have been experimentally determined (Stamm 1959) and mathematical models have been proposed by Siau (1995) based on experimental work which describe the influence of temperature and moisture content. There is an exponential increase in the diffusion coefficient for moisture flux in

the direction of the wood grain as the bound water content approaches fiber saturation. This is caused by the decreased bond energy at the sorption sites in the cell material as moisture content increases (Siau 1995). The highest reported empirical value for the diffusion coefficient at 29% MC is: $D = 14x10^{-11}$ m^2/s at approximately 27°C, parallel to the grain (Stamm 1989). Diffusion perpendicular to the grain is slower by a factor of approximately 2.5 (Siau 1995). Walker (1993) reports that the rate of diffusion parallel to grain increases by a factor of 37 from 25˚C to 100˚C. Applying Walker's (1993) factor to the diffusion coefficient results in $D = 8.2x10^{-9}$ m^2/s, indicating that even at elevated temperatures diffusion is a slow process.

Skaar, Siau, Stamm and others have made extensive investigations into the moisture movement through wood based upon the diffusion principle and the reader is recommended to look at their works listed in the bibliography. Further development in this work is beyond the scope of the research objectives. The significant point to be made is that when the steam pressure is equal to the air pressure inside of the wood, heat transfer is essentially limited to conductive heat transfer through a reasonably good insulation material (Table 2.4) and moisture (mass) transfer is limited to diffusion in a material with an extremely small diffusion coefficient. The combination of these two qualities results in a relatively slow process of conventional atmospheric steaming for bending wood, and also a relatively slow process of atmospheric pressure wood drying

2.7.1 Introduction to Differential Pressure Influenced Moisture Movement in Wood

Vacuum Steam Technology, VST, is a descriptive name that evolved out of Chen's experimentation regarding alternating cycles of vacuum and steam for phytosanitation treatment

of wood, leading to provisional patent VT09-086 (Chen and White 2009). The process is similar to cyclic vacuum and steam in vacuum kiln drying with the important difference of VST utilizing saturated steam at atmospheric pressure in place of superheated steam as in vacuum drying. VST begins with a vacuum cycle to reduce pressure inside of the wood. As soon as the desired pressure is attained the vacuum stops and steam is introduced. Steam quickly penetrates into the wood, condenses, and at the desired endpoint of the steam cycle the steam is shut off and another vacuum cycle commences. This section introduces theoretical components supporting development of the research hypotheses.

Throughout this section there will be several references made to Figure 2.12 (page 45), a schematic of a chamber with a piece of wood inside. Consider the atmosphere around the piece of wood as removed from the chamber by a vacuum pump. Simultaneously the air within the lumen is drawn out due to the lower chamber pressure. Given sufficient time under vacuum all of the void spaces within the wood will be at equilibrium pressure with the evacuated chamber. Neumann et al. (1992) experimented with vacuum drying of beech with additional convective heat gain during vacuum via the addition of superheated steam at 20 kPa. He measured the pressure within the wood and found a pressure gradient in every direction (longitudinally and both transverse directions) during drying.

Sasaki et al. (1987) studied the pressure inside wood as drying preceded and found that the pressure / time curves were divided into three periods. First, the pressure decreased rapidly depending on the permeability and location in the board. Second the pressure remained nearly constant. In the third period, after MC was below FSP, the pressure began to decrease again and approached the reduced pressure in the chamber. Since the specimens used for the

current research were already kiln dried to about 6%, the first two stages described in drying by Sasaki (1987) would not necessarily occur because the specimens would be below FSP. The important point remains that the pressure inside of the wood will become close to the evacuated chamber pressure. This was also shown in Figure 2.11 (page 43).

In comparison to Neumann et al. (1992) and Sasaki et al. (1987), the VST process for moisture regain only requires the wood and the chamber (Figure 2.12) be evacuated to develop a sub-atmospheric pressure gradient sufficient to induce WVBF moisture movement into the wood during the subsequent steam cycle. The steam cycle need only operate until the low pressure gradient in the wood has been fully exploited and the internal voids of the wood come to pressure equilibrium with steam in the chamber. Any additional steam use after pressure equilibrium would revert to diffusion based moisture movement.

A single vacuum-steam cycle will be described to illustrate the process. Assume the evacuated chamber (Figure 2.12) attained 10kPa (75 Torr or 75mm Hg). Due to pressure gradients within the wood, void space pressures would vary between the actual chamber pressure and greater. If the vacuum were operated long enough, all of the wood void spaces would equilibrate with the chamber pressure of 10kPa. The next step involves removing the vacuum from the chamber and introducing atmospheric steam (101kPa at sea level) to the chamber. The differential pressure between the void spaces and the incoming steam is 90 kPa and that pressure differential results in WVBF into the wood (Chen 1997). As steam penetrates into the wood, mass and heat transfer occurs from the steam to the wood. Mass transfer occurs as vapor phase bound water formation (Siau 1995). Heat transfer occurs until sufficient energy

has been lost to the wood and the steam condenses. During condensation the latent heat of vaporization of steam results in internal wood temperature rise.

In vacuum drying, water vapor bulk flow (WVBF) has been found to move an appreciable amount of water mass and can be modeled by Darcy's Law for the flow of gases through a porous media (Chen 1997). The reference equation to approximate the mass transfer occurring during the switch from vacuum to steam in the case of RA #1 is Darcy's Law for unsteady-state gaseous flow in parallel-sided bodies (Siau 1984):

$$\frac{\Delta m}{\Delta t} = -\frac{k_g A M_w \Delta\left(P^2\right)}{2\overline{R}T\left(\Delta X\right)} \qquad \text{Equation 2.12}$$

Where: Δm = change in the mass of the gas into or through the body (kg)

Δt = change in time (s)

k_g = superficial gas permeability [m^3 / (m·Pa·s)]

A = cross-sectional area of flow path (m^2)

M_w = molar mass of gas (kg/mol)

ΔP^2 = the square of the pressure differential between inlet and outlet (Pa^2)

$\overline{R}$ = universal gas constant [8.3145 J / (K•mol)]

T = temperature (K)

Δx = unit length of the gas pathway (m)

The negative sign indicates the flow is in the direction from higher pressure to lower pressure. For a thorough derivation of this form of Darcy's Law the reader is directed to Siau (1984, 1995).

The left side of Equation 2.12 is the rate of mass transfer of the gas into the body. In terms of VST this means the mass flow rate of steam into the wood because that is the direction of higher pressure to lower pressure.

The right side of the equation has several constants; the universal gas constant, the area of the cross section, the molecular weight of the steam (18g / mol), and the superficial gas permeability. 'Superficial gas permeability', according to Siau (1984) was first suggested because the flow value generally exceeds liquid permeability after both viscous and slip flows are corrected for. According to terminology in the field fluid mechanics, superficial mass velocity is the term used to describe the flow through a bed of solids or porous media. It refers to the resultant quantity when the measured weight rate is divided by the total cross-sectional area of the enclosure *without subtracting* the area occupied by the solid components in the porous media (Perry's 1984).

Strictly speaking the superficial gas permeability is not a constant in wood due to the heterogeneity and anisotropic nature of wood, though it is frequently treated as one. Miyara et al.(1991) found variability in the superficial gas permeability of ceibo wood (*Erythrina crista-galli.* L.) within the same pieces of wood cut to shorter lengths and retested. In addition steaming itself seems to increase the permeability (Wright 1999, Narayanappa 2005, Ping and WenJing 2009).

For the purposes of introducing the mechanisms responsible for rapid mass transport into the wood and using Equation 2.12, the value k_g; superficial gas permeability will be considered constant. Equation 2.12 will be restated after having removed the constants to clarify the important variables:

$$\frac{\Delta m}{\Delta t} \propto -\frac{\Delta\left(P^2\right)}{\Delta T \Delta x} \qquad \text{Equation 2.13}$$

In this form it is clear that under Darcy's Law for unsteady state as a model, the rate of mass transport; i.e. the steam, into the wood is a function of the square of the pressure differential. The larger the pressure differential can become, other factors remaining the same, the faster steam penetrates into wood in the case of this experiment.

2.7.2 Introduction to Thermodynamics of Steam Pertinent to the VST Process

Steam such as that used for preparing wood for bending, in a thermodynamic sense, is referred to as 'saturated steam'. The term 'saturated' means that the steam produced is in pressure and temperature equilibrium with the water from which it was produced. Pure saturated steam has material properties associated with it just as any material does. Of interest at this point is the fact that when steam is saturated, its temperature and pressure are *dependant* properties. That means there is exactly one specific temperature for every specific pressure. Pure water boils at 100^{o}C, at the standard atmospheric pressure of sea level (101.35kPa). The temperature of boiling water changes with elevations different from sea level, and the atmospheric pressure changes regularly as weather patterns change, but the basic concept of 100^{o}C corresponding to one atmosphere of pressure is the relevant point.

Within the definition of saturated steam resides another property of steam referred to as the quality. The quality of steam is a ratio of the mass of pure vapor divided by the total mass. It is defined in a manner tantamount to the moisture content of wood on a wet basis (VanWylan and Sonntag 1976):

$$X = \frac{v_m}{l_m + v_m}$$ Equation 2.14

Where: X = quality

v_m = vapor mass

l_m = liquid mass

Quality describes the amount of liquid droplet water that can exist in a dispersed mist form within pure saturated steam vapor. It should be pointed out that with any other gases present in the steam vapor; such as air or gas emitted from wood for example, the steam vapor mass will be a partial pressure of steam. This detailed analysis is beyond the scope of this work.

If saturated steam is separated from contact with the liquid water supplying it, and then either heated further or the surrounding atmospheric pressure is reduced, the steam will enter a state known as superheated steam. The amount of superheat is measured in degrees Celsius above what the saturated steam temperature would be at the same pressure. In the state of superheated steam, temperature and pressure are independent properties. Relative to saturated steam, superheated steam is hygroscopic and no longer in equilibrium with the liquid water source. Superheated steam will draw water into it until a new equilibrium is attained. If superheated steam were exposed to a supply of liquid water, the steam would gain water mass until it attained the saturated state.

In a saturated steam system the liquid water that provides for the production of steam vapor is said to be in a compressed liquid, or saturated liquid state. The compressed liquid state is similar to the superheated steam state in that temperature and pressure are independent properties.

Figure 2.13 is a pressure – temperature curve for saturated steam. The bold black curve is the equilibrium state of saturated steam; variations in steam quality from 0% to100% exist on this line. Below the line is the compressed or saturated liquid state and above the line is the superheated state.

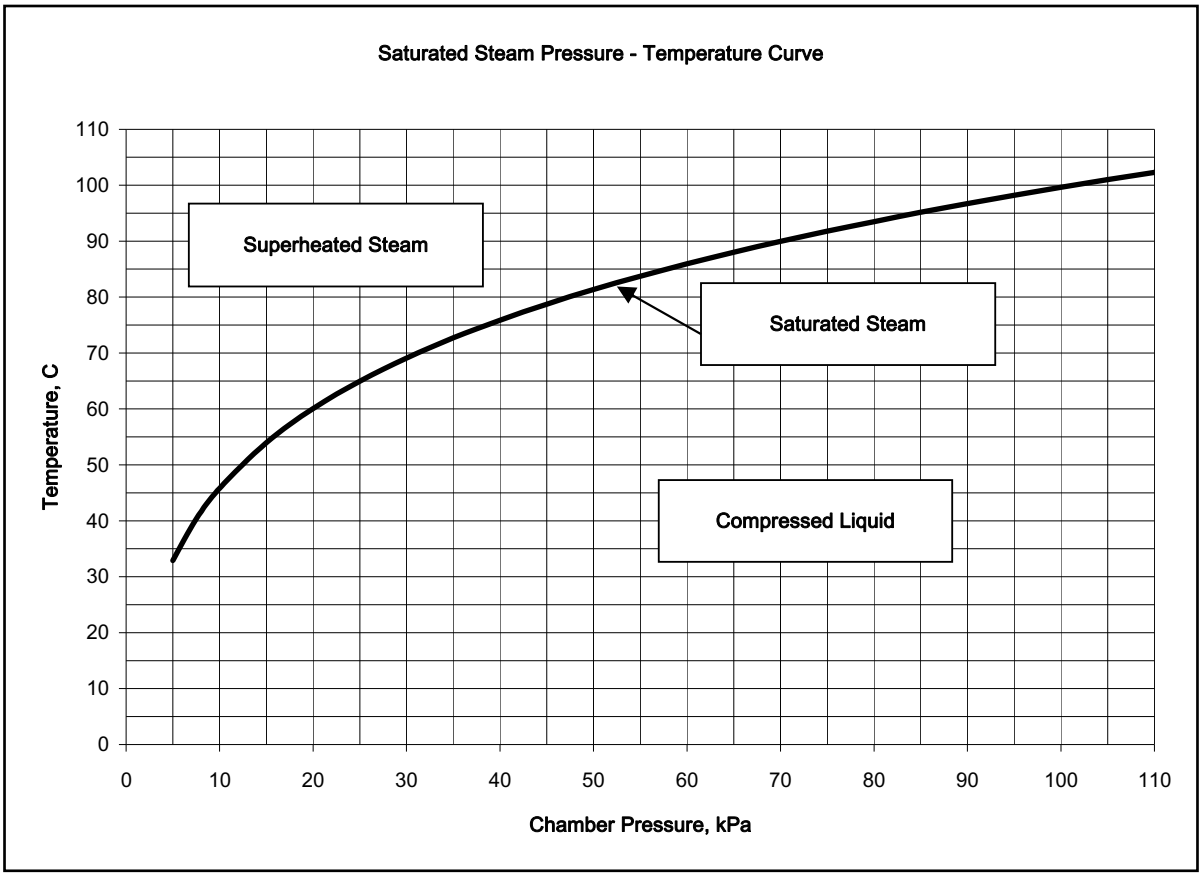

Figure 2.13 Pressure-temperature curve for saturated steam. Image produced by author 2010

2.7.3 Vacuum and Steam Behavior in the VST Process

In the VST process there exist rapid pressure fluctuations between saturated steam additions and evacuation via a pump. The fluctuations would be about one atmosphere pressure. A moisture balance must be maintained in the atmosphere during the pressure changes. As mentioned in Section 2.7.2 superheated steam is hygroscopic and would adsorb

moisture from all available sources. Several authors have published papers describing the use of superheated steam with vacuum drying as a means of heat transfer to the wood being dried (Yamsaengsung et al. 2008, Defo et al. 2004). In VST for moisture re-gain to wood that is already dry; a superheated atmosphere must be avoided. The required balance is represented by the saturated steam line in Figure 2.13.

A chamber is required to contain the wood and an atmosphere surrounding the wood plus simultaneously resist the forces due to one atmosphere pressure change at an elevated temperature; a diagram is shown in Figure 2.14. Assume a steam temperature of 100°C at 101kPa; precisely on the saturated steam curve in Figure 2.13. If a vacuum cycle began, to remain in saturated steam equilibrium the temperature must drop with the pressure in the fashion described by the saturated steam curve. Minor fluctuations could occur between 0% and 100% quality, yet remain a saturated steam environment. The vacuum process aides in reducing the temperature of the atmosphere due to gas expanding within the chamber as some portion of gas is being pumped from the chamber. The first law of thermodynamics for a Uniform State, Uniform Flow (USUF) system and a schematic of a chamber, valves and the control volume (CV) within the chamber will help illustrate why the temperature drops. The dashed line represents the CV being considered; see Figure 2.14.

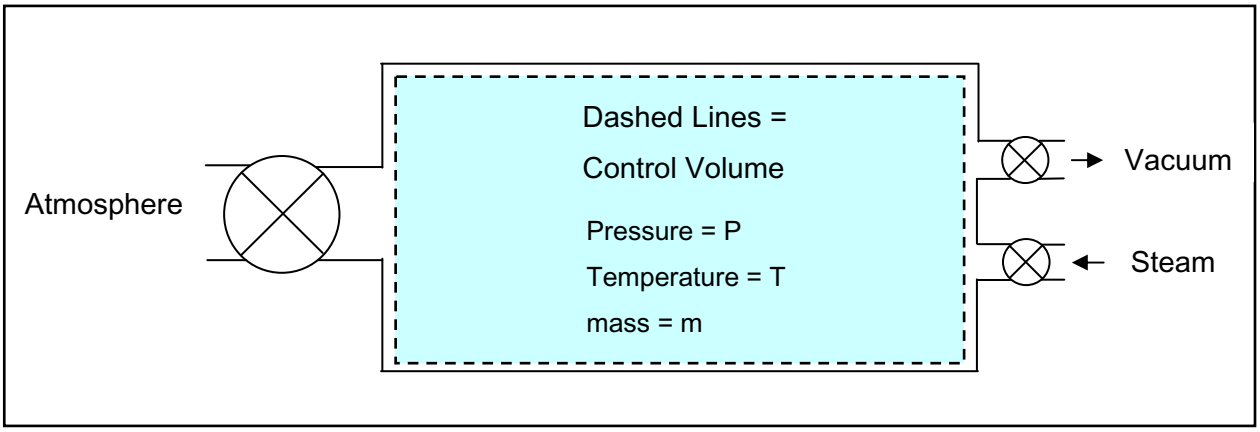

Figure 2.14 Schematic of steaming chamber, control valves, and control volume model
Image produced by author 2011

The first law of thermodynamics; USUF control volume (VanWylen 1976): Equation 2.15

$$Q_{cv} + \sum m_i\left(h_i + \frac{V_i^2}{2} + gZ_i\right) = \sum m_e\left(h_e + \frac{V_e^2}{2} + gZ_e\right) + \left[m_2\left(u_2 + \frac{V_2^2}{2} + gZ_2\right) - m_1\left(u_1 + \frac{V_1^2}{2} + gZ_1\right)\right]_{cv} + W_{cv}$$

Where:

Q_{cv} = the heat within the control volume; kJ

m_i = mass flux into (i) (or e; exiting) the control volume; kg

h_i = enthalpy flux into (i) (or e; exiting) the control volume; kJ/kg

$\frac{V_i^2}{2}$ = term for kinetic energy into (i) (or e; exiting) the control volume; m^2/s^2

gZ_i = term for potential energy into (i) (or e; exiting) the control volume; m^2/s^2

m_1 = mass in the control volume at time 1 (or time 2); kg

u_1 = internal energy in the control volume at time 1 (or time 2); kJ/kg

W_{cv} = Work done *by* or *to* the control volume; kJ

As a first estimate, time 1 is set as the point after the chamber has been preheated, atmospheric pressure air is in the control volume and all are valves closed; immediately before an initial evacuation cycle. Assume a quasi-equilibrium evacuation of air as an ideal gas with no

heat transfer from the heated chamber walls to the air in the CV (Q_{cv} = 0). Time 2 is set as the point after the chamber has been evacuated to the minimum pressure and the air volume in the chamber has been greatly reduced with all valves closed; immediately before the first steam cycle. By selecting these specific points in time there is not a need to look at the flux of air into the chamber when it is loaded (M_i=0). Kinetic and potential energy terms are negligible, and no work is done (W_{cv} = 0). Therefore Equation 2.15 simplifies and can be rearranged to:

$$(m_1u_1 - m_2u_2) = m_e(h_e) \qquad \text{Equation 2.16}$$

Equation 2.16 states the change in the total energy within the control volume from state 1 to state 2 is equal to the mass flow exiting the control volume times the enthalpy of the mass at any instantaneous moment.

The quasi-equilibrium evacuation means a change in the mass of the CV during the evacuation, so the differential form of the terms in Equation 2.16 must be utilized.

$$d(mu) = hdm \qquad \text{Equation 2.17}$$

$$mdu + udm = hdm \qquad \text{Equation 2.18}$$

$$mdu = (h - u)dm \qquad \text{Equation 2.19}$$

Equation 2.17 is the differential form of Equation 2.16. Equation 2.18 is the product rule for differentials and Equation 2.19 is an algebraic rearrangement. Thermodynamic equalities are utilized next: $du = C_v dT$ and $dh = C_p dT$ where C_v and C_p are the constant volume and constant pressure specific heats of air as an ideal gas. Both are treated as constant values (not changing over the small temperature range of the VST technique) Substituting into 2.19:

$$mC_v dT = (C_p - C_v)Tdm \qquad \text{Equation 2.20}$$

$$mdT = ((C_p/C_v) - 1)Tdm \qquad \text{Equation 2.21}$$

Introducing another thermodynamic concept; the ratio of specific heats $C_p/C_v = k$ and additional algebraic manipulation then provides:

$$\frac{1}{T}dT = (k-1)\times\frac{1}{m}dm \qquad \text{Equation 2.22}$$

Integrating both sides of Equation 2.22 between the limits of T_1 and T_2, and m_1 and m_2 respectively:

$$\int_{T1}^{T2}\frac{1}{T}dT = (k-1)\int_{m1}^{m2}\frac{1}{m}dm \qquad \text{Equation 2.23}$$

The form {*(1/T)dT*} and {*(1/m)dm*} may be recognized as the integral form of the fundamental theorem of calculus: $ln(t) = \int(1/x)dx$ for t from 1 to t. Invoking this theorem and the logarithm identity rule for the difference between two logarithms; $ln(p) - ln(x) \equiv ln(p/x)$:

$$\ln\left(\frac{T_2}{T_1}\right) = (k-1)\times\ln\left(\frac{m_2}{m_1}\right) \qquad \text{Equation 2.24}$$

Another logarithm identity; $p(ln(x)) = ln(x^p)$ and utilizing the exponential function e on both sides of the equation provides:

$$\left(\frac{T_2}{T_1}\right) = \left(\frac{m_2}{m_1}\right)^{(k-1)} \qquad \text{Equation 2.25}$$

At this point it might be recognizable that as the CV is evacuated and the mass of air in the CV at state 2; i.e. m_2 becomes small, the temperature at state 2; i.e. T_2 must also become small. If the mass term is substituted using the ideal gas law $PV = mRT$ then 3.19 can be written in terms of temperature and pressure. In this case, the volume of the control volume (chamber) is fixed and constant. The universal gas constant is R. The mass at state 1 is rewritten as;

$m_1 = (P_1V) / (RT_1)$ and the mass at state 2 is rewritten as; $m_2 = (P_2V) / (RT_2)$. Making the substitution into the quotient portion of the right hand side of Equation 2.25 and cancelling the reciprocal constants V and R:

$$\left(\frac{T2}{T1}\right) = \left(\frac{P2/T2}{P1/T1}\right)^{(k-1)} \qquad \text{Equation 2.26}$$

Additional algebraic manipulation involving exponent laws to yield a workable equation;

$$\left(\frac{T_2}{T_1}\right) = \left(\frac{P_2}{P_1}\right)^{\left(\frac{k-1}{k}\right)} \qquad \text{Equation 2.27}$$

From Equation 2.27 it can be seen that as P_2 decreases due to the evacuation of the chamber, T_2 must also decrease to maintain the energy balance controlled by the first law of thermodynamics. The assumption was made at the beginning of this derivation that there was no heat transfer to the control volume inside the chamber. Chapter 6 describes the experimental process involved in working with the reality that there was an influential amount of heat transfer from the steel chamber walls to the atmosphere within the evacuated chamber.

The literature had a few references to current research incorporating a combination of vacuum and steam. Yang et al. (2009) used a vacuum-assisted steam stripping technique to extract juglone from the ground bark of *Juglans mandshurica.* Nandanwar et al. (2006) used a single vacuum stage followed by various steam stages to determine which steam stage would best replicate an existing 72 hour standardized boil test in India for plywood wet glue strength. Mellouk et al. (2008) used a technology referred to as: DIC (De'tente Instantane'e Controle'e) and translated as: Instantaneous Controlled Pressure Drop process. The method was used to perform extractions of volatile compounds from red cedar (*Thuja plicata*) for aroma essence. It

begins with wood in a small chamber at atmospheric pressure, the chamber was evacuated, and saturated steam is introduced to a set process pressure and held for the desired process time. A receiving vessel of sufficient size to account for the expanding gas volume from the pressurized chamber (30 times the volume) had been evacuated. At the completion of the steam process time the wood in the pressurized vessel is instantaneous discharged into the evacuated chamber. Rezzoug (2009) used the same apparatus for steam extraction of oil from maritime pine needles. Chen and White (2009) have a provisional patent for the use of vacuum steam technology (VST) for phytosanitation treatments.

No literature was found that specifically discusses utilizing alternating cycles of vacuum and saturated steam for the purpose of achieving a plasticized state within wood for bending. From that perspective the research performed in this work is an original contribution to the state of the art. Chen (2009) had coined the term “VST” for Vacuum Steam Technology for phytosanitation, however the author continued the reference, but as VST for rapid plasticization of maple.

2.8 Summary of Key Principals

Atmospheric pressure steaming of wood that is also at atmospheric pressure is rate limited by thermal conductivity values and diffusion-based moisture movement of bound water (Siau 1995). Because moisture diffusion is slow in wood, the traditional technique for plasticizing wood for bending emphasizes the need to condition wood to the ideal moisture content (20-25%MC, Stevens and Turner 2008) prior to initiation of the steam process. Due to the correct MC established by conditioning, the steaming process need only heat the wood relying on

conductive heat transfer and that estimated steaming rate is about 1.8 min/mm (45min/inch) (Stevens and Turner 2008). For drier wood below 20% the suggested rate is 2.4 min/mm (60min/inch) with more time required as the wood becomes drier (Peck 1957). The additional time is required for diffusion based moisture transport. Air drying requires time and space resources that can be problematic and wood quality may suffer degrade from stains or molds.

Luthiers and other specialty wood workers must often begin with kiln dried wood (Galbreath 2008). Moisture regain to kiln dried material is problematic depending on the thickness of stock. For thicker stock either soaking wood in water or extended steaming is required (Galbreath 2008, Hollandsworth 2010). It was reported that extended steaming can decrease the wood strength (modulus of rupture) (Skaar 1976).

Vacuum Steam Technology is proposed as a method for rapid moisture and heat regain to low moisture content wood (<10%). It has been reported that vacuum can quickly reduce the pressure within the wood due to gas permeability (Sasaki 1987, Chen 1997) such that a sequential addition of steam will produce water vapor bulk flow (WVBF) of moisture deep into the wood (Chen and White 2009). Because WVBF is a fast moisture transport mechanism relative to diffusion (Chen 1997), it is hypothesized that the internal temperature gain due to a preliminary vacuum cycle before a steam cycle will be significantly faster than an atmospheric steamed specimen. If the internal temperature does increase significantly faster due to steam WVBF that implies moisture is distributed quickly and uniformly within the specimen. If both heat and moisture are faster and more uniform, then cycles of vacuum and steam should result in a significant improvement of the plastic-deformable state relative to atmospheric steamed specimens given equivalent treatment times when beginning with low moisture content wood. If

a significant improvement occurs in plasticization then the amount of work to bend VST treated wood should be less than atmospheric steamed wood given equivalent treatment times.

Chapter 3: Common Methods

3.1 Introduction

To address the objectives listed in Section 1.2 and the research hypotheses listed in Section 1.3 the following three Research Area (RA) categories were defined:

- RA #1; Internal Wood Temperature vs. Time
- RA #2; Development of Vacuum Steam Technology for Plasticization of Maple
- RA #3; Work to Bend

The methodology aspects common to all experiments will be covered in this chapter. The three Research Areas shared certain common methodologies and all used the exact same hardware and technology with different protocol for vacuum/steam. A chamber was constructed specifically for the VST process and it is described in detail in Section 3.5; from this point forward any reference to 'the chamber' refers to that hardware system. The specimens are common to all experiments and are described in detail in section 3.3. An introduction to the three RA's will be presented in this chapter but the methods specific to an individual experiment will be described in subsequent chapters:

- RA #1 in Chapter 4; contains experimentation to address Research Hypothesis #1
- RA #2 in Chapter 5; research and development experimentation for VST
- RA #3 in Chapter 6; contains experimentation to address Research Hypothesis #2

3.2 Introduction to the Research Areas

The intent of RA #1 was to test whether the addition of an initial vacuum cycle prior to steam addition would result in a faster rise in internal wood temperature compared to the

atmospheric steamed control. In the treatment experiment maple specimens were placed in the chamber, the chamber was evacuated and then atmospheric pressure steam was introduced. The time required for the internal wood temperature to reach 100°C was recorded. In the control experiment, atmospheric pressure steam was introduced to maple specimens in the chamber, also at atmospheric pressure, and the time required for the internal wood temperature to reach 100°C was recorded. RA #1 should illustrate the effects of the fundamental difference in the mode of heat and mass transfer in the case of evacuated maple. Chapter 4 describes the process of RA #1 in detail and answers Research Hypothesis #1.

The purpose of RA #2 was to establish a sequence of vacuum stages and steam stages which would result in sufficient temperature and moisture gain within the maple to permit bending of the specimen without breakage. Because this experiment was a novel application of cyclic moisture transport phenomena (cyclic vacuum-steam technology; VST), considerable iterative experimentation was required to understand the process. Chapter 5 describes RA #2 in detail.

RA #3 was a comparison of the effort to bend maple specimens treated by the two steaming methods. One set of specimens was treated according to the VST process developed in RA #2. The control specimens were steamed at atmospheric pressure for the same amount of overall time the VST process required. Immediately following the plasticization treatment specimens were placed into a bending mould fixed to a hydraulic compression testing machine and data of force versus displacement was recorded. The force vs. displacement curves generated while bending the maple were used to calculate work to bend and compare the VST treatment vs. atmospheric control. Chapter 6 covers RA #3 in detail and answers Research Hypothesis #2.

3.3 Test Specimens

For all experiments, the wood tested was acquired from a local manufacturer under a request for ‘hard maple’; the pick-ticket listed ‘maple’. The result was a possible mix of hard and soft maple woods. Maple was chosen for two reasons in this proof-of-concept developmental work. First, it is a commonly used wood for luthier applications and second, in the work of Peck (1957) at the USDA-FPL, soft maple ranked 15th (60th percentile) and hard maple ranked 17th (68th percentile) out of 25 hardwoods investigated for suitable qualities in bending, thus presenting a reasonable challenge to the technique under development.

All test specimens were machined to dimensions similar to those used by a local luthier and builder of “Buckeye Banjos”; Greg Galbreath (2010). The dimensions were modified slightly to accommodate the available hardware apparatus for treatment and testing but essentially simulate the bending of one-half of a banjo hoop of radius 152mm (6”). The specified design dimensions were: 533.4mm (21.00”) long, 63.5mm (2.50”) wide, and 4.76mm (0.1875”) thick. The pieces were machined in three different large batch operations. Some dimensional variation undoubtedly occurred as a result of the general lab storage of the specimens; that is to say they were not kept in an environmental chamber for this experimentation. This is in keeping with the realities of niche luthier capabilities for wood storage as well as the desire to demonstrate the robustness of the VST treatment. The moisture content of the specimens did vary (between 4.5% and 10.5%) over the course of the experimentation period. The technique for moisture determination is described later in this section.

Each individual specimen had its length measured in two places and averaged, width measured in four places and averaged, and height measured in six places and averaged. A dial indicator-type caliper accurate to +/- 0.01mm (0.0005”) was used for measuring width and height. A metal scale accurate to +/-0.1mm (0.005”) was used for length. After measuring each of the 163 specimens used in this research, the detail values are shown in Table 3.1:

Table 3.1 Specimen Dimensions

	Length, mm	Width, mm	Height, mm
Average (n=163)	533.6	63.46	4.70
Maximum	534.7	65.02	4.88
Minimum	531.9	62.74	4.47
Standard Deviation	0.45	0.35	0.05
Design Value	533.4 (21.0 inch)	63.50 (2.50 inch)	4.76 (0.188 inch)

Because surface defects from machining and natural grain defects within the wood can adversely affect the bending success of wood (Stevens and Turner 2008, Benson 2008), all specimens were visually graded twice; first by David Jones, Laboratory Specialist Senior and manager of wood shop in the Department of Wood Science and Forest Products at Virginia Tech and again by Greg Galbreath, a banjo luthier. RA’s #1 and #2 did not involve bending the wood; therefore, the goal was to select the best 60 specimens for the actual bending in RA #3 to address Research Hypothesis #2. The grading to select the bending specimens was based on the guidelines suggested in the above references and include: the wood be straight grained with less than 4° slope of cross grain (across the 4.76mm height in this case) less than 4° grain run-out (across the 63.5mm width in this case), clear grain without visible disruptions like knots, ingrown bark, surface checks (cracks perpendicular to the annual rings), shake (longitudinal

grain separation parallel to the annual rings), and decay. In addition, boards with surface defects from the machining process were excluded from the bending sample. The photograph in Figure 3.1 shows four specimens as machined.

Figure 3.1 Completed maple specimens prior to thermocouple insertion. Very close inspection may reveal the pencil grader marks around defects; these were not specimens for bending. Photograph by author 2010.

Whether the required 20-25% moisture content for bending had been attained could only be determined after the steaming portion had been completed via gravimetric methods and oven dry weight determination. The time-lag in determining the effect of treatment was unavoidable. The moisture content of each specimen was determined at three different points during the experimental process. Initial weights were recorded at the time the specimens were

measured (after manufacture); at the time immediately prior to whichever experimental treatment the specimen was in queue for; and immediately after the experimental treatment. At the conclusion of each treatment for RA's #1, #2, and #3, the specimens were placed in a 105°C drying oven to determine the oven dry weight (ASTM D4442-07 Method A). After the dry weight was determined, the moisture content at each of the three points could be determined. All weighing was done with a top-loading Mettler PL300 balance. Based on the dimensions previously discussed, a known moist weight, and the oven dry weight, specific gravity based on oven dry weight at moisture content 'm' was determined. The Wood Handbook (2010) and Siau (1995) define specific gravity, G, for wood specimens as:

$$G = w_o / (V \times \rho_o) \qquad \text{Equation 3.1}$$

Where: w_o= Oven dry mass; kg

V = moist volume; m^3

ρ_o = density of water; 1000kg/ m^3

The specific gravity values determined from Equation 3.1 were variable in the particular moisture content ('m') at which each specimen was measured. As mentioned the moisture content of the specimens varied from 4.5% to 10.5%. To be meaningful, specific gravity values must be at the same moisture content because wood swells with water, changing the dimensions and ergo changing the apparent density or specific gravity. The Wood Handbook (2010) provides a modeling equation whereby wood specific gravity of differing moisture contents can be normalized to a specific gravity based upon the green state, which is considered to be at the fiber saturation point of wood or 30% moisture content. Referencing the Wood Handbook (2010) page 4-9, equation (4-11):

$$G_x = G_b / [1- 0.265G_b(1 - MC_x / MC_{fs})] \quad \text{Equation 3.2}$$

Where: G_x= specific gravity based on volume at moisture content MC_x

G_b= basic specific gravity at green volume (published data)

MC_{fs} = moisture content at fiber saturation point (assumed to be 30%)

Equation 3.2 was rearranged and solved for $G_b = f(G_x)$ to provide:

$$G_b = G_x / [1+ 0.265G_x(1 - MC_x/30)] \quad \text{Equation 3.3}$$

Equation 3.3 was then used to normalize the specific gravity values at the variable moisture content 'm' for each specimen to an approximate corresponding value *as if* the specimens' dimensions had been measured at the green wood volume. These normalized specific gravity values were evaluated and a histogram was produced to illustrate whether the possibility did exist for a mixture of hard and soft maple species.

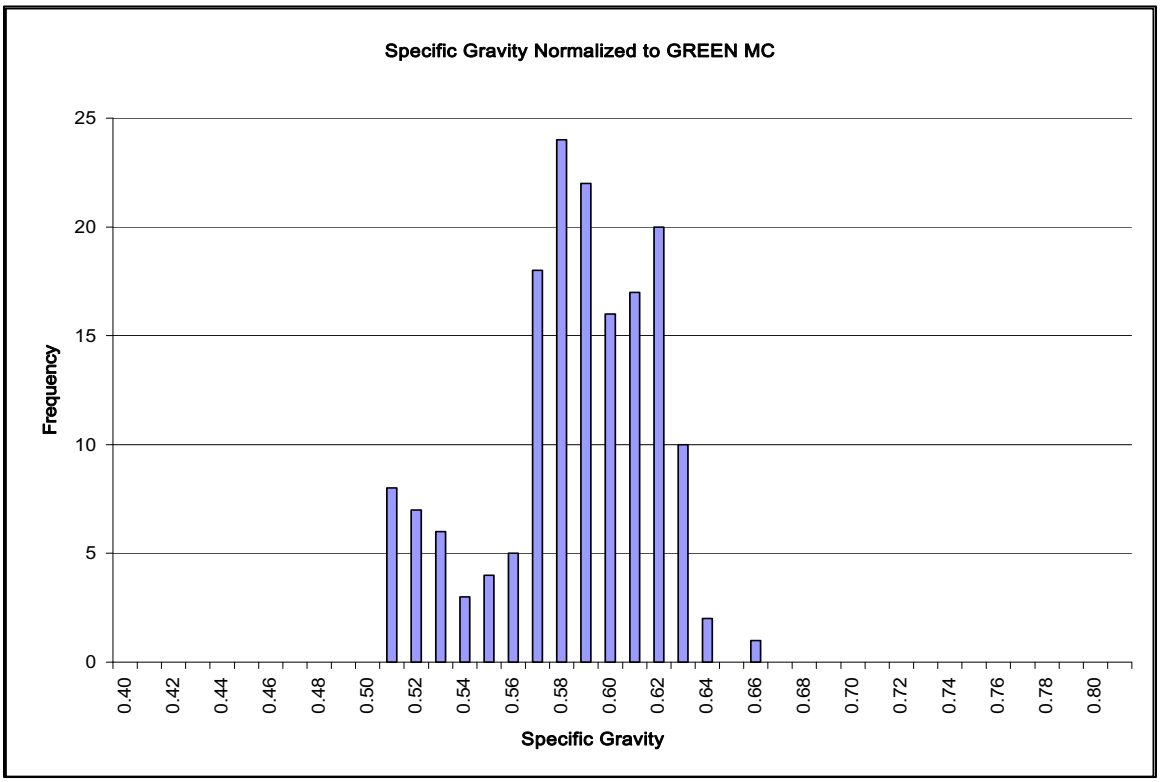

Figure 3.2 Frequency histogram for complete sample of 163 research specimens, showing specific gravity values normalized to 30% moisture content (green volume). By author, 2010

Figure 3.2 seems to indicate the possibility of two density populations. From the data, it is known that 24 specimens comprise the apparent lower density population and of those, 22 were involved with RA #2 and two were in RA #3. The data points are specifically identifiable to the specimen number. Figure 3.3 shows a scatter plot of the individual data points to help illustrate the distribution. In this figure the green triangles toward the left and the two light grey-blue 'x' marks are the lower specific gravity specimens.

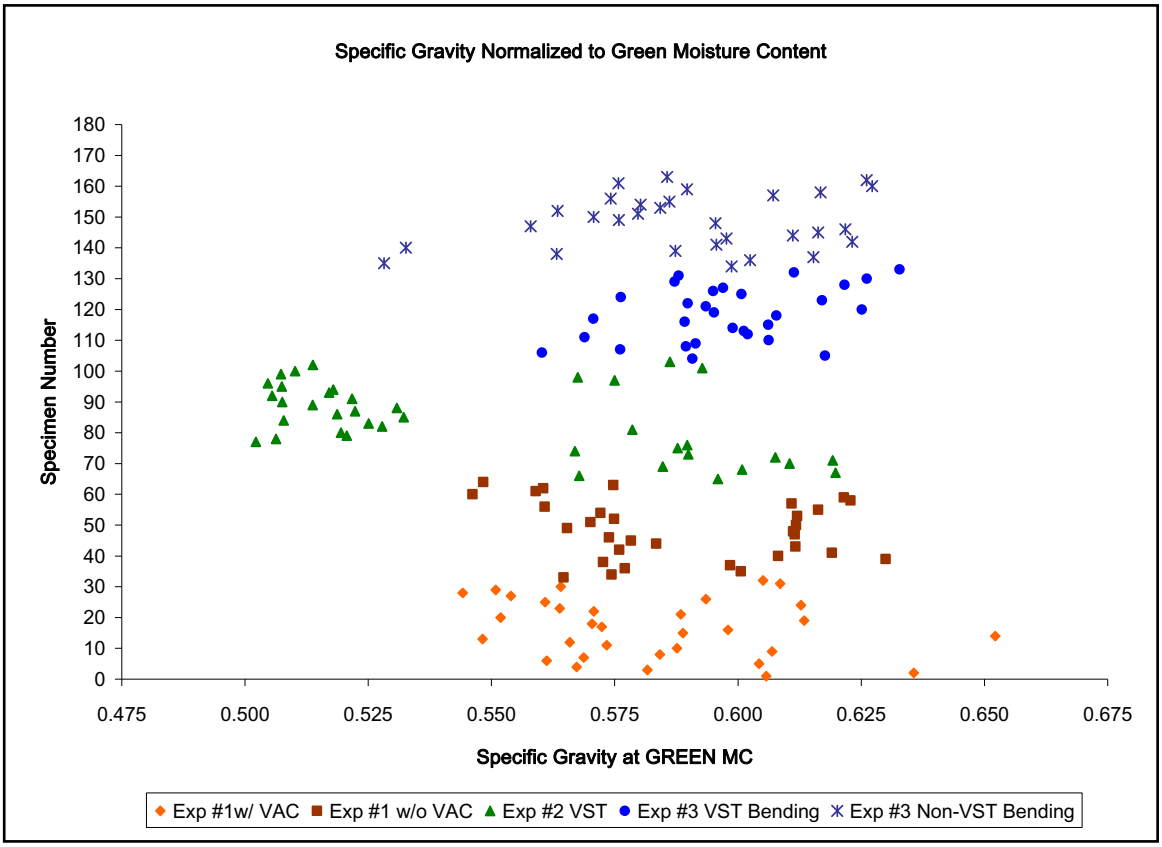

Figure 3.3 Showing individual data points for 163 specimens with specific gravity adjusted to a green volume equivalent for direct comparison. By author, 2010

In the Wood Handbook (2010) two species of soft maples; red and silver, have a green specific gravity statistical value of 0.49 and 0.44 respectively. Two species of hard maples; black and sugar, have a green specific gravity value of 0.52 and 0.56 (with an approximate

coefficient of variance 10%) respectively. This information is a strong indication that all specimens in RA #1 were hard maple, all but two in RA #3 were hard maple, and RA #2 may have been split between hard and soft maple.

From the data the mean for the 24 specimens of apparent low density was compared to the mean of the remaining 139 specimens of apparent high density. Levene's test for heterogeneity of variance was performed and the t- statistic was -10.5, t-Critical two tailed was 1.97 and P=0.001; therefore at alpha = 0.05, unequal variance was used. The two tailed t-test for difference in means of the density samples was significant with a t-statistic of -28.8, t-critical two tailed was 1.99 and P=0.001 therefore at alpha=0.05 the null hypothesis was rejected and Figures 3.2 and 3.3 do indicate two different samples of specific gravity. Peck (1957) made an attempt to correlate bending quality with specific gravity and rate of growth (number of annual rings per inch). He concluded that no correlation was found and the best bending wood was nearly identical to the worst bending wood in both specific gravity and rate of growth. In light of Peck's conclusions it was anticipated that a mix of hard and soft maple would not have a significant effect on the experimental results.

3.4 Common Mechanical System and Data Recording Requirements

The experimentation required hardware (see Figures 3.4 and 3.5) which could provide and control atmospheric steaming and vacuum conditions for variable periods of time and to enable rapid transitions between the two. The chamber, defined as a thermodynamic control volume, had to be adiabatic relative to external environmental conditions so that only the introduction of steam or evacuation would affect the specimens inside.

It was necessary to rapidly measure and record temperatures in the chamber and in the wood, plus the span of time from the initial temperature to the final temperature. Parameters had to be identified which would indicate the beginning and end of treatment in a repeatable fashion with sufficient accuracy for comparison. The internal temperature of the maple was measured using a Type K twisted wire thermocouple inserted into the center (detailed in Section 4.2). A final internal maple temperature of 100°C was the obvious stop point for measuring time to temperature due to the literature supported evidence that around 100°C was optimal.

A challenge arose in determining at what point the timing of the temperature rise should begin. Because the null hypothesis states there is not a difference in time-to-temperature when a preliminary vacuum cycle was utilized, it was essential to begin the timing at *the* point when temperature *could* begin to increase in both the control and the treatment. That is to say, the measured time interval must begin as soon as steam was introduced into the chamber but it was not acceptable to wait until a temperature increase was noticeable via a thermocouple signal to begin the measured time interval. The steam pressure signal was the reasonable solution to this challenge. Pressure within the chamber was measured directly with a transducer attached to the chamber (see Figure 3.4; explained in detail in Section 3.5). Steam used for preparing wood for bending is saturated steam. A change in chamber pressure would be immediately detectable and would provide an immediate indication of when the temperature *could* begin to rise when steam was added.

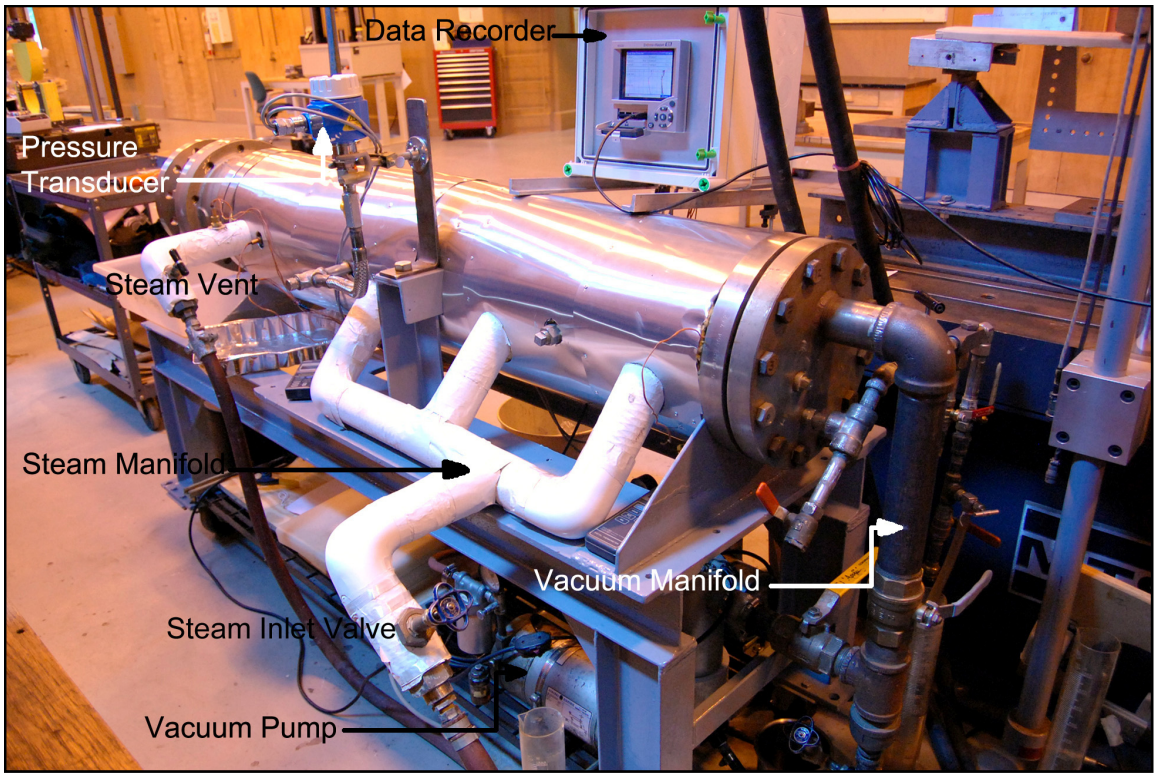

Figure 3.4 Rear 3/4 view of chamber. Image shows steam inlet valve and manifold, vacuum manifold, pressure transducer, steam vent, data recorder, cart and vacuum pumps on shelf. Photograph by author 2010.

3.5 Vacuum Steam Technology (VST) System Hardware Development

A mechanical system was necessary to enable experimentation with moisture transport in wood in a range of pressures from approximately 10 to 130 kPa. Available equipment limitations dictated that minimum pressure would be about 10 kPa. If a higher minimum pressure became important through the development process that would simply be a matter of switching valves (see Figure 3.6). The pressure of 130 kPa corresponded to a maximum saturated steam temperature of approximately 107°C. Though greater than the goal temperature, it will be shown in Chapter 4; Section 4.4.1, that boiler control fluctuation determined the need for a slightly higher maximal temperature so that the average uniform state

temperature was approximately 100°C. The essential components included: a chamber, a vacuum system, a steam generating system, and a data recording system.

The chamber (see Figures 3.4 and 3.5) had to have an easy method of loading and unloading, it had to be resistant to corrosion from steam and it had to have structural integrity for the potential maximum steam delivery from the boiler in the event of a system problem. It was re-serviced from a previous research project and had withstood pressures up to 3.55 MPa and temperatures up to 240 ^{o}C. This was a factor of 4.5 times the pressure that the steam generator was capable of producing The body of the chamber was constructed from a short section of ASME/ANSI B36.19, 152mm (6”) schedule 80 (wall thickness 10.9mm), 304L stainless steel pipe. ANSI B16, class 300, slip-on 316 stainless steel weld flanges were fitted to each end and seal welded in place.

A class 300, full-port 152mm 316 stainless steel ball valve (see Figure 3.5) was fit to one end to facilitate easy loading and unloading of specimens. Three steam inlets were manifold from a single supply, and had been placed near the rear end of the chamber up to approximately half the length of the chamber. The inlet ports were fit into the chamber wall in to produce an entry of steam that was tangential to the interior wall surface. Other 12.5mm (½”) female national pipe thread fittings were welded onto the chamber wall with holes drilled to the inside. These would serve as access ports for thermocouple wires, the pressure transducer signal, and other instrumentation as necessary.

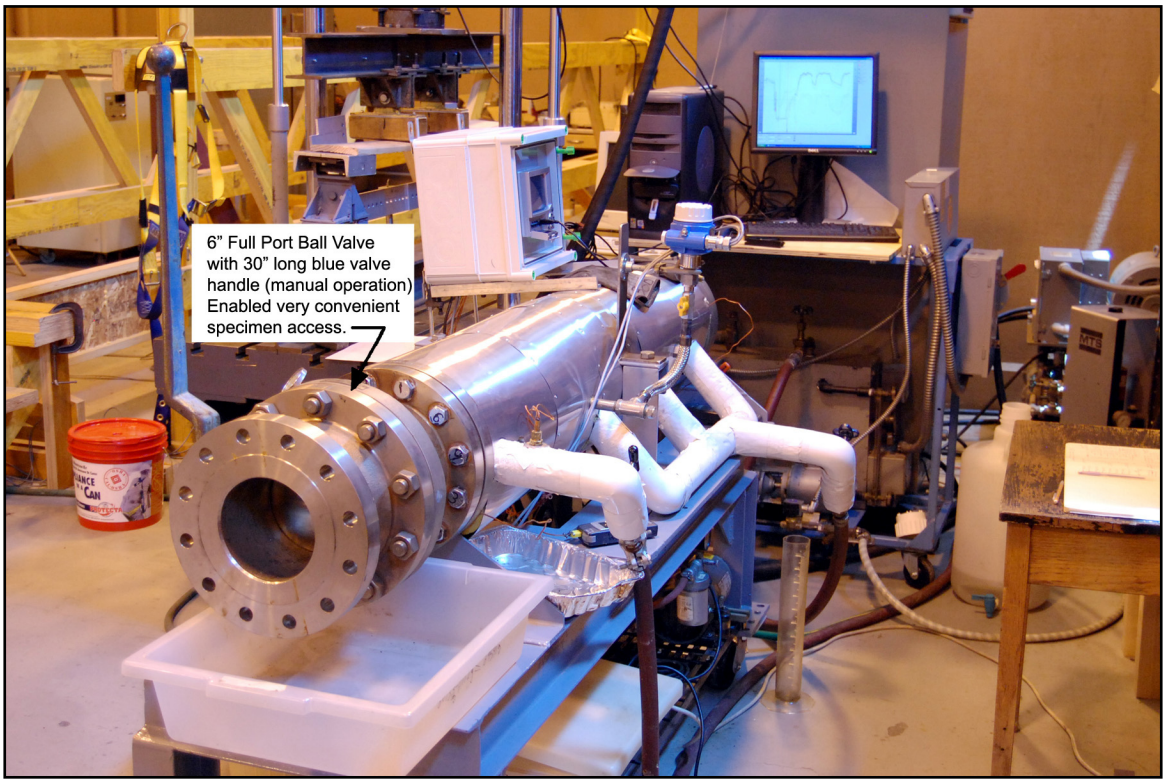

Figure 3.5 Large, six-inch inside diameter ball valve for specimen loading / unloading. Photograph by author 2010.

A class 300 ANSI B16 blind flange (see Figure 3.6) was used on the other end of the chamber because that would enable locating the positions of necessary connections via drilling and tapping holes. The blind flange was fitted with a 50mm diameter vapor vent at the topmost point on the circumference. This vent was piped to the vacuum system and to an optional path to atmosphere with isolation valves to control flow. A liquid drain was fit to the bottommost point on the circumference. This port was piped to the condensate outlet controlled by a disc steam trap in one direction, and to a valve controlled sample port in another direction.

The chamber atmosphere was manipulated by valve position and sequence for all experiments. The valve identification and sequence for switching between vacuum and steam follows (Figure 3.6).

#1: Chamber Drain Valve

#2: Steam Trap Trim Valve

#3: Chamber Vent Valve

#4: Atmospheric Vent Valve

#5: Vacuum Valve

#6: Condensate Collection Valve

#7: Condensate Drain Valve

#8: Condensate Blocking Valve

#9: Steam Trap Blow-Down Valve

#10: Vacuum Vent to Atmosphere (green hose to outside; no valve)

#11: Disc Steam Trap

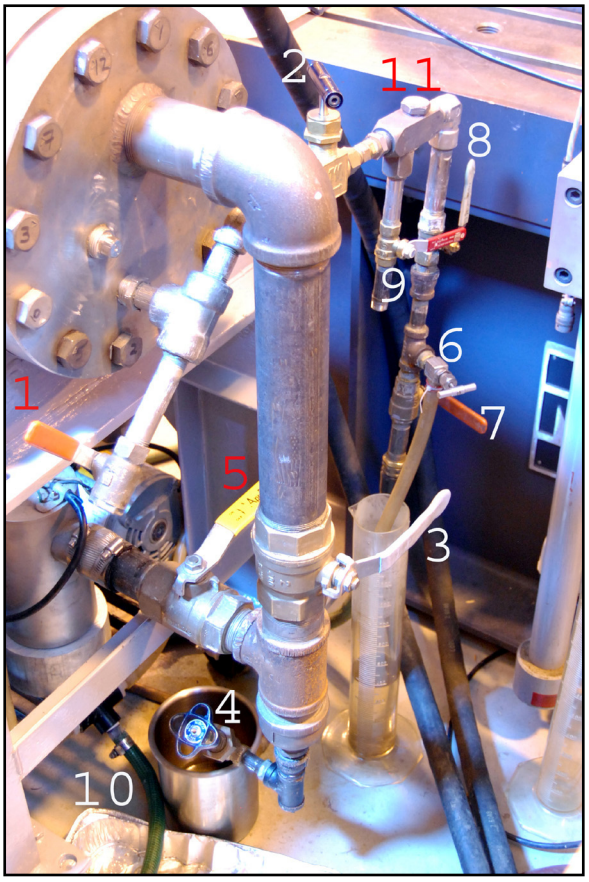

Figure 3.6 Rear view of modified blind flange with pipe and valve configuration. Photograph by author 2010.

Valve Sequencing used in all experiments (referencing Figure 3.6 unless noted otherwise):

Warm-up Phase – steam inlet valve (Fig. 3.4) fully open, steam vent valve open 1.5 turns (Fig. 3.4), steam trap valve #2, valves #7 and #8 fully open; all other valves closed.

Steam Cycle - steam inlet valve (Fig. 3.4) fully open, steam vent valve closed (Fig 3.4), Steam trap valve #2 open to a 45° (see Figure 3.7), #8 and #6 fully open; all others closed.

Vacuum Cycle - steam inlet valve closed (Fig. 3.4), steam vent valve closed (Fig 3.4), steam trap valve #2 (Fig. 3.7) remains open to a 45°, valve #4 open first, then #3 to vent steam, #4 closed and then vacuum valve #5 open.

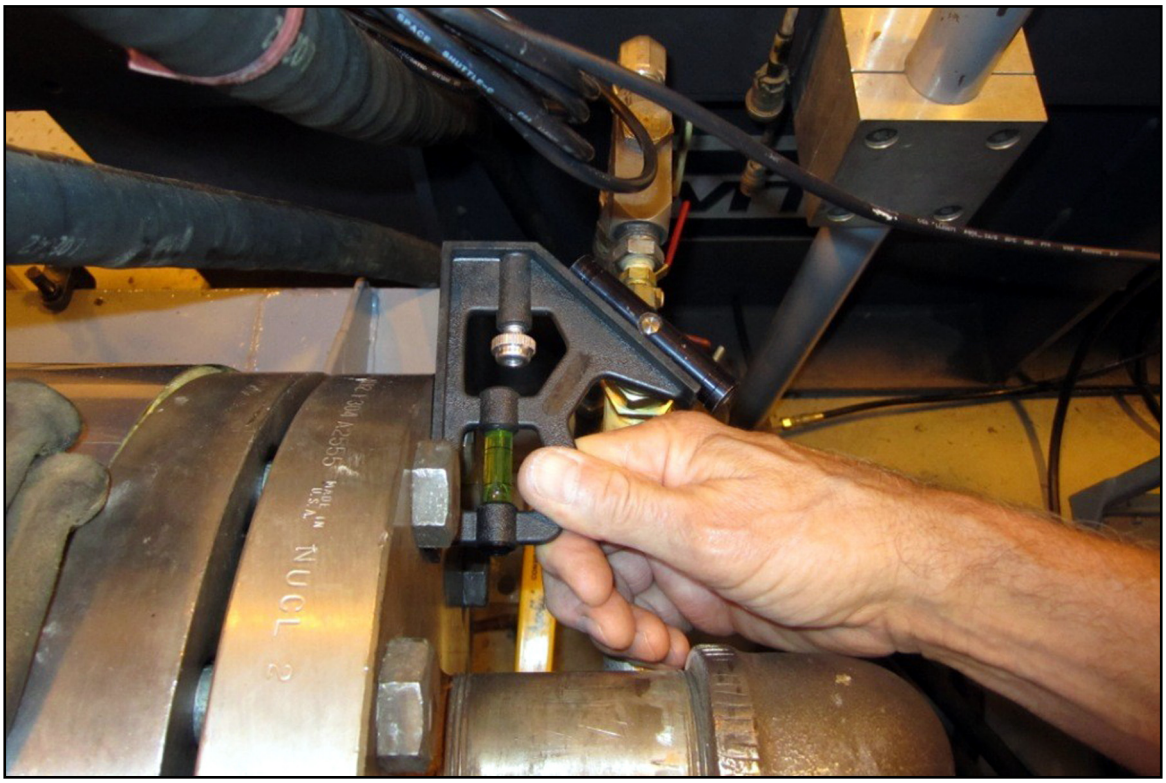

Figure 3.7 Method for steam trap valve trim adjustment (valve #2 in Fig 3.6)
Photograph by Richard Goff, used with permission.

The steam trap trim valve seen in Figures 3.6 (valve #2) and 3.7 above was an embellishment to the system performed between RA's #1 and #2. RA #1 used a 90° turn ball valve carefully positioned to 56° closed (90° = fully closed). During tests the trim (degree of restriction on the inlet to the steam trap) proved to be beneficial in maintaining a saturated relative humidity within the chamber during VST cycles. Chapter 5 elaborates on the details of this performance characteristic of the system.

The entire chamber body was insulated with 75mm dense fiberglass pipe insulation and then covered in a thin aluminum sheet skin to contain the fiberglass and serve as a modest radiant heat return. The chamber itself was fitted onto a structural cart with casters for

maneuverability. A lower shelf (Figure 3.8) provided the location for the vacuum system and specimen storage

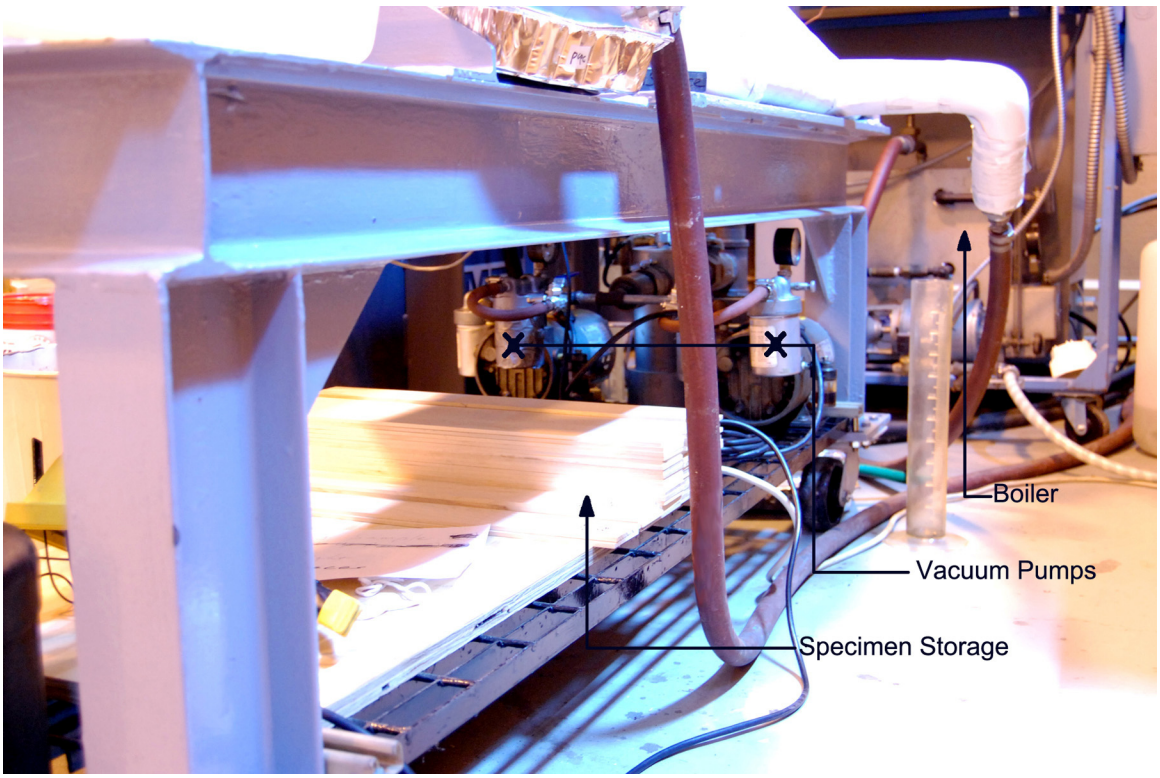

Figure 3.8 Lower shelf showing vacuum pumps indicated with "X", boiler and specimen storage with "←". Photograph by author 2010.

The vacuum system (Figure 3.8) had to be capable of evacuating hot steam at a rate sufficiently fast to minimize radiant heat gain from the hot steel vessel walls to the atmosphere inside the chamber and thence to the wood during the vacuum phase. Any heat gain to the wood during the vacuum phase would increase the potential for evaporative loss from the wood (Chen 1997).

The vacuum system was re-serviced from another research project and that dictated the pump type. Two rotary-vane, oil sealed vacuum pumps each rated (when new) at 0.0015 m^3/s (1.5 liter/s) free air displacement were utilized. The pumps were piped in parallel through a high

capacity molecular sieve bed for moisture separation, up to the topmost vent in the blind flange. Both pumps together could attain a pressure of 10 kPa when pumping down a blanked-off, empty and cool chamber (see Graph 4.1). During the actual conditions of the extended 20 minute vacuum cycles used in RA #1 (with four low moisture content ($<7\%$) wood specimens inside), the chamber would pump down from atmospheric pressure to the minimum pressure in about 30 seconds. The average minimum pressure with wood was about 12 kPa.

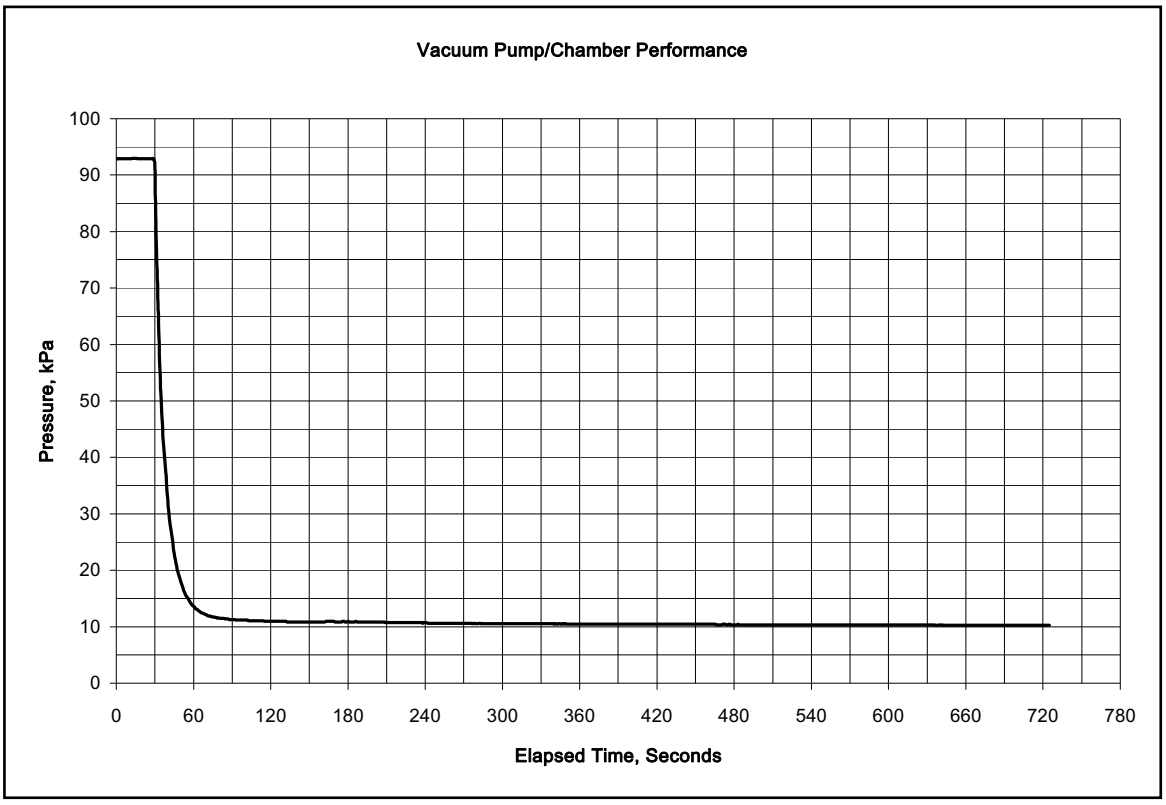

Graph 3.1 Performance curve for both vacuum pumps; empty and cool chamber

The steam generating system was a 15 kW, 785 kPa (100psi) maximum working pressure electric steam boiler manufactured in 1981 by the Electro-Steam Generator Corporation of Alexandria, VA. During preliminary testing the 15 kW power output proved

suitable for a reasonably short (less than 30 minute) warm-up cycle and more than enough to maintain the chamber temperature during the experimental procedures.

The boiler control was a conventional Honeywell “Pressuretrol” diaphragm-based pressure sensor. As pressure within the boiler dropped due to steam usage, the pressure switch would turn on the heater and bring the pressure up to the set point. After some preliminary testing a set point was established that controlled within a narrow range of pressure and temperature around the desired control set point of 101 kPa and 100°C. Following the completion of RA #1 with 11 cumulative hours of steaming conditions, the average chamber pressure was 111.9 kPa with a standard deviation of 1.5. This corresponds to an average saturated steam temperature, based on saturated steam table data, of 102.8°C with a standard deviation of 0.4. The same data was investigated for average chamber temperature. The total cumulative time was 7 hours after the chamber had achieved thermal equilibrium. The average chamber temperature was 103.5°C with a standard deviation of 1.04 (see Table 3.2).

Table 3.2 Cumulative average pressure and temperature for the chamber; RA #1 during Uniform State, Uniform Flow conditions.

Experiment #1 Specimens	USUF Pavg; kPa	USUF Tsat; °C @ Pavg	USUF Tchmbr avg; °C
1 - 4	114.4	103.4	102.3
5 - 8	110.1	102.3	103.6
9 - 12	110.5	102.4	102.7
13 - 16	108.9	102.1	103.1
17 - 20	112.1	102.8	105.3
21 - 24	111.8	102.8	105.9
25 - 28	111.8	102.8	103.9
29 - 32	111.5	102.7	102.9
33 - 36	115.2	103.6	104.1
37 - 40	112.7	103.0	104.1
41 - 44	112.8	103.0	102.9
45 - 48	111.4	102.7	102.3
49 - 52	112.0	102.8	104.5
53 - 56	112.4	102.9	102.7
57 - 60	111.3	102.6	103.4
61 - 64	111.6	102.7	103.0
Average	111.9	102.8	103.5
Std. Deviation	1.5	0.4	1.0

The first temperature column is based on steam table data corresponding to the recorded pressure. The second temperature column is actual recorded data. Agreement between the columns is within 0.68% or about 0.7°C. This is within the accuracy of thermocouples in general. The operating point of 103°C was well within conventional guidelines for stream bending of wood.

The data acquisition system (Figure 3.4 and 3.9) was an Endress and Hauser EcoGraph T (model RSG30-B1B3FEA1) and software. It had five thermocouple inputs, one pressure input, and a data collection rate of 1 Hz to capture the rapid changes during the non-equilibrium portions of the experimentation. There were four specimens tested per run in RA #1, each had a

thermocouple (TC) sealed in place and one other TC was used to measure the chamber temperature for five TC's total. Type K thermocouples were used. The sixth input was for a pressure signal that came from a pressure transducer mounted with direct access to the chamber atmosphere. The pressure transducer was a Cerabar M (model PMP41-RC24P6A11G1) capable of constant monitoring of the chamber pressure from 0.0 to 1.03 MPa. It was calibrated accurate to 0.07% of calibration pressure within the range of pressures used for this research and 0.14% maximum deviation across the full range of capability.

A desktop personal computer was used to interface with the EcoGraph recorder and provided real-time output in the form of a continuous display of all six inputs. The screen was set up with two different ordinate axes; one referenced the chamber pressure and the other referenced one of the five thermocouple inputs. The pressure signal was presented in the form of percent of full range. Since the full range was 1.034 MPa (150 psia), a real-time pressure signal of 5% actually meant 51.7 kPa (7.5psia). The temperature scale was presented in degrees Centigrade. All five thermocouple signals were transmitted simultaneously and were easily distinguishable.

The transducer had to be thermally remote from the chamber and protected from direct contact with steam condensate. During the vacuum cycle, there could not be any steam condensate trapped between the transducer and the chamber as that would affect the pressure influence on the transducer. The author designed a simple installation involving a long-radius 90^{o} angle in the inlet pipe via a flexible braided stainless steel pipe section installed with a slight grade away from the pressure transducer, back toward the chamber.

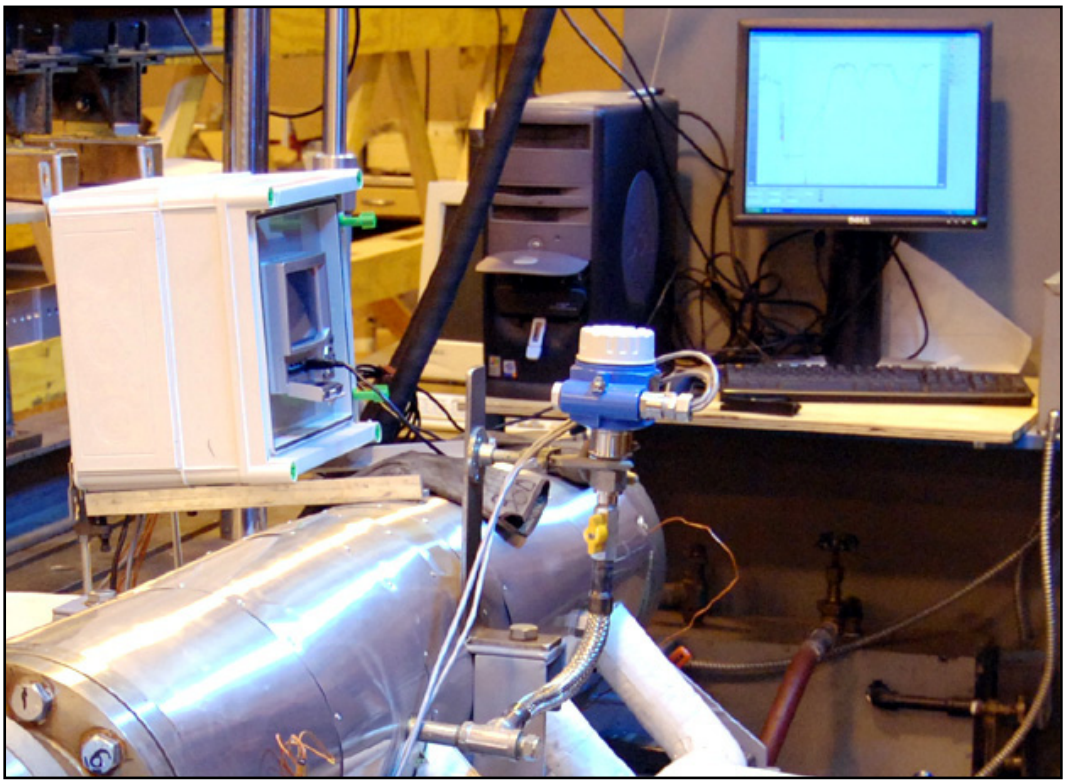

Figure 3.9 Data acquisition system. Image shows data recorder, computer, pressure transducer (blue), and 90° curved stainless steel pipe at bottom center. Photograph by author 2010.

The transition for the TC wires through the chamber wall was accomplished via the ½" NPT threaded couplings welded to the side of the chamber as mentioned above (see Figure 3.10). Approximate 40mm lengths of 9.5mm (3/8") diameter copper tubing were used to make sleeves in which the TC wires were to be sealed for vacuum and steam containment. The copper tubing was readily adapted to common tubing and pipe hardware that permitted leak-tight connections to the welded couplings.

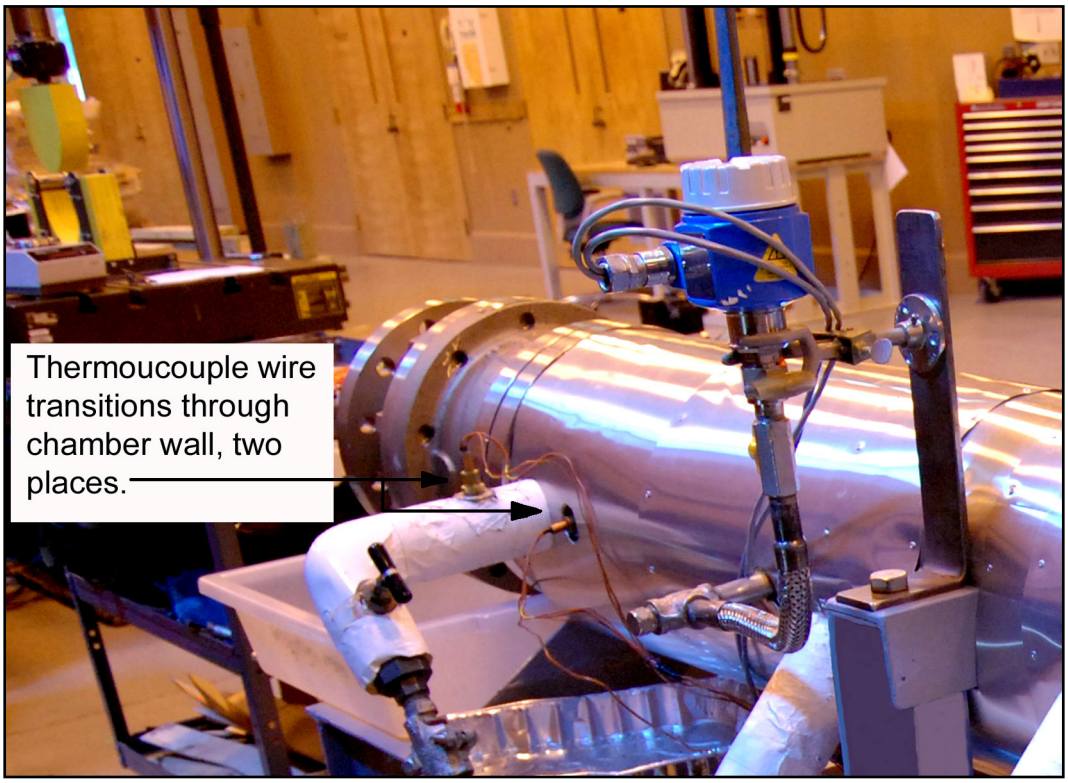

Figure 3.10 Thermocouple transitions through chamber wall in two places. Photograph by author 2010.

The TC wires were sufficiently long on the inside of the chamber to allow them to both reach the end of the chamber when the maple specimens were in place and to reach out through the entrance valve for connection to the maple specimens when loading (Figure 3.11). The wires were initially sealed into the copper tubing with high temperature copper-compounded silicone sealant; second generation transitions used a high temperature, two-part epoxy. The change is described in greater detail in Section 4.4.2.

The TC wires mounted through the chamber wall were fit with thermocouple mini-plugs. This allowed the pre-assembly of multiple maple specimens with short sections of TC wire sealed in place and a mating mini-plug. Some questions regarding TC installation were

addressed during testing and will be discussed in greater detail in Chapter 4. Thermocouples were used in this fashion for Experiments #1 and #2.

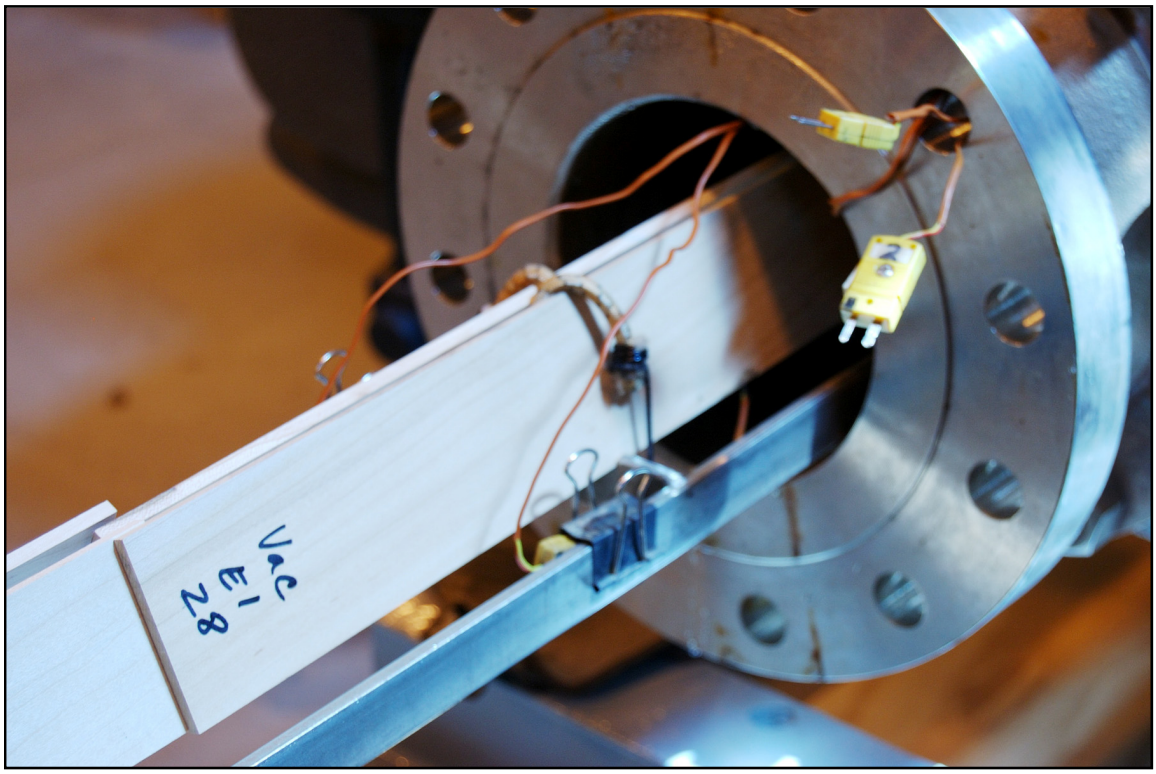

Figure 3.11 Thermocouple connections. Image shows wires from within chamber connected via mini-plugs to the thermocouples sealed inside of the maple specimens (see Figure 4.1 next chapter). Photograph by author 2010.

Chapter 4: Internal Wood Temperature vs. Time

4.1 Introduction to Research Area #1

The intent of RA #1 was to test whether the addition of an initial vacuum cycle prior to steam addition would result in a faster rise in internal wood temperature compared to the atmospheric steamed control. It should provide empirical evidence that would support the theoretical concepts presented in Section 2.6 and Figure 2.10 which shown the calculated difference between diffusion and Water Vapor Bulk Flow (WVBF) of approximately two orders of magnitude (Chen 1997). Preliminary experimentation was performed to determine an appropriate thermocouple sealant material and an analytical technique to quantifiably demonstrate whether a difference in the time to temperature metric did exist between the treatment and the control groups.

System limitations not realized during development of the methodology resulted in deviations from the original experimental plan during execution of the plan which addressed Research Hypothesis #1. The limitations are discussed in this chapter and the outcomes of the deviations from the experimental plan were not detrimental to a successful determination of Research Hypothesis #1.

4.2 System Limitations

Three limitations of the system were recognized at different points during experimentation. One had been mentioned in Section 3.6; the control for the boiler system had an oscillation resulting in a uniform state pressure fluctuation. A second concerned the selection of sealant material part of the way through experimentation with the statistical sample. A third was recognized after studying graphs from the maple which had been processed through the

experimentation designed to address RA #1. The problem came from heat gain to the vacuum treated boards during the 1200s vacuum cycle. Following a vacuum cycle those specimens began the steam cycle hotter than the atmospheric specimens. While the discussion of these limitations incorporates specific experimental results, the system limitation discussion should not be confused with methodology, results and conclusions that follow later in the chapter.

4.2.1 Steam Pressure Limitations

The steam pressure was not constant and therefore the temperature was not constant at any time. This was due to the type of control on the boiler output; an industry typical diaphragm actuated normally closed switch. The controller turned the boiler heater on when the diaphragm indicated a low pressure condition and turned the heater off when the upper set-point pressure was reached via movement of the pressure diaphragm. The resultant pressure delivery was constantly changing about a narrow differential pressure and the graph of this somewhat resembles the teeth of a saw blade. The temperature is a dependent property of pressure and so it was constantly changing about a narrow differential as well. It was important to understand how this constant flux would affect the uniform state of the chamber, and so an experiment was performed with an empty, pre-heated chamber and the bare (or neat) thermocouple junctions were secured to the rack in a manner which approximated their position as if they were inside a wood specimen. That experiment is shown in Graph 4.1.

The extremely tight cluster of temperature signals indicates consistency. The temperature traces for TC's 2, 3, 5, and 6 were looked at individually and compared to the chamber temperature. From those graphs it was possible to determine the average temperature during the uniform state of boiler pressure oscillation, from time = 2000 seconds to the end of

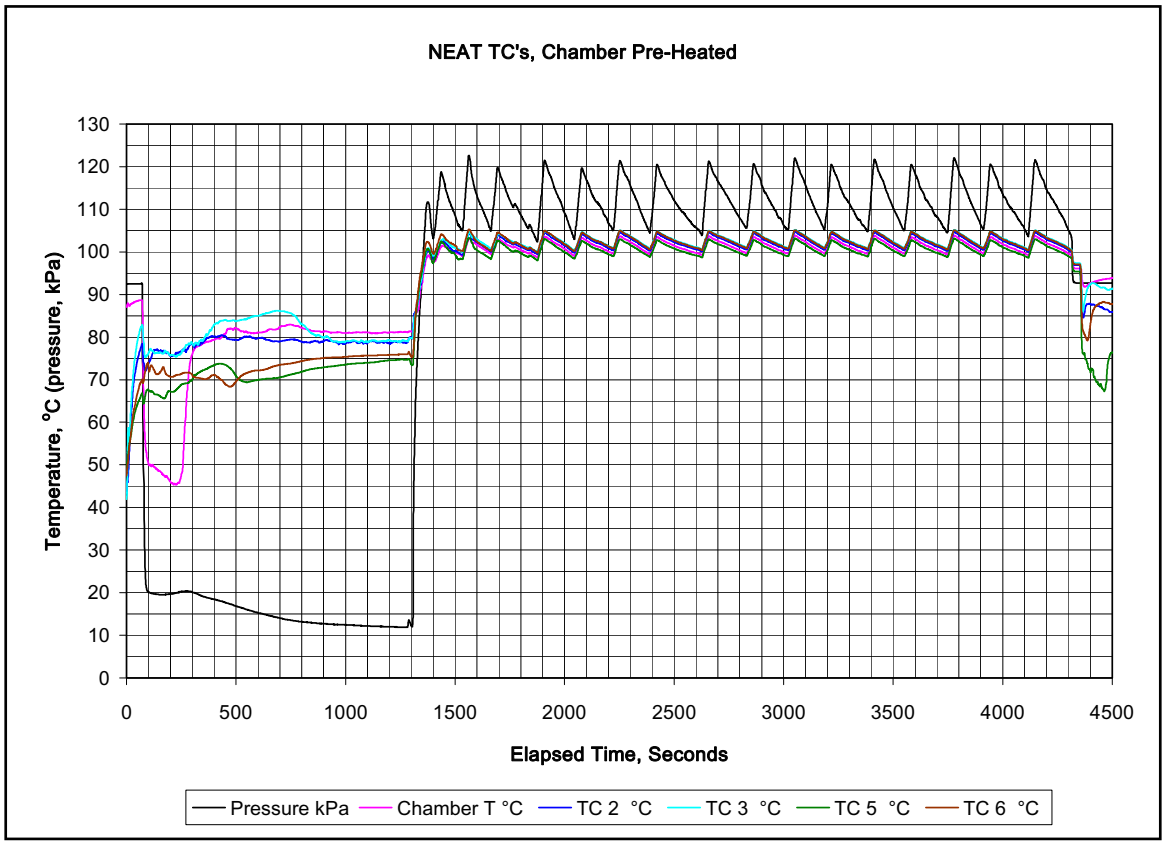

Graph 4.1 Showing the pressure and temperature signals characteristic of the system

the experiment. The chamber pressure and temperature were compared to published saturated steam table data, Table 4.1:

Table 4.1 Uniform state pressure and temperature values characteristic for Graph 4.1

$P_{chamber}$ = 113.1kPa	TC #2 = 102.5 ˚C
$P_{saturated}$ = 109.7kPa @$T_{average}$ = 102.2 ˚C	TC #3 = 103.0 ˚C
$T_{average}$ = ($T_{chamber}$+TC#2+TC#3+TC#5+TC#6) / 5	TC #5 = 101.0 ˚C
$T_{chamber}$ = 101.7 ˚C	TC #6 = 103.0 ˚C

There was a small discrepancy between the thermocouple readings, ranging from 101˚C to 103˚C. For manufactured type K thermocouples the accepted tolerance is ∓ 1.5˚C and the

twisted wire thermocouples met that tolerance (http://en.wikipedia.org/wiki/Thermocouples, accessed 8-March, 2010). The graph below is typical of the four used to aid in determining chamber performance for RA #1.

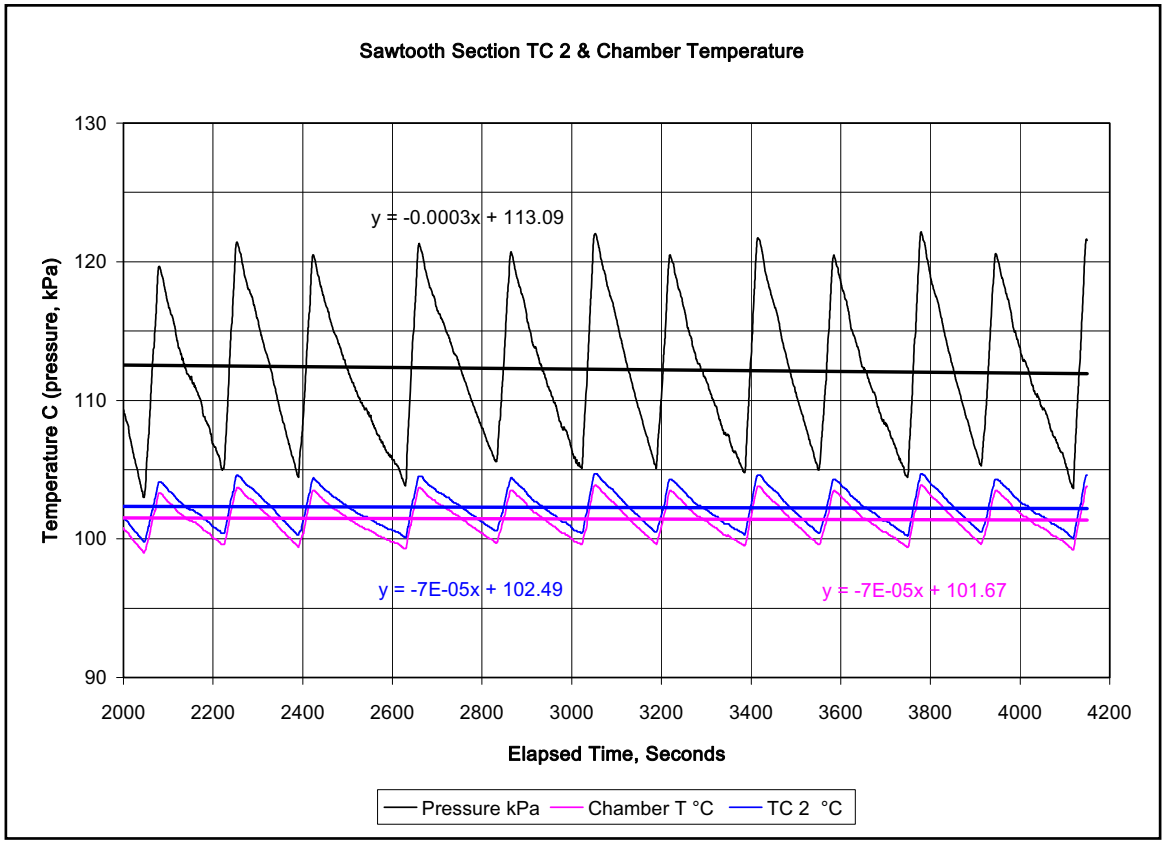

Graph 4.2 Showing expanded scale image of uniform state chamber operation

The trend lines and line equations are color-coded to identify the signal traces to the corresponding measurement location. The equation is written in the point-slope form of:

$$y = mx + b \qquad \text{Equation 4.1}$$

Where: y = ordinate axis value (pressure or temperature)

m = slope of the line

x = abscissa axis value (elapsed time)

b = y-axis intercept

The slope for all three trend lines (pressure, chamber temperature and TC temperature) is essentially zero indicating a horizontal line. At the condition of uniform state, one would expect the average of the oscillations to be a constant and this graph demonstrates that. The ‘b’ value or y-axis intercept is the uniform state, i.e. average of the oscillations, for the corresponding variable. Graph 4.2 indicates the uniform state pressure for the neat TC test experiment to be 113.09kPa, the uniform state chamber temperature to be 101.67°C, and the uniform state for the neat TC #2 temperature to be 102.49˚C (significant to one decimal point). Because the author was curious about the effect of constant fluctuation over extended periods of time, the data for all specimens 1-64 addressing Research Hypothesis #1 were looked at in the portion of the graph where uniform state had been attained. This data is presented in Results, Section 4.4. Ultimately, the differences were very minor and considered negligible.

4.2.2 Sealant Limitations

The vacuum phase was the treatment being tested; therefore, it was necessary to have confidence that sealant around the thermocouple wire in the specimen would block the effects of the chamber atmosphere during experimentation. The sealant had to prevent the thermocouple hole from being evacuated. If the hole around the wire leaked under vacuum, it would also leak under steam. If steam were permitted to leak into the evacuated thermocouple hole a false rate of temperature rise would result relative to temperature gain due to steam permeating into the wood via the anatomical pathways.

Preliminary testing was performed to determine an appropriate sealant material. Four sealant materials were tested with one cycle of vacuum and steam: A) High temperature silicone vacuum grease, B) Oatey high pressure pipe joint compound, C) Permatex High-Temp silicone gasket maker, and D) Permatex Ultra Copper high-temp silicone gasket maker. Four pieces of maple, each with a different sealant around the TC wire, were placed in the chamber and the TC mini-plugs were connected. The chamber was evacuated for 15 minutes and then steamed for a 25 minutes. The data recorded were inspected for differences in the rate of temperature rise at the onset of steam, and the sealant was visually inspected for deterioration. Both silicone sealants were much slower to gain temperature than either of the other sealants. It was concluded that both silicones were better suited than the vacuum grease and the pipe joint compound. Graph 4.3 shows the results of this preliminary test.

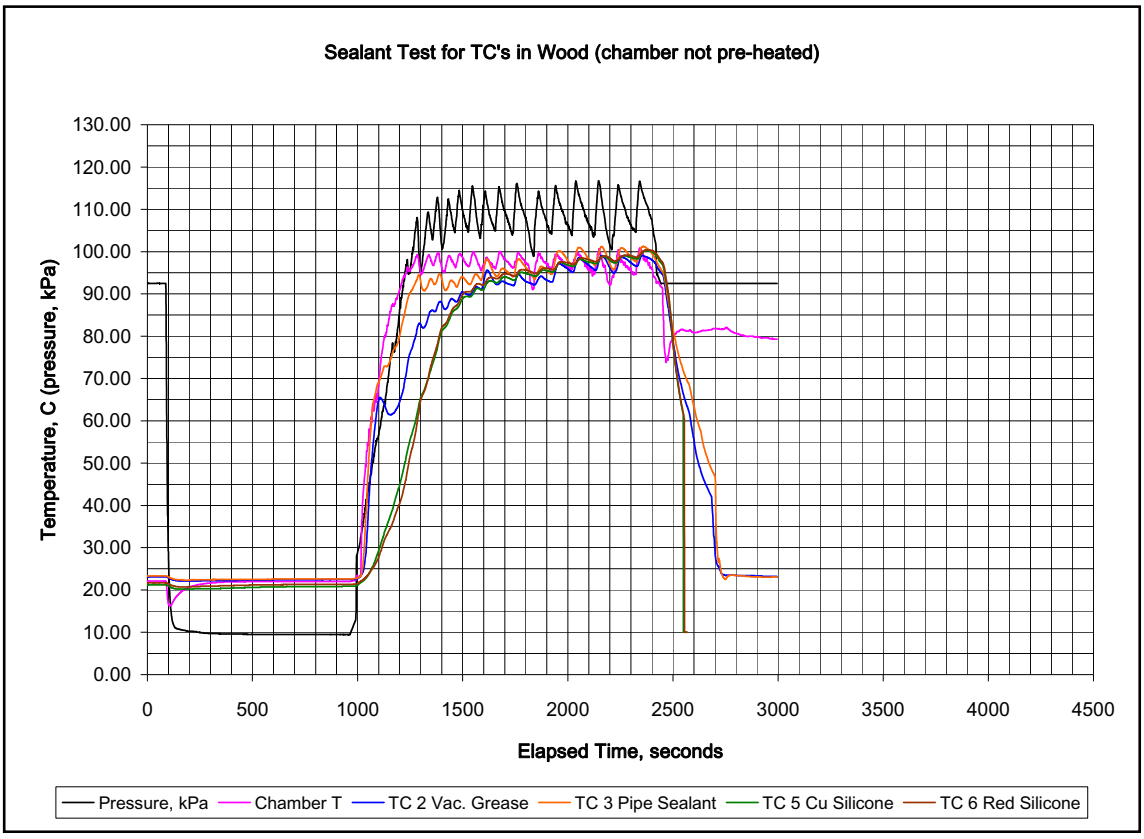

Graph 4.3 Showing results to determine sealant type for actual experimentation.

In following the black trace for the chamber pressure in Graph 4.3, at the beginning of the experiment (far left on the trace) it displays the local atmospheric pressure (at about 600m above sea level) of 94 kPa. Vacuum is applied and the chamber pressure reduced to about10 kPa in about 100 seconds. The low pressure was held for an extended period to lower the internal pressure of the maple. After 900 seconds or 15 minutes, the vacuum was shut off and steam was introduced at the elapsed time of 1000 seconds. Immediately after the steam valve was opened the chamber pressure began to rise, as did the chamber temperature. Both of these traces are virtually on top of each other. This would be expected because they registered the properties of saturated steam in the chamber without restriction to the instrument sensors. Also the scales on the ordinate (Y) axis are 0-100°C and 0-100 kPa; they are the same.

The slopes of the temperature traces of TC 2 and TC 3 had a fast temperature response to the steam addition which essentially followed on top of the chamber temperature. The implication is that the sealant had probably leaked around the TC wire and permitted an opening for steam penetration directly to the thermocouple junction in the center of the specimen.

When comparing the traces for TC 5 and TC 6 to those of TC 2 and TC 3, the slope is noticeably shallower for both of the silicone sealant materials. The implication is that the hole was sealed and the thermocouple junction inside of the specimen responded to steam permeating through the maple. The conclusion was that either silicone sealant should work for the actual Research Hypothesis #1 experimentation. Both silicones were rated for continuous use up to 316°C, but upon verifying the chemical composition of them the red silicone was an acetic acid based solvent system and the ultra copper was based on a formulation which did not require acetic acid and was not corrosive (an oxime based solvent). The absence of acetic acid

was important because acetic acid in the sealant might result in some interaction with certain chemical constituents in the maple (acetyl groups on the hemicellulose) in the vicinity of the TC, potentially causing micro-exothermic reactions and erroneous temperature readings (Frazier 2010). The Copper Silicone sealant was selected. The same sealant was used to seal around the thermocouple wires in the transitions through the chamber wall.

Despite the evaluation process the sealant did fail in the chamber transitions for the TC wires during the first experiment with specimens 1-4. This test included a vacuum stage before they were steamed. During the steaming stage of this experiment the Permatex® Ultra-Copper silicone sealant used on the TC wires through the chamber wall developed visible leaks of steam in the transition ports. This occurred after a cumulative exposure to a 100°C (∓2.5°C) saturated steam environment of five hours. This time included several system tests in addition to the first experimental run. The sealant failure occurred despite being rated to operational temperatures a factor of three times higher than the temperature of experimentation. The silicone-sealed ports were removed from the chamber and new ones were built using a waterproof high strength two part epoxy rated to working a temperature of 121°C (Devcon “plastic steel epoxy” product # 62345). The epoxy ports were installed and performed without any visible evidence of leakage for the duration of experimentation; approximately 62 hours of cumulative time exposed to the saturated steam environment during three different experiments.

The steam leak through the silicone-sealed transition port in the chamber raised the question of whether the silicone seal between the maple and the thermocouple wire in the research specimens might have leaked. The result was the choice to change the sealant used for the thermocouple wires in the maple specimens. The change occurred at the mid-point of the

sample so that specimens 1-16 and 33-48 (treatment and control, respectively) were sealed with silicone and specimens 17-32 and 49-64 (treatment and control, respectively) were sealed with epoxy (Devcon “plastic steel epoxy” product # 62345).

4.2.3 Temperature Limitations

The 1200s vacuum stage specimen tests in the hot chamber (about 85-100°C) gained sufficient radiant heat that the internal maple temperature could drift up to an average temperature of 63-64°C; before any steam had been introduced. In contrast the control group of specimens 33-48 had an average temperature immediately prior to steam addition of 41°C. It was not clear what effect the difference in wood temperatures would have on the elapsed time to achieve the design temperature of 100°C.

To address the temperature differential it was decided to change the non-vacuum procedure for specimens 49-64. The change would permit the non-vacuum treated specimens an equivalent amount of time resting in a pre-heated, atmospheric pressure chamber prior to the introduction of steam for a time period equal to the vacuum period, or 1200 seconds (20 minutes).

A wood temperature anomaly occurred with some specimens regardless of sealant type. Thermocouple readings inside of the maple specimens were greater than the chamber temperature. It had been shown in Table 4.1 that the thermocouple performance was within standards for this instrumentation. It was hypothesized that a micro-climate, similar to Frazier’s (2010) micro-exotherm theory developed within the void area occupied by the thermocouple that resulted in temperatures within the wood at uniform state registering higher temperatures than the steam within the chamber. The following two graphs (4.4 and 4.5) depict this phenomenon.

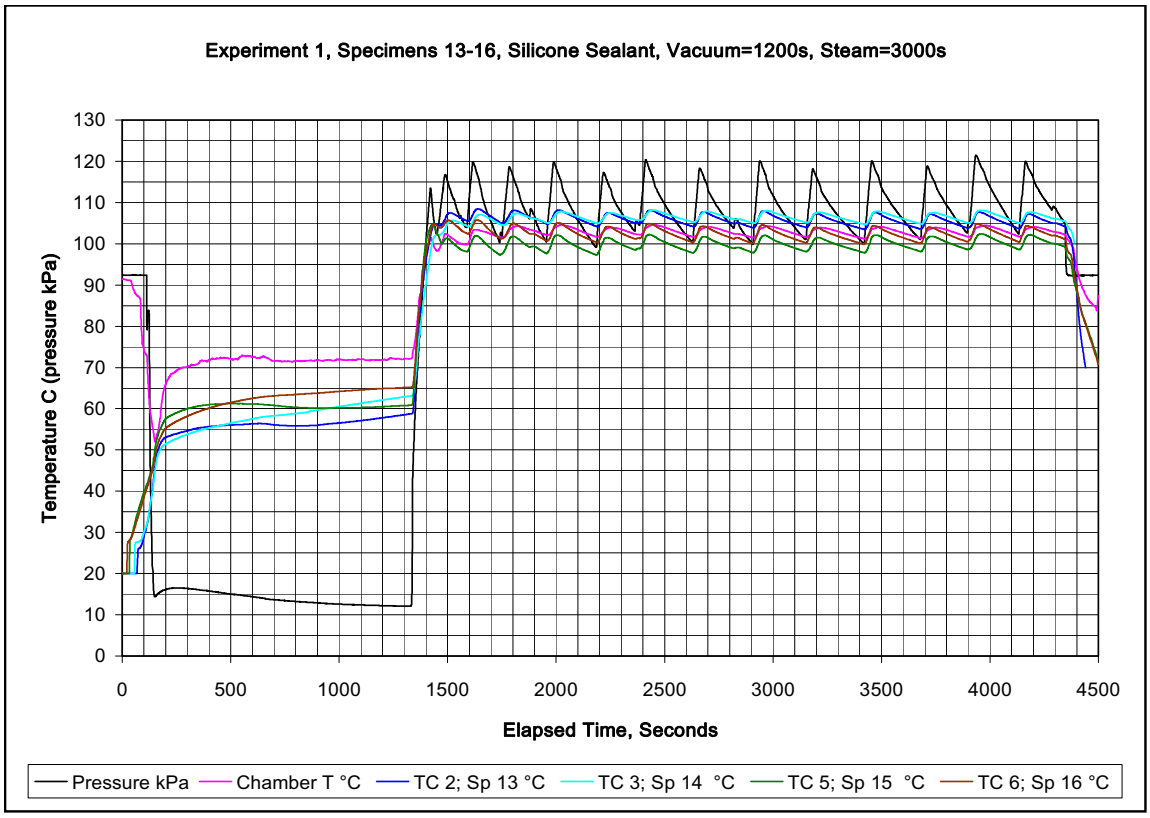

Graph 4.4 Showing TC readings in wood with 20 minute vacuum and 50 minute steam cycle

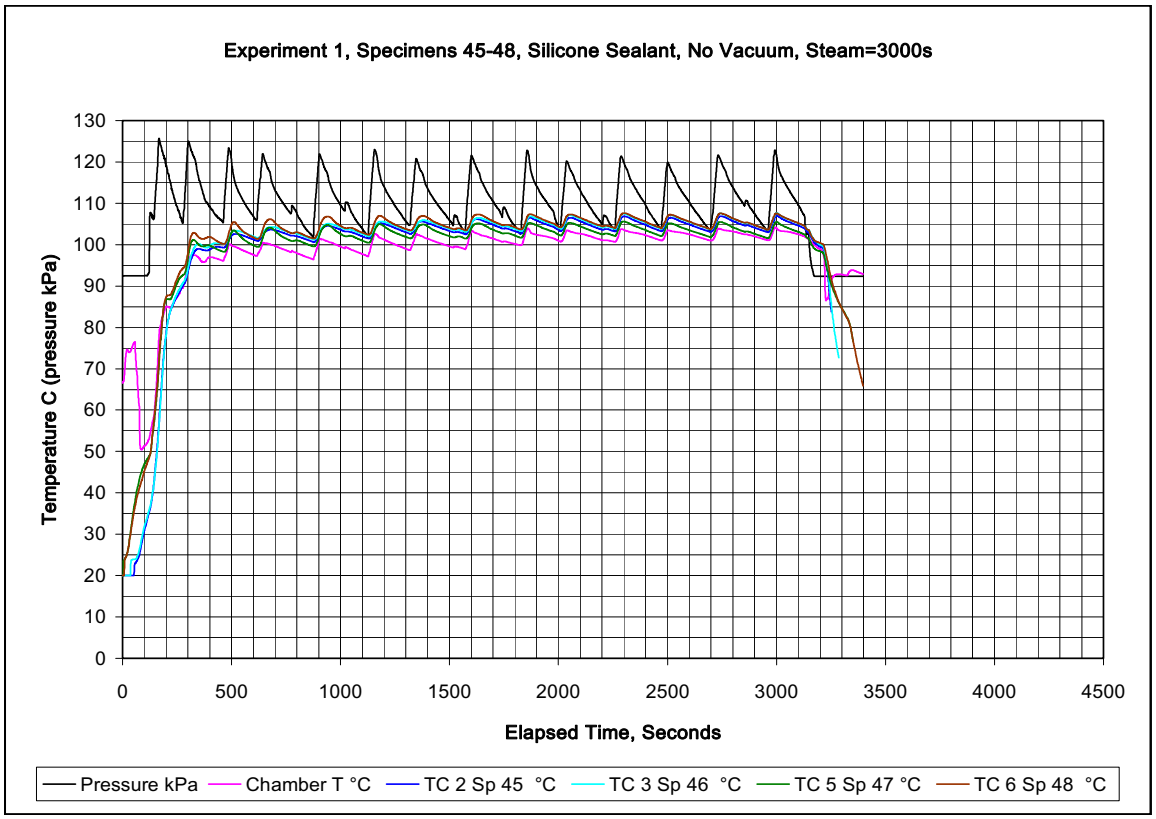

Graph 4.5 Showing TC readings in wood without vacuum and a 50 minute steam cycle

Graph 4.4 is representative of all graphs for the vacuum treated sample. Graph 4.5 is representative of all graphs for the atmospheric steamed sample. These two graphs will be referenced in the next section.

4.3 Methodology

- Research Hypothesis #1: There is not a difference in the time required (elapsed time) to attain the goal internal wood temperature due to a preliminary vacuum cycle relative to the classic process of atmospheric steaming when beginning with low moisture content (<10%) maple.
- Alternate Hypothesis #1: There is one technique which is faster than the other.

To evaluate Research Hypothesis #1 the treatment experiment placed maple specimens in the chamber, the chamber was evacuated, then atmospheric pressure steam was introduced. The elapsed time required from the moment the steam was introduced until the internal maple temperature to reach 100°C was recorded. In the control experiment atmospheric pressure steam was introduced to maple specimens in the chamber, also at atmospheric pressure, and the time required for the internal maple temperature to reach 100°C was recorded. One vacuum/steam cycle would be used to avoid the possibility of cumulative changes in maple superficial gas permeability during multiple steam cycles as mentioned in Section 2.4.

Sixty-four maple specimens comprised the experimental sample for Research Hypothesis #1. The boiler setting was held constant and essentially identical steam cycles were administered to each specimen. Thirty-two specimens were steamed with an initial vacuum step and 32 were steamed without a vacuum step. The methodology is shown in Table 4.2.

Table 4.2 Research Hypothesis #1, Internal Wood Temperature vs. Time Experimental Plan

Internal Wood Temperature vs. Time: Temperature ≅ 100˚C	
Treatment; With Vacuum Cycle	Control; Without Vacuum Cycle
Single vacuum phase applied to maple specimens prior to steaming phase. a) Weigh each specimen immediately prior to placing into chamber. b) Pre-heat chamber to testing temperature and hold at temperature (T) c) Vent steam from chamber, open to atmospheric pressure, add specimens, close chamber. d) Begin evacuation of chamber and simultaneously begin timed cycle for vacuum phase. Maintain vacuum phase for 1200sec. e) At time = 1200sec., Isolate vacuum and immediately add steam to chamber. Record time required to attain the 100^{o}C internal temperature. e) Continuous steaming to investigate performance characteristics of the VST chamber in treating maple. f) Weigh each specimen immediately after.	Maple specimens subject to steaming phase from ambient pressure. a) Weigh each specimen immediately prior to placing into chamber. b) Pre-heat chamber to testing temperature and hold at temperature (T) for time (t) ≅ 10 minutes. c) Vent steam from chamber, open to atmospheric pressure, add specimen(s), close chamber. d) Immediately add steam and simultaneously begin timing. Record time required to attain the desired internal temperature. e) Continuous steaming to investigate performance characteristics of the VST chamber in treating maple. f) Weigh each specimen immediately after.

The specimens used in research area #1 required holes drilled into the center of the specimen for thermocouples to monitor internal wood temperature during experimentation. A jig was made to support the specimens on their narrow edge at a 90° angle to a drill press platform. The jig also ensured each specimen was drilled in the same location; at the center of the longitudinal axis and at the center of the thin 4.76mm face. A #44 size drill (2.18mm) was

used to make a hole to the center across one-half of the width; approximately 31.5mm deep. A drill stop was used to ensure the hole stopped in the center of the transverse dimension. The diameter of the hole *just* permitted the insertion of the individually insulated Type K thermocouple wires with the outer sheath removed. The thermocouple junction was formed by removing the individual insulation from the final 5mm of each thermocouple wire and tightly twisting the ends together with pliers and a small vice. The remaining two-wire insulated portion was super-glued together to add rigidity during insertion of the thermocouple to the end of the hole. Sealant was placed around the insulated wire portion upon insertion to block out the effects of the chamber atmosphere during testing such that the thermocouple was only affected by transport mechanisms through the maple. Figure 4.1 is a cut-away model of the placement and sealing of the thermocouple wire.

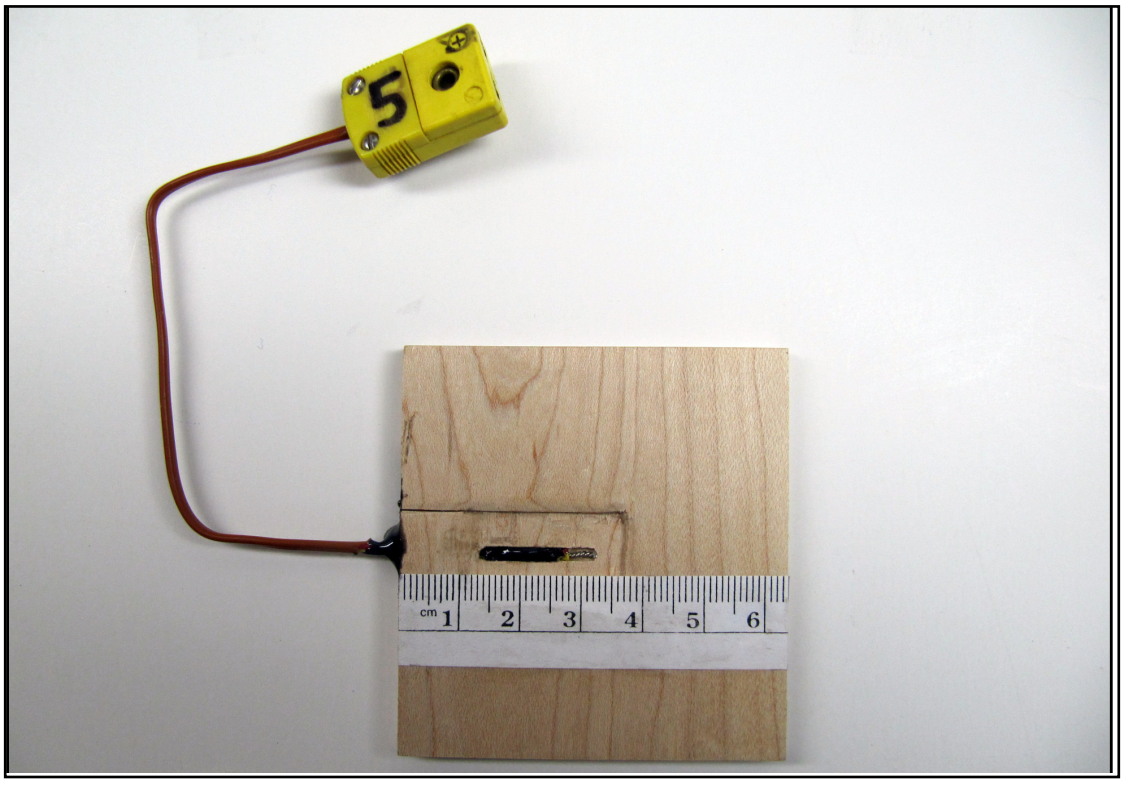

Figure 4.1 Cut-away model of thermocouple location and sealant. By author 2010.

Figure 4.2 shows four specimens with thermocouple wires inserted and quick-connect plugs installed on the wires. The arrangement of Figure 4.2 is typical of all specimens for RA #1 (and RA #2)

Figure 4.2 Specimens for Research Hypothesis #1 showing thermocouple placement Photograph by author 2010.

The quick-connect mini-plugs in Figures 4.1 and 4.2 were used to connect with mini-plugs on the ends of the thermocouple wires which were permanently sealed in transition ports through the wall of the chamber and then directly to the data recorder. Figure 4.3 shows four specimens during loading, mounted on a shelf for support of the maple specimens. The shelf was welded together from 316 SS bar stock. Four wires can be seen coming out of the chamber with mini-plugs and in position waiting for the specimens to be moved further into the chamber prior to connection of the thermocouple wires (also seen in Figure 3.11).

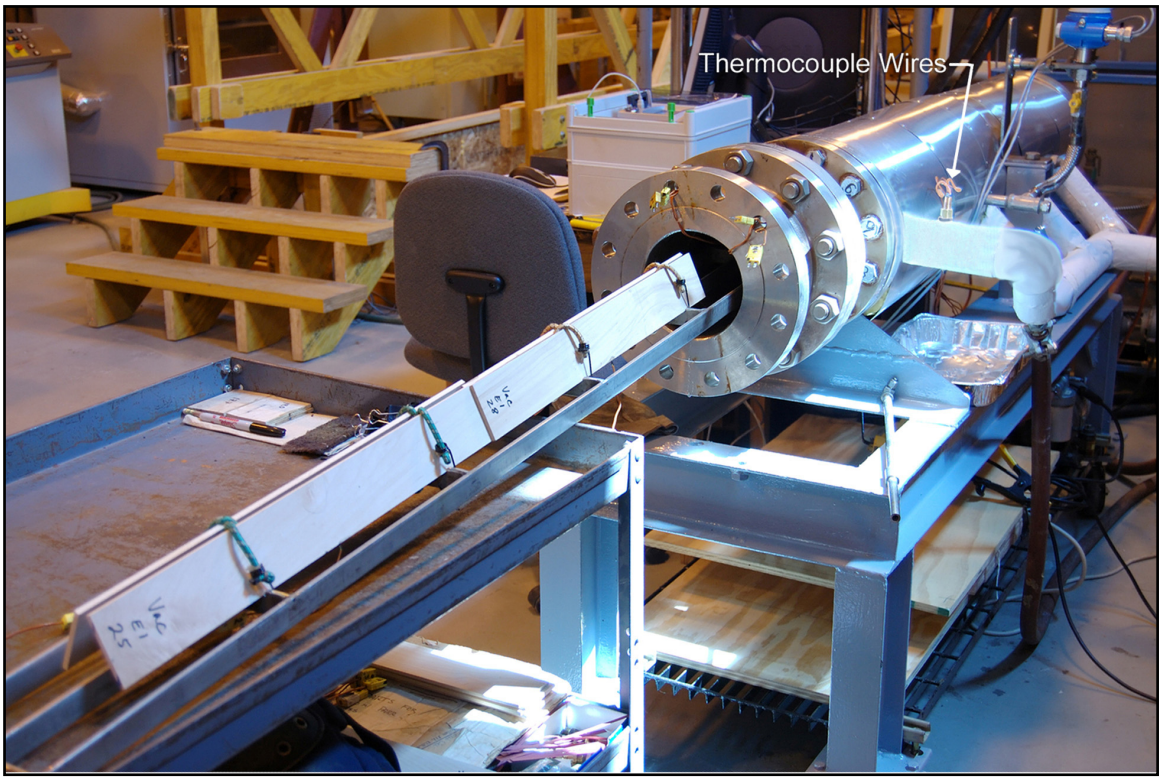

Figure 4.3 Front ¾ view showing maple specimens on stainless steel rack being loaded into chamber. Boards are positioned so thermocouple wires exit from the bottom edge; protected by the support shelf. Also shows chamber thermocouple wires at a sealed access port through chamber wall. To the right in Figure 4.3 some of the wires passing through a vertical sealed transition port can be seen in an area bright from sunlight (also seen in Figure 3.10). Photograph by author 2010.

Specimens were prepared as shown in Figure 4.2 in batches of 12 or 16 and then four were used per experiment. Each experiment performed in RA #1 to evaluate Research Hypothesis #1 was done so in accordance with the experimental plan in Table 4.2. The EcoGraph T data logger would display and record each maple specimen internal wood temperature, the chamber temperature and the chamber pressure. Reference Figure 4.4 for a typical vacuum treatment experiment graph and Figure 4.5 for a typical atmospheric, non-

vacuum experiment graph; these graphs illustrate the narrow zone of the time-to-temperature curve critical to the evaluation of Research Hypothesis #1.

In both graphs the black trace is the chamber pressure. The instant of steam addition is immediately recognizable as the abrupt and nearly vertical deviation from the otherwise essentially horizontal line. In Graph 4.4 this occurred near 1300 seconds and in Graph 4.5 this change occurred near 100 seconds. This abrupt change was referred to in Section 3.4 as the moment the wood temperature *could* begin to rise because this is the moment the 100°C steam was introduced to the maple. The data were recorded at 1 Hz, hence it was extremely easy within the data file to select the individual one second interval when the steam was introduced to the chamber.

This point became time zero for determination of the internal wood temperature vs. time rate. At time zero the internal wood temperatures for each specimen loaded into the chamber was noted in a separate file. The data were next carefully scanned looking for the one second interval when the internal wood temperature attained 100°C. Due to the steam pressure limitations mentioned in Section 4.2.1, occasionally the boiler was on a decreasing steam pattern as a specimen was attempting to reach 100°C. In those events the author used the highest attained temperature. In Figure 4.4 the heat-up phase ended around 1400s and in Figure 4.5 the internal wood temperature heat-up ended around 300s. Precise determinations were made through the data file.

4.4 Results

Results reported in this section reflect specific research experiments conducted according to the experimental plan of Table 4.2. Due to two limitations; Sealant Limitations, Section 4.2.2 and Temperature Limitations, Section 4.2.3 the results section must be broken into multiple sub-categories. For example, not only is there a vacuum treatment vs. a non-vacuum control, there is also silicone sealed vacuum and epoxy sealed vacuum groups and silicone sealed and epoxy sealed non-vacuum groups. The inclusion of a pre-heat option due to Section 4.2.3 added another variable. Each variation was addressed from the research perspective questioning how different one option was from another?

4.4.1 Uniform State Chamber Performance

Uniform state uniform flow (USUF) chamber performance during steaming for all experimental runs in RA #1 was defined as the internal wood temperatures reaching the 100°C point through to the end of the steaming period. This section brings resolution to the steam pressure limitations mentioned in Section 4.2.1. While not a specific research objective, it was important to determine how repeatable the chamber performance was. Repeatable performance would enable research objective-related comparisons to be made. Referencing the previous graphs in Section 4.2.3, Graph 4.4 would begin the uniform state around time = 1500s and for Graph 4.5 around 400s. This time period approach was used to investigate each experimental run of four specimens in RA #1. The cumulative uniform state elapsed operating time was in excess of 10 hours. The average chamber pressure was 111.9 kPa with a standard deviation of 1.5, the average chamber temperature was 103.5°C with a standard deviation of 1.0 (see Table 4.3). The steam table value for the saturated steam temperature at the chamber average

pressure of 111.1 kPa was 102.8°C. This was well within the accuracy of the TCs. The steam table value for the saturated steam pressure at the chamber average of 103.5°C was $P_{saturated}$ = 113.6 kPa. This is a very minor difference of 1.7 kPa, or 1.5% from the actual data for the average pressure and was considered insignificant to the outcome of the experiment.

Table 4.3 Uniform state performance of steaming chamber

Experiment #1 Specimens	USUF Pavg; kPa	USUF Tsat; °C @ Pavg	USUF Tchmbr avg; °C
1 - 4	114.4	103.4	102.3
5 - 8	110.1	102.3	103.6
9 - 12	110.5	102.4	102.7
13 - 16	108.9	102.1	103.1
17 - 20	112.1	102.8	105.3
21 - 24	111.8	102.8	105.9
25 - 28	111.8	102.8	103.9
29 - 32	111.5	102.7	102.9
33 - 36	115.2	103.6	104.1
37 - 40	112.7	103.0	104.1
41 - 44	112.8	103.0	102.9
45 - 48	111.4	102.7	102.3
49 - 52	112.0	102.8	104.5
53 - 56	112.4	102.9	102.7
57 - 60	111.3	102.6	103.4
61 - 64	111.6	102.7	103.0
Average	111.9	102.8	103.5
Std. Deviation	1.5	0.4	1.0

4.4.2 Internal Wood Temperature vs. Time

The rate of wood heating was the critical metric of this experiment to evaluate the research hypothesis. The determination of the rate of temperature increase was accomplished with three metrics: The first metric was based on an estimation of the steepest slope in the heat-up phase of each individual maple specimen. Second was an overall slope calculation based on the `time zero' point described in Section 4.3 and then the end point of 100°C. The third method was the best match for Research Hypothesis #1 and the elapsed time from time zero to time at 100°C for every specimen was evaluated.

In the review of the graphs of data, such as Graphs 4.4 and 4.5, it was immediately apparent to the author that the slope of the lines represented by the TC values in the maple specimens was almost twice as steep for the vacuum treated specimen relative to the non-vacuum treated specimen. Looking at the narrow range of time on graphs 4.4 and 4.5 when the steam valve was first opened; the vacuum treated maple went from about 50°C to 100°C in about 100 seconds and the same approximate temperature change in the non-vacuum treated maple required about 200 seconds. The slope, $\Delta T/\Delta t$, was utilized to determine if there was a difference between treatment and control.

The maximum slope was estimated by generating graphs of every individual TC over the time interval from time zero until the TC registered 100°C. Those graphs were produced on expanded scales to better visualize the slope, and then the author selected what appeared to be the steepest portion of the slope to make a linear regression approximation of the data. From the trend line a slope value was determined. The slopes could then be compared between the treatment and the control experiments. See Graph 4.6 from a non-vacuum, control experiment and Graph 4.7 from a vacuum treated experiment as examples of the date manipulation. Note the slope value ‘m’ from the trend lines in Figure 4.6 and Figure 4.7: slope =0.41 for the vacuum treated specimen and 0.17. In this example the vacuum treatment produced a $\Delta T/\Delta t$ value two and a half times greater than the control.

Evaluation of the estimated maximum slope values ($\Delta T/\Delta t$) data for all specimens in the experimental sample for Research Hypothesis #1 was accomplished. Without consideration for the sealant or temperature limitation issues (Section 4.2.2 and 4.2.3) and looking only at the difference between vacuum treated steaming compared to non-vacuum control steaming,

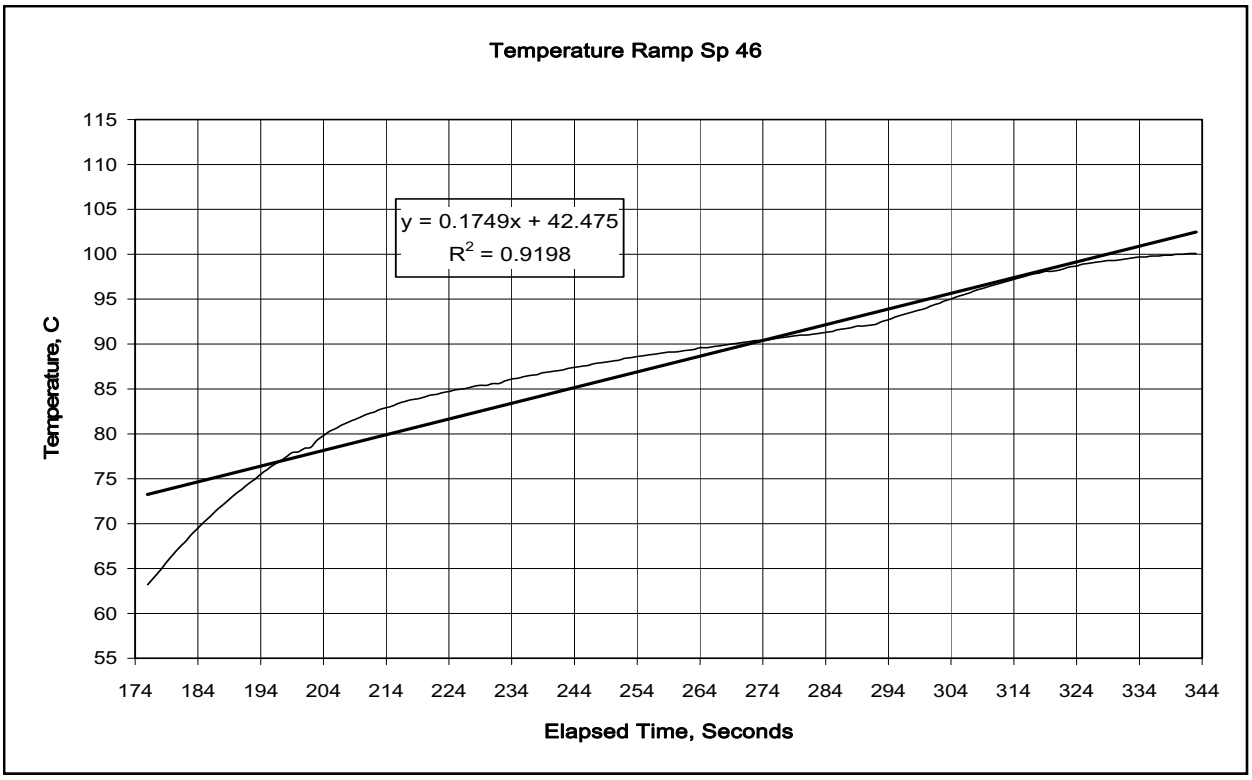

Graph 4.6 Slope of TC #3, Sp #46, Control, (ref. Graph 4.5) on expanded axes for analysis.

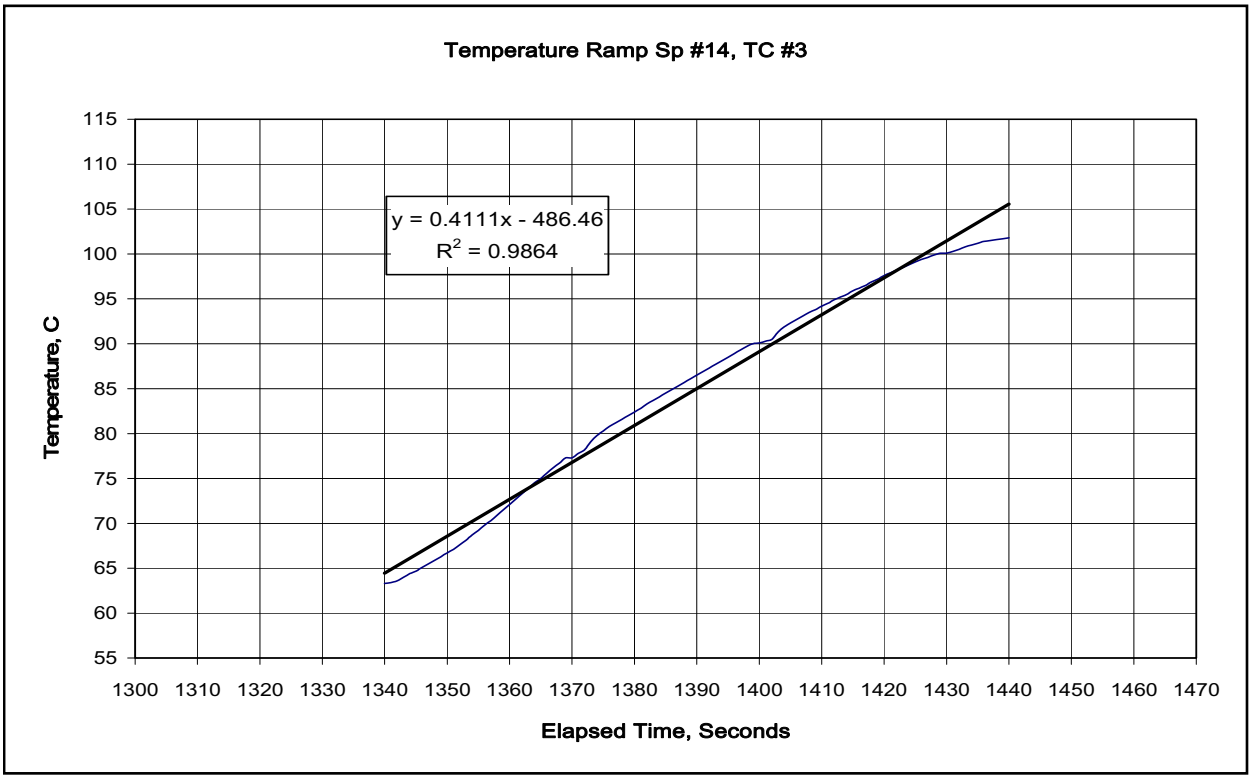

Graph 4.7 Slope of TC #3, Sp #14, Treatment, (ref. Graph 4.4) on expanded axes for analysis.

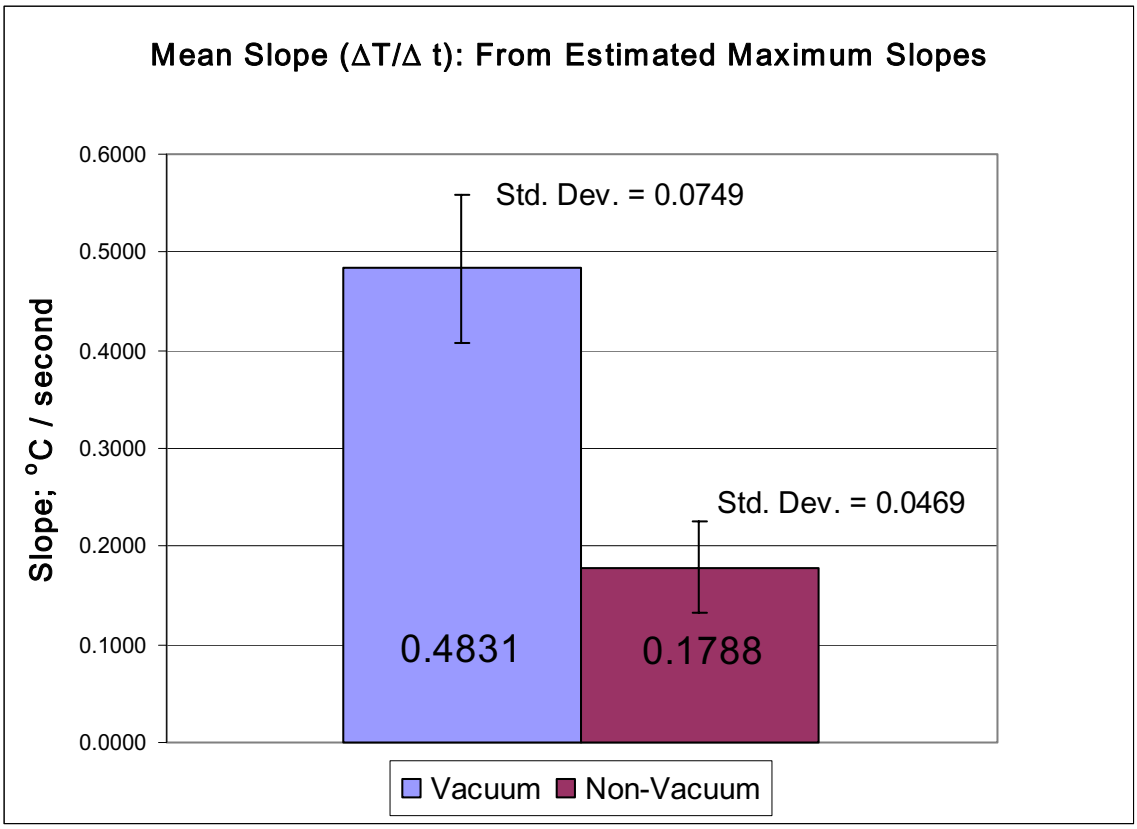

Figure 4.4 Sample means of the maximum slopes during initial heating. Internal wood temperature vs. time, °C / second. Means in columns and standard deviation above Produced by author 2010.

Figure 4.4 demonstrates quite clearly that a vacuum stage preceding the steaming stage results in the internal temperature of the maple heating faster than traditional steaming by a factor of 2.7 (0.483 /0.179 = 2.7). The data were evaluated for heterogeneity of variance with Levene's test prior to performing a t-test. The t-statistic in the Levene two tailed test was 2.04 with t-critical at 2.03 and P= 0.049 for alpha = 0.05; therefore, we fail to reject the null hypothesis and the variance are equal. The subsequent two-tailed t-test with equal variance for the combined slope data produced a t-statistic of 19.4 with t-critical at 2.0 and P= 0.001 and on this basis the null hypothesis was rejected. The application of a vacuum stage prior to steaming

significantly increased the rate of heat gain ($\Delta T/\Delta t$) compared to the control by a factor of 2.7 (0.483/ 0.179).

After having looked at the data for Research Hypothesis #1 based on estimated maximum slope, the influence of subjective judgment regarding the `steepest section' of the $\Delta T/\Delta t$ data was in question. Therefore, the data were looked at in the very strict sense of time from the second the steam was introduced to the chamber (at internal wood temperature 'T_1') to the second the internal wood temperature registered 100°C (at internal wood temperature 'T_2') or a temperature maxima that occurred very close to 100°C in the event the boiler heater had cycled off at that time (see Section 4.2.1).

Ten specimens in the non-vacuum control experiment did not reach the goal of 100°C internal temperature during the initial temperature ramp. The reason was the boiler had cycled through its' heating cycle and began the periodic pressure/temperature decay characteristic of the system. These specimens did eventually reach the goal temperature, but the boiler had to cycle through a second heat cycle. In these ten cases the author selected the time mark at the initial highest attained temperature (note; the lowest of these ten was 97.1°C)

When the data were compared as: (total temperature change) / (total elapsed time), the result was slightly different slope values. Figure 4.5 below shows the mean slope values based on total elapsed time. A significant result from the Levene test for heterogeneity of variance dictated a t-test assuming unequal variance. A t-test was performed on the elapsed time slope data represented by Figure 4.5. The t-statistic was 11.4 and t-critical two tailed was 2.0 resulting in P = 0.001 and on this basis the null hypothesis was rejected; the conclusion is the same; heat

gain is significantly greater for the vacuum/steam combination when compared to steaming alone by a factor of 2.2 (0.512/ 0.232).

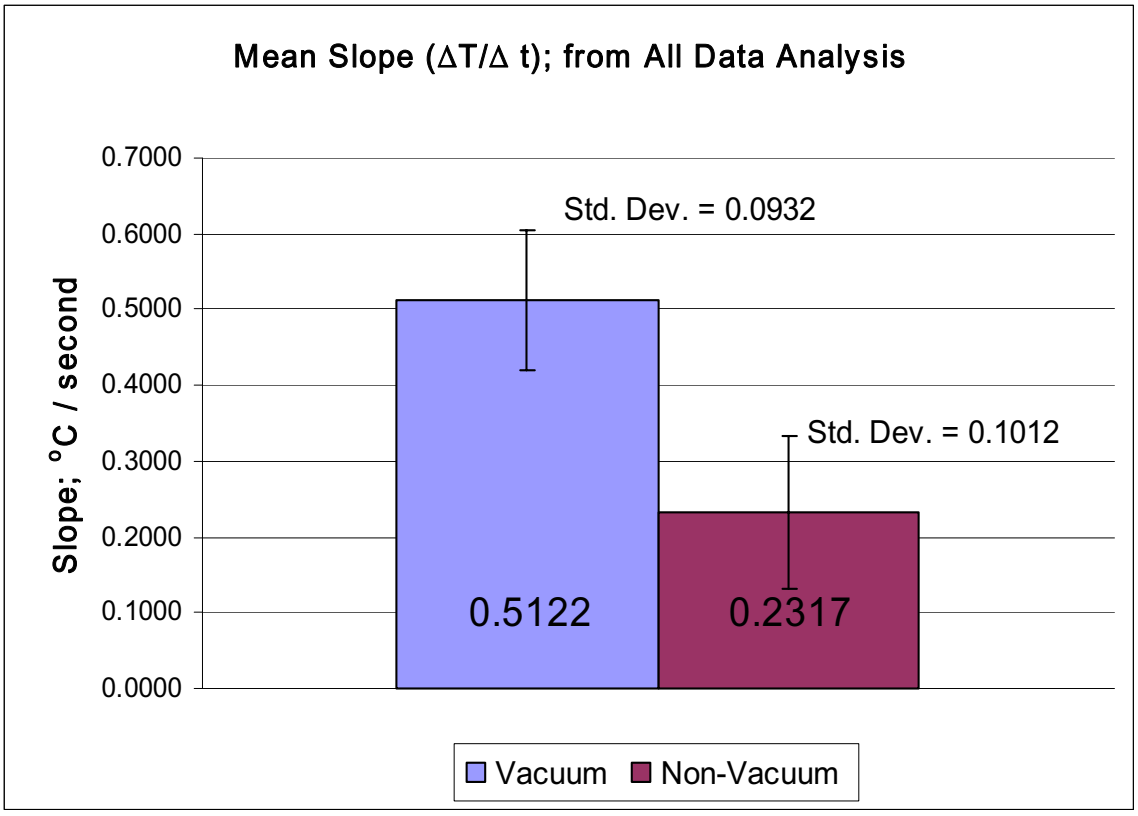

Figure 4.5 Sample means of cumulative slopes; initial heating. Internal wood temperature vs. elapsed time data; means in columns and standard deviation above.
Produced by author 2010.

The third metric utilized for evaluating the relative performance between the vacuum treated sample and the non-vacuum control sample was elapsed time data for the initial heat-up ramp from time zero to time at 100°C. These data were calculated for each maple specimen. The time-only data is the most explicit response to Research Hypothesis #1. In Figure 4.6 it is

clear that the mean elapsed time to attain the goal temperature of 100°C for the non-vacuum control sample was more than twice as long as the vacuum/ steam treatment.

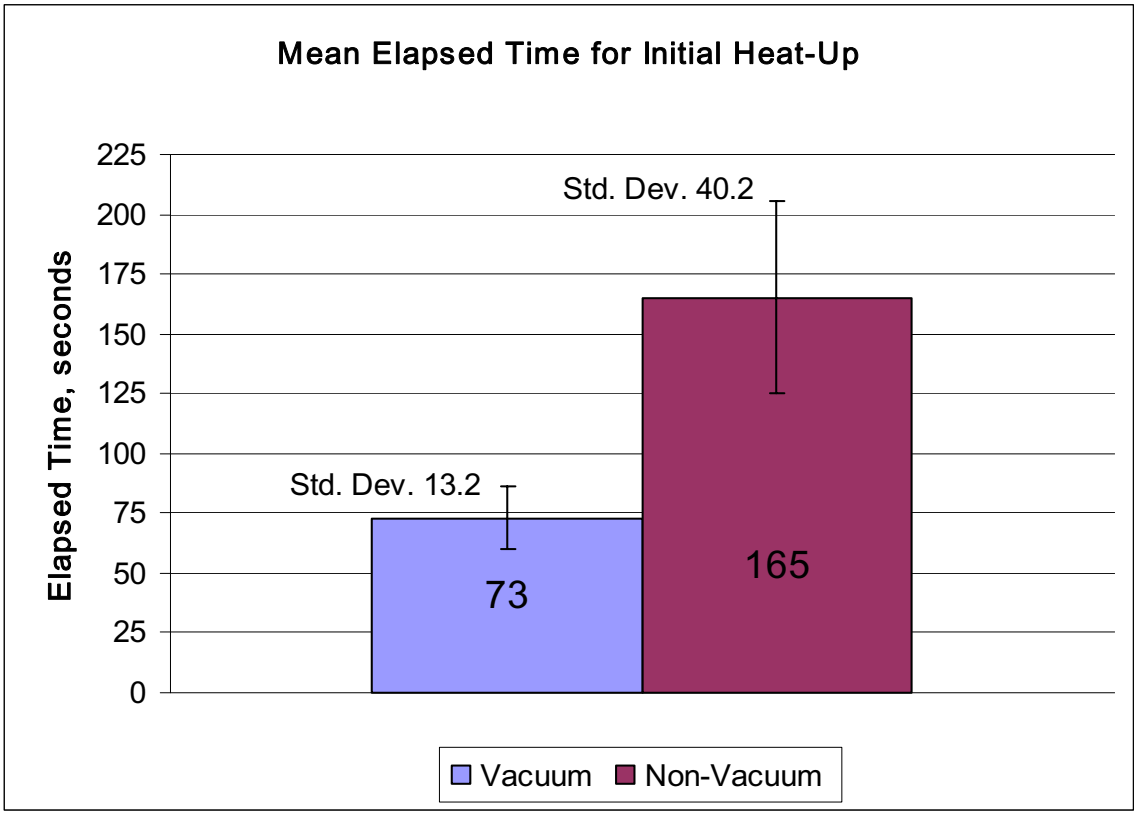

Figure 4.6 Mean elapsed time; initial heat-up. Time in seconds shown in column for the vacuum treatment and the non-vacuum control. Produced by author 2010.

Based on a significant result from the Levene test for heterogeneity of variance, a t-test assuming unequal variance was performed on the elapsed time data represented in Figure 4.6. The t-statistic was -12.3 and t-critical two tailed was 2.0, resulting in P=0.001. Therefore, on an elapsed time basis the null hypothesis was rejected and it was concluded that there is a significant decrease in the time required for kiln dried maple to attain an internal wood temperature of 100°C when an initial vacuum cycle is used before a steam cycle by a factor of 2.3 (165/ 73) due to the Water Vapor Bulk Flow.

Three methods were utilized to evaluate the data that was produced from the experimentation performed in determination of Research Hypothesis #1; the average of an estimated maximum slope ($\Delta T/\Delta t$) for the vacuum treated sample and the non-vacuum control. That result was the vacuum treatment slope was 2.7 times greater than the non-vacuum control. The next comparison was based on the full time range between time zero and the time when the maple specimens reached 100°C. In this instance the vacuum treated sample had a mean slope that was a factor 2.2 times greater than the non-vacuum control. The last comparison was based on elapsed time only from time zero to the time when the maple specimens reached 100°C. The vacuum treated sample mean was 2.3 times faster than the non-vacuum control. We reject the Research Hypothesis #1:

> There is not a difference in the time required (elapsed time) to attain the goal internal wood temperature due to a preliminary vacuum cycle relative to the classic process of atmospheric steaming when beginning with low moisture content (<10%) maple.

We accept the alternate hypothesis:

> There is one technique which is faster than the other.

We conclude the overall average result that the vacuum treatment steamed sample was 2.4 times faster than the non-vacuum control steam process for heat gain to the goal temperature in low moisture content maple specimens, and this result is significant at alpha = 0.05 two-tailed.

4.5 Discussion of the System Limitations and Their Affect on Experimental Results

As mentioned in Section 4.2.2 there was concern regarding the possibility of sealant failure between the TC wire and walls of the thermocouple hole in the maple. A choice was

made to change sealant materials halfway through the specimen set for this experiment. As mentioned in Section 4.2.3 the internal wood temperature at the time immediately before steam was added to the chamber was extremely different (approximately 40°C) between the vacuum and the non-vacuum specimens (see Graphs 4.4 and 4.5 in Section 4.2.3 for a typical example). A choice was made to change the procedure of the non-vacuum control group halfway through the specimen set and permit a non-steam preheat.

One obvious question was: How did either change affect the results? Evaluation of this question required segregation of the data files corresponding to specimens into subsets and then conducting data analysis on the subsets. The specimens were broken down into four subsets to enable comparisons between them. For the control, non-vacuum sample of 32 the first 16 became `silicone, non-vacuum' and the second 16 became `epoxy, non-vacuum with pre-heat'. For the vacuum treatment sample of 32 the first 16 became `silicone, vacuum' and the second 16 became `epoxy, vacuum'.

Determination of whether the silicone sealant leaked was not possible because there was not a mechanism to measure internal wood pressures. However, a t-test was used to compare the silicone, vacuum and the epoxy, vacuum subsets to indicate how the two different sealants behaved relative to each other. Because there were no visible leaks of steam around the TC wires that were epoxy sealed into transitions through the chamber wall during 62 hours of cumulative run time with the reactor at operating pressure and temperature, there was circumstantial evidence that the epoxy sealed TC's in the wood probably did not leak during a single 70 minute experiment. If the performance difference were not significant from the t-test then by reasonable implication the silicone-sealant probably did not leak.

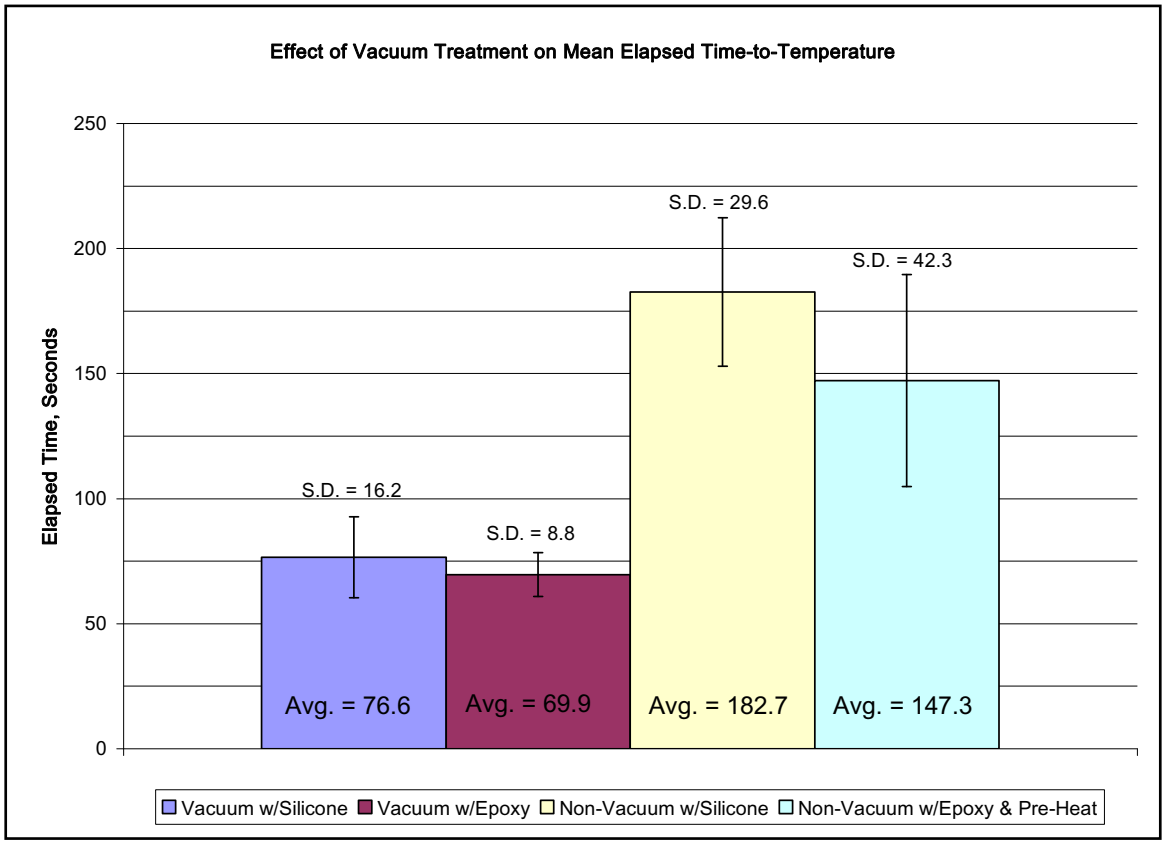

Figure 4.7 Mean elapsed time-to-temperature of subsets of vacuum-treated group and non-vacuum control group, with standard deviation shown. Produced by author 2010.

Figure 4.7 shows the four subsets of the experimental sample and the average elapsed time-to-temperature of each subset. In the vacuum treated group, the mean for the two sealant types are quite close to each other with the silicone sealant being 6.7 seconds greater than the epoxy sealant. Silicone sealant exhibited a larger standard deviation, indicating larger variability among the specimens comprising that group. Variability might be construed as evidence of leakage, but the fact that the elapsed time-to-temperature is greater for that subset is contrary to the effect of leakage around the TC wire; i.e. a leak path for steam to enter would influence the temperature to rise more quickly.

Several t-tests were performed on data from the vacuum-treated subsets of silicone and epoxy because the author felt is was important to ascertain that the silicone sealing material did perform adequately well in the context of single-use, individual experimental specimens for the duration of individual experiments (about 70 minutes). If the silicone material did leak, it may have leaked on the atmospheric steamed specimens as well and the result would be essentially useless data for Research Hypothesis #1.

Three parameters were investigated for the subsets of the vacuum treated group; elapsed time (Δt), overall slope ($\Delta T / \Delta t$), and the change in temperature (ΔT). In each case the Levene test for heterogeneity of variance was used to determine the proper variance condition to be applied to the subsequent t-test. The null hypotheses were: There is not a difference in the { (Δt), ($\Delta T / \Delta t$), (ΔT) } between silicone-vacuum and epoxy-vacuum. See Table 4.4:

Table 4.4 t-test for sample means comparing vacuum treated silicone and epoxy

Variable	Levene Result	t-statistic	t-critical, two-tailed	P Value	Result at alpha =0.05
Δt	unequal variance	1.477	2.080	0.154	fail to reject null hypothesis
$\Delta T / \Delta t$	equal variance	-0.443	2.045	0.661	fail to reject null hypothesis
ΔT	unequal variance	1.259	2.069	0.221	fail to reject null hypothesis

Table 4.4 clearly indicates that at the alpha=0.05 confidence level in the two-tailed t-test there is not a significant difference in the means of the two samples; vacuum with silicone sealant and vacuum with epoxy sealant, for three critical performance metrics. Bearing in mind the observation of no visible leakage around the epoxy-sealed TC wires entering the chamber

during 62 hours of operation, it can be implied that the epoxy sealed TC wires entering the maple specimens probably did not leak. Consequently it can be implied from Table 4.4 indicating no significant differences between the sample means that the silicone sealant material probably did not leak around the TC wires entering the maple specimens for the vacuum treatment group. Finally, for the atmospheric steamed control group sealed with silicone, it can be reasoned that if the silicone sealant did not leak during the more extreme environmental conditions of vacuum followed by steam, it probably did not leak during atmospheric steaming.

Comparisons were made between the silicone sealed atmospheric control sample and the silicone sealed vacuum treatment sample (Figure 4.7) to address the null hypothesis for these two subsets of elapsed time-to-temperature. The Levene test for heterogeneity of variance concluded unequal variances and the t-test produced a t-statistic of -12.47 and t-critical, two-tailed value of 2.06, P=0.001 and so at alpha=0.05 we reject the null hypothesis and conclude there is one technique faster than the other; The mean elapsed time values show that in the silicone sealed subset of specimens a vacuum cycle preceding a steam cycle significantly reduces the elapsed time required for low moisture content maple to attain the goal temperature of 100°C by a factor of 2.4.

A similar comparison for elapsed time-to-temperature was made between the two subsets of epoxy sealed specimens of Figure 4.7; the atmospheric control sample with additional pre-heat and the vacuum treatment sample. Both samples had 16 specimens. The pre-heat phase resulted in an average temperature of 80.5°C before any steam was introduced. The average temperature of the vacuum treated sample before any steam addition was 64.4°C.

The Levene test concluded unequal variance and the t-test resulted in a t-statistic of -7.19 with t-critical two-tailed at 2.12, P = 0.001 and therefore at alpha = 0.05 the null hypothesis is rejected for this subset. Despite beginning the steam cycle 16°C cooler than the atmospheric sample, the time-to-temperature was significantly shorter for the vacuum treated sample by a factor of 2.1 (Figure 4.7).

4.5.1 Discussion Regarding Specific Gravity Affect on Results

Peck (1957) had concluded that specific gravity does not have an influence on bending qualities based on research with a large sample of oak. Specific gravity does have an effect on many qualities of wood chiefly all mechanical strength properties (Wood Handbook 2010): The experiments in RA #1 of this work did not involve bending, just steaming of maple via two different techniques. Since steam bending is comprised of two critical components: steaming and bending, the question arose as to whether the one or both components (steaming or bending) were equally unaffected by specific gravity. Figure 4.8 below plots the slope of $\Delta T/\Delta t$ (change in temperature over change in time) based on the actual elapsed time, against specific gravity for all specimens in RA #1. The figure illustrates that specific gravity within the range tested does not seem to have a strong affect on the rate of temperature gain for maple beginning at low moisture content as evidenced by no visual correlation in the scatter plot. This may be due to competing effects within the wood. The Wood Handbook (2010) states that thermal conductivity of wood increases with specific gravity and moisture content, but Siau (1995) states that moisture diffusion decreases with increasing specific gravity due to increased resistance of the cell wall paths.

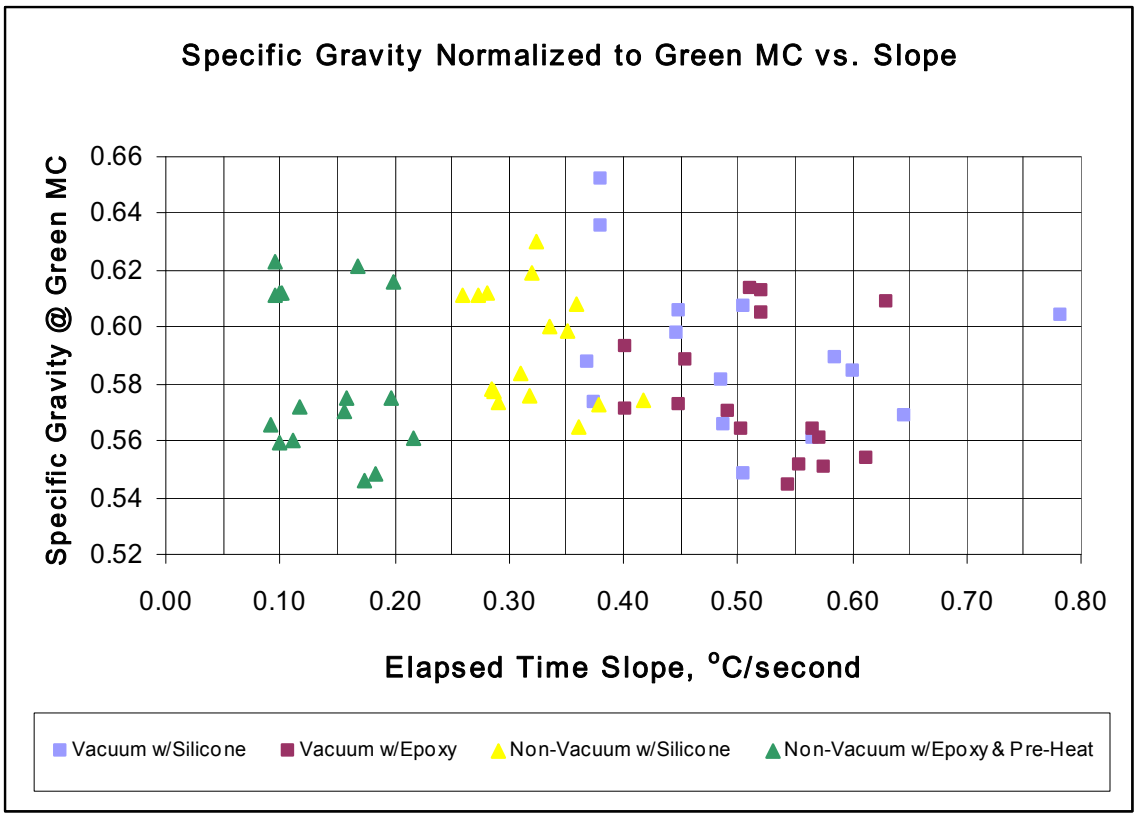

Figure 4.8 Showing individual specimen specific gravity vs. elapsed time-based slopes of temperature rise. No noticeable correlation. Produced by author 2010.

4.5.2 Discussion of Moisture Content Results

Following either steaming procedure utilized in the experiments of Research Area #1, none of the maple boards had attained a bendable state. The overall average final moisture content for the atmospheric control group of 32 specimens was 11.0%. The overall average final moisture content of the vacuum-treated sample of 32 was 14.4%. There was evidence supporting the WVBF transport mechanism allowing more moisture gain, since the vacuum treatment group with one vacuum cycle regained 3.4% more water on average. One vacuum cycle was insufficient to optimize the potential of the gain to 20% or 25% MC. The temperature gain was 2 to 2.5 times faster with a preceding vacuum cycle, but not a comparable gain in MC.

The conclusion from the experiments in RA #1 were that a single vacuum cycle before a steam cycle can result is much faster internal wood temperature gains, but is limited on moisture gain. The extrapolation of the idea of moisture gain per cycle led to the experiments and effort of RA#2; Development of Vacuum Steam Technology for Plasticization of Maple

4.6 Summary of Results for Research Area #1

- The vacuum cycle preceding the steam cycle resulted in a faster temperature rise compared to the atmospheric steam control in every case, with either silicone sealant or epoxy sealant, by a factor ranging from 1.9 to 2.6 depending upon which mean values are compared from Figure 4.7.
- A single vacuum cycle preceding the steam addition resulted in a very small increase in the overall mean moisture content compared to the atmospheric control of 3.4% (14.4% vacuum cycle and 11.0% non-vacuum). This indicated the need for:
- An additional experiment was needed to develop cyclic vacuum-steam technology moisture addition to the maple specimens used in this research work.

Chapter 5: Development of Vacuum Steam Technology for Plasticization of Maple

5.1 Introduction to Research Area #2

In RA #1, it was shown that a single vacuum stage prior to addition of steam into the chamber resulted in a significantly faster gain of internal temperature but insufficient moisture to adequately plasticize the kiln-dried maple specimens for bending. The reasonable and logical next step was exploration into multiple vacuum / steam cycles to enable repeated rapid moisture gains within the wood due to the WVBF transfer mechanism. The pattern of cycles for Vacuum / Steam Technology (VST) as developed by this author was comprised of an initial vacuum cycle for some as-yet-to-be-determined duration as in RA #1, followed by an initial steam cycle, followed by a series of vacuum / steam cycles for some as-yet-to-be-determined duration and number of cycles; ultimately to attain a plasticized maple state suitable for bending.

The unavoidable consequence of repeated vacuum cycles was the removal of some amount of moisture from the wood with each vacuum cycle; just as in vacuum drying of wood. The crux of the technique to be developed lay in a methodology that would provide a real-time indication of when the wood began to give up moisture during the vacuum cycle. At the point of incipient moisture loss from the wood, the vacuum cycle had to be terminated and the next steam cycle had to commence. A companion consideration was how long each steam cycle should be. Determination of the extent and the duration of each cycle to attain a bendable state from kiln dried wood were the goals for RA #2.

The experimental design to accomplish both goals was based on a teaching pedagogy referred to as: ‘whole-part-whole’. An initial ‘whole’ VST test was performed using four pieces of maple with thermocouples inserted and subjecting them to a sequence of vacuum / steam

cycles of assumed duration and number. That test data was inspected, manipulated, and analyzed to gain as much knowledge as possible about the thermodynamic states within the chamber during VST and the response of the wood to those states (chiefly moisture content, bend-ability). An extensive series of were then designed and carried out (tests spanning 14 cumulative hours) to address specific questions ('parts') about the system dynamics as evidenced from the first test. The information from investigating the 'parts' was synthesized into a standard operating procedure. The procedure was then used to treat the 'whole' of the research sample of 27 specimens.

The first test will be described in detail to elucidate the variables identified and the challenges encountered in developing the prototype standard operating procedure for the VST treatment to plasticize maple. The extensive subsequent tests will be described in a brief list of results. The application of the VST technique to the research sample will then be presented in Section 5.5; Methodology. The results from the 27 specimens are in Section 5.6.

5.2 The First VST Test

The first test was performed with small maple specimens, essentially cut-offs from the machining process for the statistical specimen set. The test had a beginning which resembled the vacuum treated samples in RA #1 with a 20 minute vacuum cycle followed by a 30 minute steam cycle. After the first steam cycle a sequence of four additional vacuum / steam cycles occurred that were nominally consistent in the wood temperature attained during the vacuum cycle and the length of the pressure cycle. Vacuum cycles in this test were controlled based on the lowest internal wood temperature. When the internal wood temperature dropped to 70°C, it

was hypothesized that a low temperature would favor steam condensation within the wood during the next steam cycle. It was coincidental that the chamber pressure was consistently about 20kPa at the turn-around point because chamber pressure was not considered as a controlled variable during the first VST test. Steam cycles had a duration of 6-7 minutes with the fourth one being more than 12 minutes, resulting in a total test period of 110 minutes, or about 230 minutes / centimeter (585 minutes / inch), and a moisture content change from 6.5% to 16%. It was clear from these results that it was further necessary to reduce time and increase moisture content. See Graph 5.1.

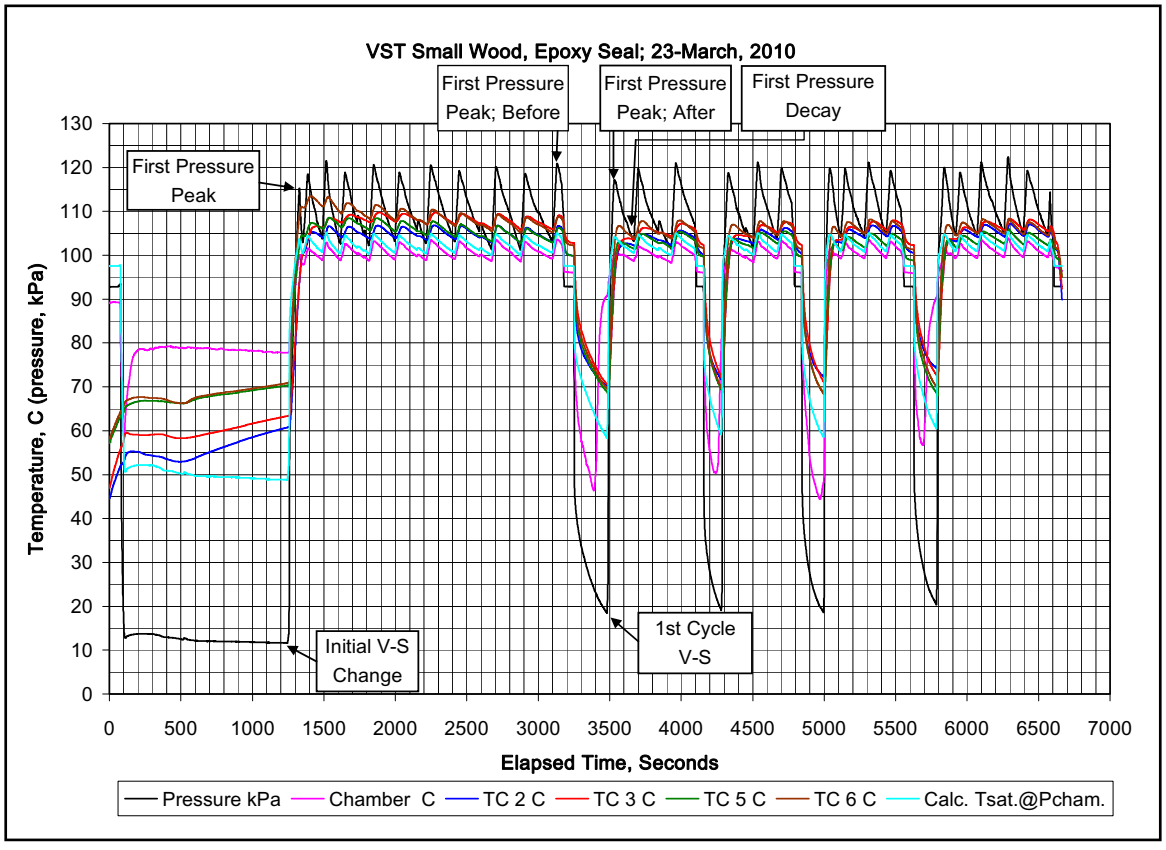

Graph 5.1 First VST test data with some developing VST terms labeled

Details of the test:

- Chamber pre-heated to steel about 100°C (varied between 97.6°C to 100.7°C)
- Steam trap trim valve (ball-type) set to 56° angle closed (90°= fully closed)
- Run initial vacuum cycle as in RA #1 (20 minute duration, about 11.5 to 12kPa)
- Run initial steam cycle approximately as in RA #1 (30 minute duration)
- Control subsequent vacuum cycles based on attainment of 70°C wood temperature (about 20kPa) to favor steam condensation during subsequent steam cycles
- Assume the duration for subsequent steam cycles

5.2.1 First VST Test Results

Graph 5.1 is representative of the real-time data available for each VST test or experiment. In the real time VST experimentation there were always differences in the range of the pressure swings and in what temperatures actually occurred in the wood and in the chamber. However, the basic data available for analysis and insight remained similar to the data represented in Graph 5.1. One challenge was to understand how every possible interrelationship within the chamber was reflected in deflections of temperature or pressure signals on the real time graph so that the information could be used to control the chamber atmosphere. Astute observation was very important to the VST development. The temperature of the maple specimens is represented by thermocouple numbers 2, 3, 5, and 6. The chamber temperature used thermocouple 4 and is labeled “Chamber”. The black trace is the chamber pressure.

Evidence that the chamber was pre-heated can be seen at the far left where the chamber atmospheric temperature (pink trace) began at approximately 90°C whereas the internal wood temperatures ranged from 45°C to 60°C. As soon as the vacuum (black trace) was started at about 80s, expanding gas in the chamber atmosphere resulted in the chamber temperature dropping to about 60°C (pink), but it quickly began to regain temperature from radiant heat of the hot steel walls, eventually reaching almost 80°C. The wood specimens showed a more gradual decrease in temperature until about 500s and then began to increase in temperature. It was hypothesized that the initial cooling of the wood was due to a combination of gas expanding as it was evacuated from the wood but also moisture may have been removed resulting in evaporative cooling to a minimum temperature for each piece. The minimum temperatures indicated either or both; fully evacuated wood, or completely dehydrated wood. The wood began to increase in temperature while under a 12kPa vacuum and this was taken as an indication of extremely dry, evacuated wood gaining radiant heat energy from the steel walls. There was reason to believe the MC of the wood at the end of the initial vacuum cycle was dryer than the initial average MC of 6.5%. This was an extremely undesirable result for the initial vacuum cycle. Evaporation of additional moisture from a piece of kiln dried maple had to imply bound water removal. Local atmospheric conditions for bound water removal from wood are the complete antithesis of the desired conditions during VST for moisture regain. Determination of when to stop the initial vacuum cycle became one developmental goal.

The initial vacuum / steam transition is labeled with a text box. The transition was a matter of shutting a valve (valve #3, Figure 3.6) to isolate the running vacuum system from the chamber and then open the steam inlet valve (Figure 3.4). The transition required less than five

seconds to accomplish, resulting in no discernable bump in the pressure or temperature traces. The initial steam cycle shows that wood temperatures increased at about the same rate as the steam pressure increase, attaining steady state temperature in 200s – 300s. The oscillatory pattern of boiler pressure and all temperature traces remained essentially constant for the duration of the 30 minute steam cycle. It was hypothesized that during the extended steam cycle diffusion was the only moisture transport mechanism at work. Diffusion was not the desired mechanism for moisture transport and determination of the duration of the steam cycle to favor predominantly WVBF became another goal of development.

At the end of every steam cycle the transition to vacuum required an involved valve sequence and more time to accomplish. The steam inlet valve had to be closed (Figure 3.4), the steam within the chamber had to be vented to the outside (valves #3 and #4, Figure 3.6) until no more vapor could be seen or heard escaping, the atmospheric vent valve (#4, Figure 3.6) had to be closed, and finally the vacuum valve (#5, Figure 3.6) had to be opened. The time required ranged approximately from 20s – 40s. The pressure and temperature traces in Graph 5.1 show this transition as a constant atmospheric pressure, almost constant temperature step immediately preceding the precipitous drop in pressure and temperature at the beginning of the vacuum cycle. This would become a performance characteristic of the hardware system.

The first vacuum cycle (labeled: "1st Cycle V-S") and each subsequent vacuum cycle were moderately consistent regarding minimum wood temperature and minimum chamber atmospheric pressure, but the chamber temperature did not behave consistently. One aspect was thought to be understood; when the chamber temperature increased as the chamber pressure continued to decrease, such as in the first vacuum cycle at the elapsed time of 3400s

in Graph 5.1, the chamber atmosphere was probably superheated steam. The implication of a superheated steam environment was moisture removal from the wood as the gas attempted to achieve a saturated atmosphere. This was not a desired outcome and understanding of the phenomena during the vacuum cycle became a goal of the development. Results from the first VST test indicated a need to: (1) determine the endpoint for the initial vacuum cycle, (2) determine the duration of the steam cycle to favor WVBF and not diffusion, and (3) understand the chamber phenomena during the vacuum cycle.

5.2.2 Vapor-Pressure Curve Graph Technique for Post-Test Analysis

Given the evidence for potential superheated steam environments during each vacuum cycle, a better means to gain knowledge of the actual state of the atmosphere was needed. A graph technique that plotted temperature against pressure from thermodynamics was employed; the vapor-pressure curve (VanWylen and Sonntag 1976). The graph places chamber pressure on the abscissa and chamber temperature on the ordinate. The beginning of each vacuum cycle was defined to be the point of maximum chamber pressure immediately before a vacuum cycle began, and the end point of the vacuum cycle was defined to be the point of maximum chamber pressure immediately after the vacuum cycle. Both of these points are labeled in Graph 5.1. The resultant vapor-pressure curve became a powerful analytical tool for determining what changes were necessary. Graph 5.2 below is the first such graph generated from the data of the first vacuum cycle in Figure 5.1 (differentiated from the initial vacuum cycle).

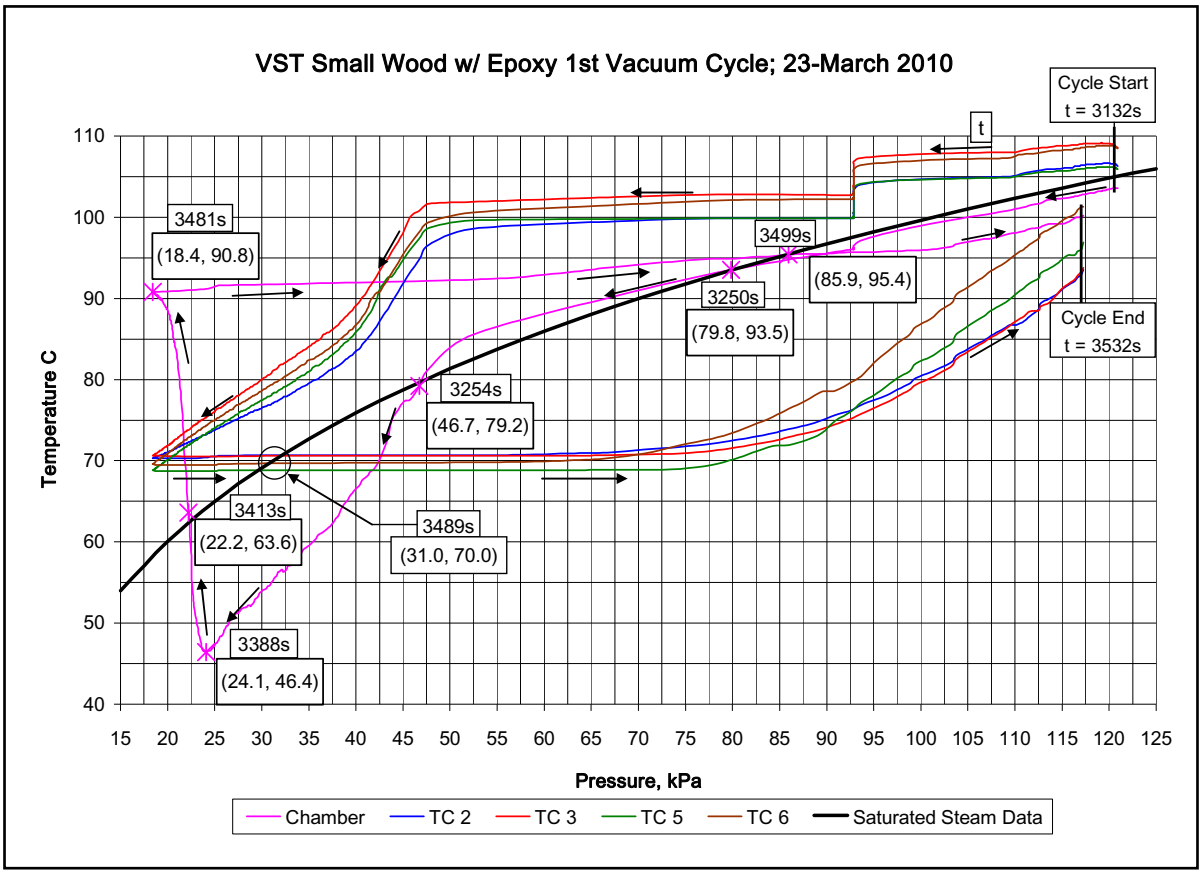

Graph 5.2 Vapor-pressure curve of the first vacuum cycle from Graph 6.1. Produced by author 2010.

Time has no reference in a vapor-pressure curve. However, because these graphs represent a cycle, time obviously was a component and in an effort to help understand how time progressed during the cycle, a series of black arrows indicates the passage of time from the cycle start point of t = 3132s to the cycle end point of t = 3532s; 400s total. The time values reference the abscissa of Graph 5.1, but are also shown in boxes in Graph 5.2. The wood specimens used thermocouple numbers 2, 3, 5, and 6 just as in Graph 5.1 and have the same colors as used in Graph 5.1. The chamber temperature uses the pink trace. There is not a chamber pressure trace in Graph 5.2 because the chamber pressure functioned as the dependant variable.

The bold black curve essentially splitting Graph 5.2 diagonally from upper right to lower left is generated from saturated steam table data. It is the pressure and temperature data for tabulated values of pure, “dry”, 100% saturated steam. The term “dry” means that there is not any condensed water entrained within the steam, just the ideal gas steam.

Above the saturated steam line is a thermodynamic state referred to as super-heated steam. This means that the steam is not saturated and is hygroscopic. The extent of superheat is described by the degrees Centigrade above the saturation line and the greater the degree of superheat the greater the propensity for the steam to absorb water from whatever source might be available; such as wood in the chamber during a VST process. To the extent possible avoidance of a superheated state in the chamber atmosphere at all times had to be accomplished for the VST technique to work.

Below the saturated steam line a state of “super-saturation” exists where condensation can occur within the chamber, producing liquid water. This zone is referred to as a compressed liquid state implying the pressure is greater than saturation pressure at that temperature. The desired condition within the chamber to minimize moisture loss from the wood during a vacuum cycle is on the saturated steam curve or below the curve. If the atmospheric state within the chamber (control volume) is that of saturated steam or compressed liquid, the relative humidity within the chamber will be 100% and evaporative loss from wood within the chamber will be minimized during a vacuum cycle.

The statement regarding 100% relative humidity in the chamber can be evaluated using the ideal gas law and considering saturated steam to be an ideal gas. By selecting a point on the black curve of saturated steam in Graph 5.2, the temperature and pressure become fixed.

Assume an experiment attains the point where; T = 83.7°C and P = 55 kPa. The volume of the chamber was calculated by the author after subtracting the volume of the shelf and found to be: $V_{chamber}$ = 0.0245 m^3. The ideal gas constant for steam is: R = 0.4615 kJ/(kgxK). Substituting into the ideal gas law and solving for mass:

$$m_{H_2O} = \frac{PV}{RT} = \frac{55 \times 0.0245}{0.4615 \times 356.9} = 8.17 \times 10^{-3} kg \qquad \text{Equation 5.1}$$

From saturated steam table data at the same temperature and pressure the density of steam is given as 0.33736 kg/m^3. Multiplying this by the volume of the chamber:

$$0.33736 \times 0.02447 = 8.26 \times 10^{-3} kg \qquad \text{Equation 5.2}$$

One definition of relative humidity is the mole fraction of water vapor in a mixture to the mole fraction of saturated water vapor at the same conditions. The moles can be attained for the above masses by dividing them by the molecular weight of water; 18.02 g/mole. Since the molecular weight occurs in both the numerator and denominator they cancel and the ratio of masses becomes the relative humidity:

$$\frac{8.17}{8.26} = 0.989 = 99\% \text{ Relative Humidity} \qquad \text{Equation 5.3}$$

Therefore, assuming pure steam in the chamber without any other gasses (such as air that had not been removed or volatile emissions from hot, moist wood), if the chamber trace remained on or below the saturated steam line during a vacuum cycle, then the chamber atmosphere would essentially be 100% relative humidity. If the chamber atmosphere were saturated, then moisture loss from wood during a vacuum cycle would be minimized.

5.2.3 The Chamber Pressure-Temperature Trace

As shown in Graph 5.2, the chamber trace did not remain at or below the saturation line during the entirety of the first vacuum cycle. It began the cycle below the saturation line, but the vacuum had not yet begun because by definition the cycle began with the shutting the steam inlet valve and venting the chamber steam to atmosphere. This section of the graph demonstrates that during the depressurization stage the chamber atmosphere remained saturated. At a point very close to 92.5kPa the waiting period for steam vapor to leave the chamber is seen as the constant pressure decrease in temperature. At the end of the constant pressure stage, the pressure decreases very rapidly because the vacuum valve to the chamber had been opened. The chamber trace remained below saturation briefly at the beginning of the evacuation, but crossed into the superheated state and that point was marked and labeled. The cross to superheat occurred at 3250s, at the pressure, temperature coordinates (P, T) of (79.8, 93.5). This was 110s after the start of the cycle. The length of time within the superheated state was a very brief 4s as seen by the next data point marked at 3254s, (46.7, 79.2). The temperature drop due to expanding gas during evacuation resulted in the chamber atmosphere entering a compressed liquid state. The state remained compressed liquid through the minimum temperature point at 3288s, (24.1, 46.4). This part of Graph 5.2 revealed that the atmosphere did not become superheated as soon as the chamber temperature began to rise during the vacuum cycle. At the point 3413s, (22.2, 63.6), before minimum pressure had been attained, the chamber atmosphere re-entered the superheated state; this point is also marked on Graph 5.2. The atmosphere diverged to 27°C superheat by the point (marked on Graph 5.2) of minimum pressure at 3481s, (18.4, 90.8). This point at 3481s was the transition from vacuum to steam

but the chamber atmosphere remained superheated until 3499s, (85.9, 95.4) when it crossed into the compressed liquid state again and remained through to the end of the cycle. For a combined elapsed time of 90s out of the total cycle time of 400s the chamber atmosphere was in a superheated state. To preclude excessive drying of the maple specimens in the chamber the amount of time during the vacuum cycle that the chamber atmosphere was in a superheated state had to be reduced.

5.2.4 The Wood Specimen Pressure-Temperature Traces

The vapor-pressure curve for gas within wood as represented by the curves for TC's: 2, 3, 5, and 6 shown in Graph 5.2 are quite different from the chamber trace. Due to the fact that the physical make-up of the gas within the wood is not known and could not easily be determined, inference of knowledge about the conditions within the wood could only be estimated from the vapor-pressure curves shown in Graph 5.2.

One estimate made was the proportion of total cycle time apparently spent within the superheated state. From the data for this test the time where the traces for TC's2, 3, 5, 6 crossed from superheat to compressed liquid was determined to be 3489s at (31, 70); this collection of points are shown on Graph 5.2. The cycle began at 3132s and the wood apparently began the cycle in the superheated state, therefore 357s of the total 400s cycle time (3489-3132) was in a superheated state.

Due to the uncertain composition of gas within the wood which could include a combination of steam, volatile extractives from the wood, and perhaps trace amounts of air, utilization of the pressure-temperature graph technique was not applied to the wood specimens

during the further development of the VST process. An important realization occurred as a result of noticing the very different form of traces (chamber and wood), and that was the maple might be contributing volatile organic compounds to the chamber atmosphere affecting the assumption of pure steam in the chamber. For this reason all subsequent testing to develop the VST technique was performed with no wood and only thermocouples positioned approximately where they would be had they been in wood, plus the chamber TC. The hypothesis to govern further choices in the developmental work then became; determine a standard operating procedure that will enable the chamber atmosphere to remain in the saturated or compressed liquid state throughout all stages and the wood will then 'follow' the chamber atmospheric relative humidity, plus the influence of Water Vapor Bulk Flow from VST.

5.2.5 Calculated Saturated Steam Temperature Graphing Technique

A second post-test graphing technique was utilized during development. A state equation had been developed by Abata (1982) to calculate saturated steam temperature in degrees Celsius* based on pressure values in pounds per square inch absolute (psia). It is a cumbersome equation, but once programmed into spread sheet software it became extremely helpful during the developmental work. Equation 5.4 is shown on the next page

*Abata first published in terms of Fahrenheit, the author incorporated terms for the unit conversion.

Saturated Steam Temperature (Tsat.), °C =

((101.74419+(77.052576+(11.951549+2.0562054x0.43429448xLN(P))x0.43429448xLN(P))x 0.43429448xLN(P)+(0.42070502+(-0.068410987+0.0625368x0.43429448xLN(P))x0.43429448x LN(P))x(0.43429448xLN(P))^4-0.0065948781x(0.43429448xLN(P))^7)-32)x5/9 Equation 5.4

Where: P = the real-time chamber pressure in psia

The trace generated by this equation is shown by the turquoise color and labeled: “Calc. Tsat.@Pcham.” in Graph 5.1. The utility of incorporating this trace is in the knowledge that a chamber temperature greater than the saturation temperature had to be within the superheated state, assuming pure steam in the chamber atmosphere. Conversely a chamber temperature less than saturation temperature had to be in the compressed liquid state.

After addition of the saturated temperature trace evaluation of the extent and duration of various process steps became a visual inspection effort. As examples of the observations made: (a) The initial vacuum stage in Graph 5.1 for example was almost entirely within the superheated state by 30°C; driving the kiln dried maple to a drier state, and (b) In vacuum cycle #1 we see the chamber trace nearly indistinguishable from the Tsat trace until about 78°C when the chamber drops below Tsat into the compressed liquid state. This corresponds very well with the vapor-pressure curve of Graph 5.2. Careful observations between a system graph such as Graph 5.1 with the Tsat curve added, and individual vacuum cycle pressure-temperature curves such as Graph 5.2 enabled informed process changes during the subsequent test and development effort.

5.3 Standard Operating Procedure Development Tests

Due to the strong evidence of radiant heat gain to the chamber atmosphere from the hot steel walls while under vacuum one hardware change was made before the testing began. A radiant heat barrier was built and installed in the chamber to protect the chamber TC from excessive heat gain. See Figure 5.1.

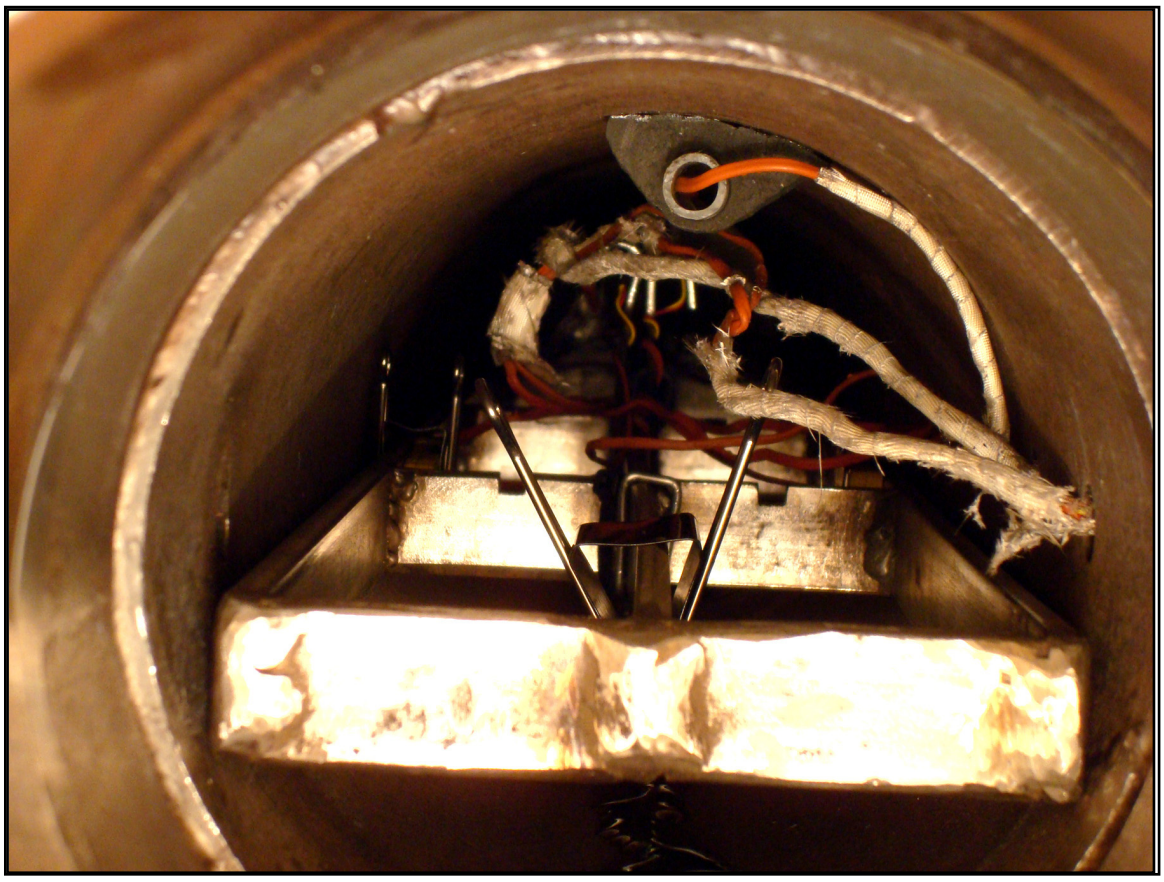

Figure 5.1 Radiation shield for Chamber TC to mitigate heat effect due to radiation from hot steel sidewall during vacuum cycle. Photograph by author, 2010.

Testing proceeded without wood in the chamber through 12 separate VST experiments. The chamber TC was mounted as shown in Figure 5.1. The other four thermocouple wires were attached to the clips that normally hold the wood so that the bare TC junction was positioned as

if it were in wood. There were essentially five TC's providing a temperature profile from the front to the rear of the chamber. See Figure 5.2.

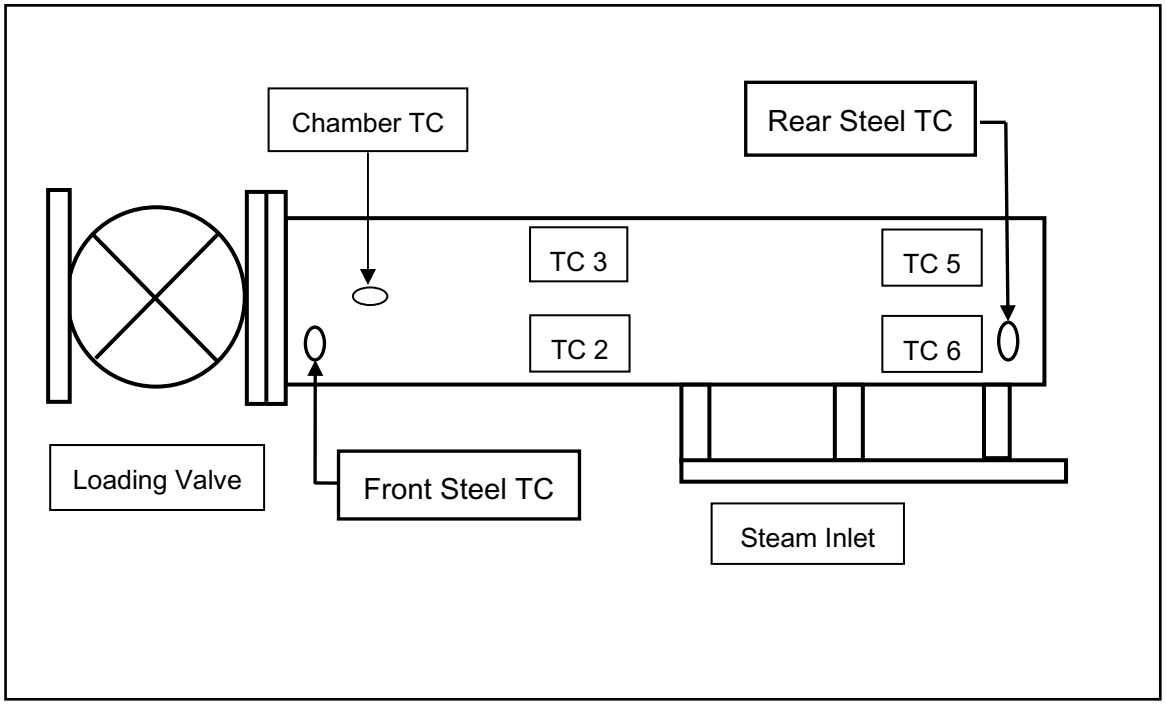

Figure 5.2 Schematic of thermocouple layout during VST developmental work. Produced by author 2011.

At the completion of 14 hours of testing and the evaluation of 73 graphs as described in Section 5.2 several details of operation were better understood. On the next page is a list comprised of a combination of process variables and/or procedural steps that were found to exhibit a noticeable influence on the chamber atmospheric conditions.

Intermediate determination of functional process variables:

a) The chamber must be pre-heated
b) Temperature of the steel chamber walls (after pre-heat)
c) Following the pre-heat, the empty chamber must be evacuated prior to any further steam addition for accurate saturated pressure-temperature data
d) The amount of condensate pooled within the chamber seemed optimal between 50ml and 200ml
e) The position of the steam trap trim valve; affects (d) above
f) There exists a practical duration of the steam cycle beyond which the VST process did not gain further benefit
g) There exists a practical extent (pressure) of the vacuum cycle beyond which the VST process did not gain further benefit due to a superheated environment
h) There exists a practical duration of the initial vacuum cycle for the VST process
i) The portion of the chamber closer to the loading valve where TC's 2 and 3 resided consistently registered a superheated temperature whereas TC's 5 and 6 and the chamber TC remained saturated or below

5.4 Procedural Outcome of the Developmental Tests

Several procedural aspects for experimental repeatability were identified and included: the initial vacuum cycle, the VST steam cycle, pooled condensate in the chamber, the VST vacuum cycle and the number of VST cycles. These topics are detailed in the next 5 sub-sections.

5.4.1 Determination of the Initial Vacuum Cycle

It was concluded that the vacuum cycle of RA #1 was unnecessarily long. The change of internal wood pressure due to evacuation of the chamber atmosphere should require approximately the same amount of time that was required for the evacuated wood specimens in RA #1 to reach 100°C when steam was introduced into the evacuated chamber. In RA #1 it was concluded that the sealant around the TC wires did not leak and therefore the internal temperature rise was due to WVBF of steam through the interstitial spaces of the wood to reach the TC junction in the center of the wood. Consider the following:

Steam progressed through the anatomical pathway in the mean elapsed time of 73 seconds at an initial differential pressure of approximately one atmosphere (reference Figure 4.6). The empty chamber vacuum pump performance attained 99% of the minimum possible chamber pressure in 60 seconds (reference Graph 3.1). Chen (1997) had produced evidence that the internal wood pressure curve during evacuation approximately paralleled the combined pump / chamber pressure performance curve (reference Figure 2.11). Therefore it was hypothesized that the maple used in this research would achieve an *initial* evacuated state in approximately 30 to 90 seconds from the point the *initial* vacuum cycle was begun.

The emphasis on the word `initial' is due to the critical distinction between the first vacuum cycle and the VST vacuum cycles when beginning with kiln dried wood. Graph 5.1 shows that kiln dried wood apparently lost very little temperature during the first 300s after vacuum was started and probably very little moisture during the same period. Reasonable insurance that the void spaces deep within the wood were evacuated would provide the best opportunity for the initial steam cycle to penetrate deep into the wood. The initial vacuum cycle

was established to mean the period from the opening of the valve between the chamber and the vacuum system to the point where the real-time instrumentation trace of the chamber pressure first reached a minima as observed on the computer screen. Referencing Graph 5.3 below, the pressure drops precipitously during the first 20 seconds after the vacuum began and then asymptotically approached its absolute minima. The *initial* vacuum cycle was terminated as soon as the pressure trace appeared to have reached the onset of the asymptotic section of the curve.

Graph 5.3 Modified, expanded scale and abbreviated trace from VST specimens #65 and #66 showing pressure trace of the initial vacuum cycle only and the chamber temperature.

In Graph 5.3 the black pressure trace initially followed local atmospheric pressure. The vacuum commenced around 82s, was stopped and switched to steam around 121s. From actual one-second interval data the total initial vacuum cycle in the case of specimens #65 and #66 was 39s.

5.4.2 Determination of the Steam Cycle

In Chapter 2 the discussion of the VST process for moisture re-gain posits that the only requirement for each steam cycle be the penetration of steam to the innermost regions of the wood, followed by condensation at that location. The moment that the vacuum induced pressure differential becomes neutralized by the influx of steam determines the moment that any subsequent moisture movement within the wood is dependant upon diffusion-based phenomena.

RA #1 determined that steam had reached the center of the evacuated wood specimens and caused an internal temperature increase to 100°C in an average of 73 seconds. The maximum elapsed time was 108 seconds; therefore, 108 seconds should have been a sufficiently long steam cycle for the size of specimens in this experiment.

However, due to the cyclic pressure control of the boiler (Section 4.2.1), attainment of the temperature 100°C did not reflect the endpoint of the first boiler pressure cycle following a vacuum cycle. Since the boiler steam pressure and therefore the chamber steam pressure were still increasing, the pressure differential within the wood had not been completely exploited until a chamber pressure maximum had been reached.

Close inspection of Graph 5.1 will reveal that the chamber pressure reached the first maximum after each vacuum cycle in less than 100 s for this test and the pressure decay period ended some time after that. Notes on the graph identify the data points typical of those reported in Table 5.1 below.

Table 5.1 Elapsed time data used to evaluate the duration of the steam cycle

V-S	$P_{min.}$	$P_{max.}$	P_{decay}	t_{Pmin}	t_{Pmax}	t_{Pdecay}	$t_{Pmax} - t_{Pmin}$	$t_{Pdecay} - t_{Pmin}$
Initial	11.58	115.31	102.90	1245	1329	1353	84	108
1st	18.41	117.28	103.21	3481	3534	3669	53	188
2nd	19.13	118.83	101.56	4281	4331	4506	50	225
3rd	18.62	119.76	104.15	4996	5040	5115	44	119
4th	20.37	119.97	104.56	5786	5840	5917	54	131
Avg.	17.62	118.23	103.28	n/a	n/a	n/a	57	154 (σ=50)

(Pressure (P) is in kilo-Pascal, time (t) is in seconds)

The last column in Table 5.1 is the elapsed time between the transition from vacuum to steam, to the point where the chamber pressure decay reached a minimum. The average time was 154 s. However, subtracting one standard deviation of 50 s had the potential result of some specimens not reaching 100°C. It was decided to add one standard deviation and then round to the nearest minute for ease of timing during the actual experimentation. The result was the choice to set the duration of the steam cycle to 3 minutes, or 180s.

5.4.3 Determination of the Benefit of Pooled Condensate within the Chamber during VST

In one test with ten VST cycles the condensate had been manually drained from the chamber after every steam cycle and measured. The steam trap trim valve setting permitted a

portion of the total condensate to be automatically discharged from the chamber during the steam cycles, and that was measured. Comparing the condensate drained from the chamber relative to the amount discharged by the trap was the metric for how to set the trap trim valve. Manually draining the residual condensate allowed observation of the effect of zero condensate in the chamber via the P-T graph. The following vapor-pressure graph of the 10th vacuum cycle is an indication of the importance of residual condensate in the chamber during the vacuum cycles as well as careful control of the steam trap trim valve. The fact that all thermocouple readings are essentially horizontal and are above the saturation line demonstrates a superheated steam environment during a vacuum cycle when residual condensate is zero.

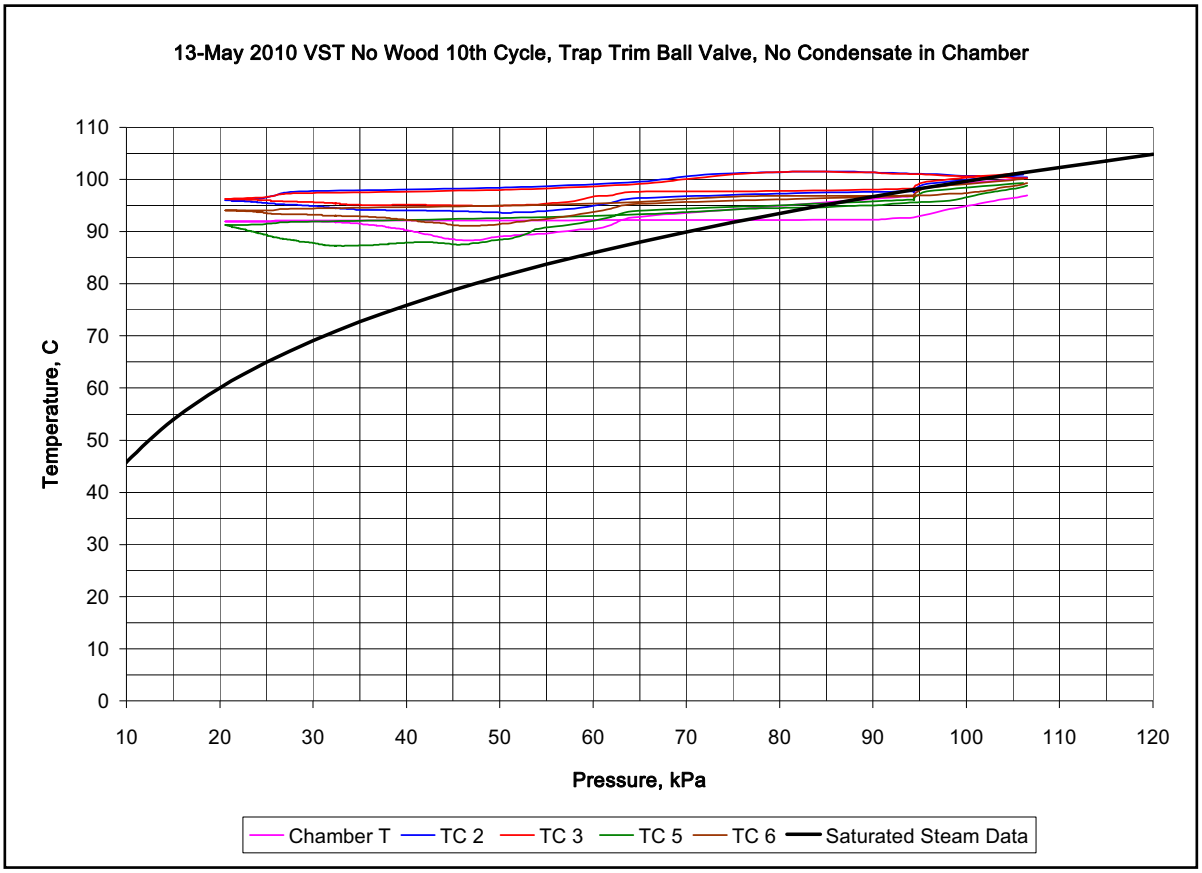

Graph 5.4 Pressure-Temperature data for the 10th vacuum cycle of a non-wood experiment

A needle valve had been installed to improve the steam trap trim adjustment. By setting the trap trim valve at different measured angles open and measuring the volume of condensate exiting from the trap a narrow range of positions was identified. The range of open positions was about 30° to 60° and between 50 ml and 100 ml condensate would be drained from the chamber after a 3 minute steam cycle.

The next graph is from a non-wood, 5-cycle VST test that only had condensate removed through the trap with the trim valve set at 60° open (no condensate had been drained manually). The benefit of condensate within the chamber on the chamber atmosphere can be seen where TC's 5, 6 and the chamber TC remain on or below the saturation line with the P-T graphing technique. Ultimately a 45° angle was found optimal (reference Figure 3.7, page 80).

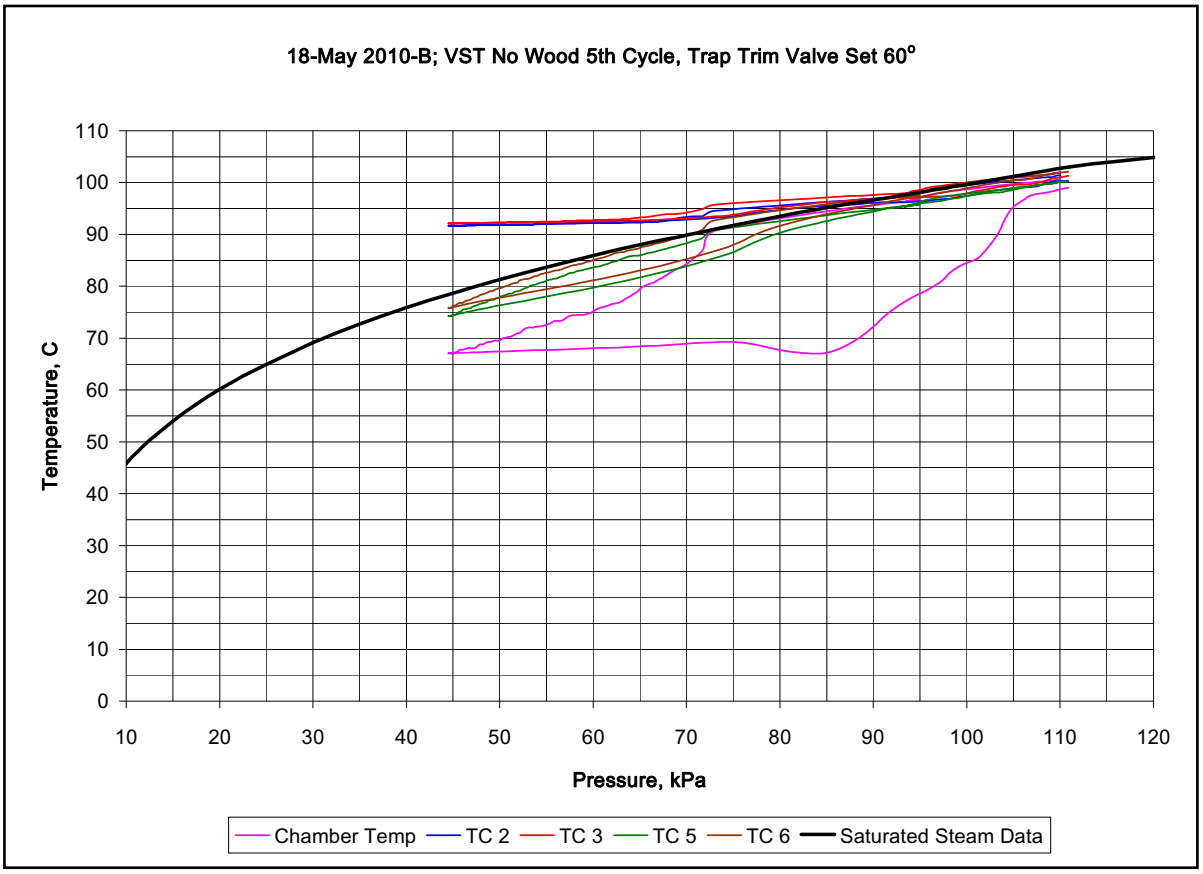

Graph 5.5 Showing very good chamber atmosphere control during vacuum cycle

5.4.4 Determination of the VST Vacuum Cycle

Section 2.7 discussed: (i) the pressure drop within the chamber and the wood, (ii) the temperature drop within the chamber and in the wood and (iii) the importance of minimizing moisture loss during the vacuum cycle. These are three critical attributes to understand and control for moisture regain with the VST treatment. The pressure within the wood (i) must be reduced below atmospheric pressure to enable the WVBF moisture transport mechanism to predominate. The temperature drop within the wood (ii) must be sufficient to permit the phase change of the steam to water within the wood so the heat of vaporization is given to the wood for rapid heat regain. Above all however was the need to minimize the moisture loss from the wood during the vacuum cycle (iii) as otherwise moisture would just circulate into the wood in one cycle and circulate out of the wood in the next cycle with undesirable results.

Several experiments were made with various minimum pressures during the vacuum cycles, which indicated that the consistency of control of the chamber atmosphere was not acceptable and a better control scheme was required. Graph 5.5 displays the tendency for TC's 2 and 3 to remain within the superheat state for reasons that were not determined, but was typical during many tests. TC's 5, 6 and the chamber TC remained below the saturated steam line. This result pointed to a degree of uncertainty regarding the use of TC's 2 and 3 when testing with wood. It was determined that wood specimens would not be placed on the front half of the shelf. Only the rear half of the shelf was to be used and therefore only two specimens per test regardless of whether the VST or atmospheric steam protocol were used.

As a result, two thermocouples became available and they were converted into a wet-bulb / dry-bulb (WB/DB) configuration for monitoring the chamber atmosphere during the

vacuum cycle. During the steam cycle the chamber was always in a saturated state or slightly compressed liquid state and under those conditions the wet-bulb always read practically identical to the dry-bulb because of the saturated conditions. Evaporation from the wet bulb would only occur during the vacuum cycle and that is precisely where the added measure of control was needed.

It was not a conventional usage of the WB/DB technology at and above the atmospheric boiling point of water, inside of a pressure vessel. One peculiarity observed was the WB registered a higher temperature than the DB during large segments of the vacuum cycle. It was hypothesized that the wet bulb cup of water in the chamber retained sensible heat of the water while the dry bulb thermocouple junction, positioned in the chamber atmosphere, had no such local energy store. As the atmosphere was removed by the vacuum pumps, expanding gas in the vicinity of the DB thermocouple caused it to cool while the WB thermocouple inside of the wet bulb sock which was soaking in about 100°C water did not cool down as quickly.

Despite these problems the WB/DB concept did prove useful during the latter portion of most vacuum cycles. The VST vacuum control point was determined to be when the DB temperature exceeded the WB temperature by 2°C, which was an indication of the chamber atmosphere drying out. If the chamber atmosphere were drying out, the wood specimens inside the chamber would begin to lose moisture also. The two degree WB/DB differential became a recognizable turn-around point in the real-time temperature trace generated during the experiments. On occasion when the WB continued to read hotter than the DB, a secondary control point minimum chamber pressure of 5% (52kPa) became the turn-around point. When the WB/DB two degree differential did work properly, 52kPa was the average pressure.

Figure 5.3 shows a close up of the wet bulb/dry bulb arrangement and the final version of the specimen placement ‘as tested’ for RA #2.

Figure 5.3 Wet bulb/Dry bulb arrangement. Wet bulb cup with wick over the TC and the dry bulb twisted wire TC near the cup, two specimens in position with clips securing the TC mini-plugs on the rack Photograph by author 2010.

5.4.5 Determination of the Number of VST Cycles to Plasticize Maple

Two tests were performed on full-sized maple specimens. One test incorporated the initial vacuum/steam cycle and seven additional VST cycles, the second test incorporated the initial vacuum/steam cycle and four VST cycles. As an example of how far the development of the standard VST procedure had evolved, Graph 5.6 shows the 7th vacuum cycle of one of the tests. Full sized maple specimens were instrumented with TC's 5 and 6, utilizing the WB/DB control technique.

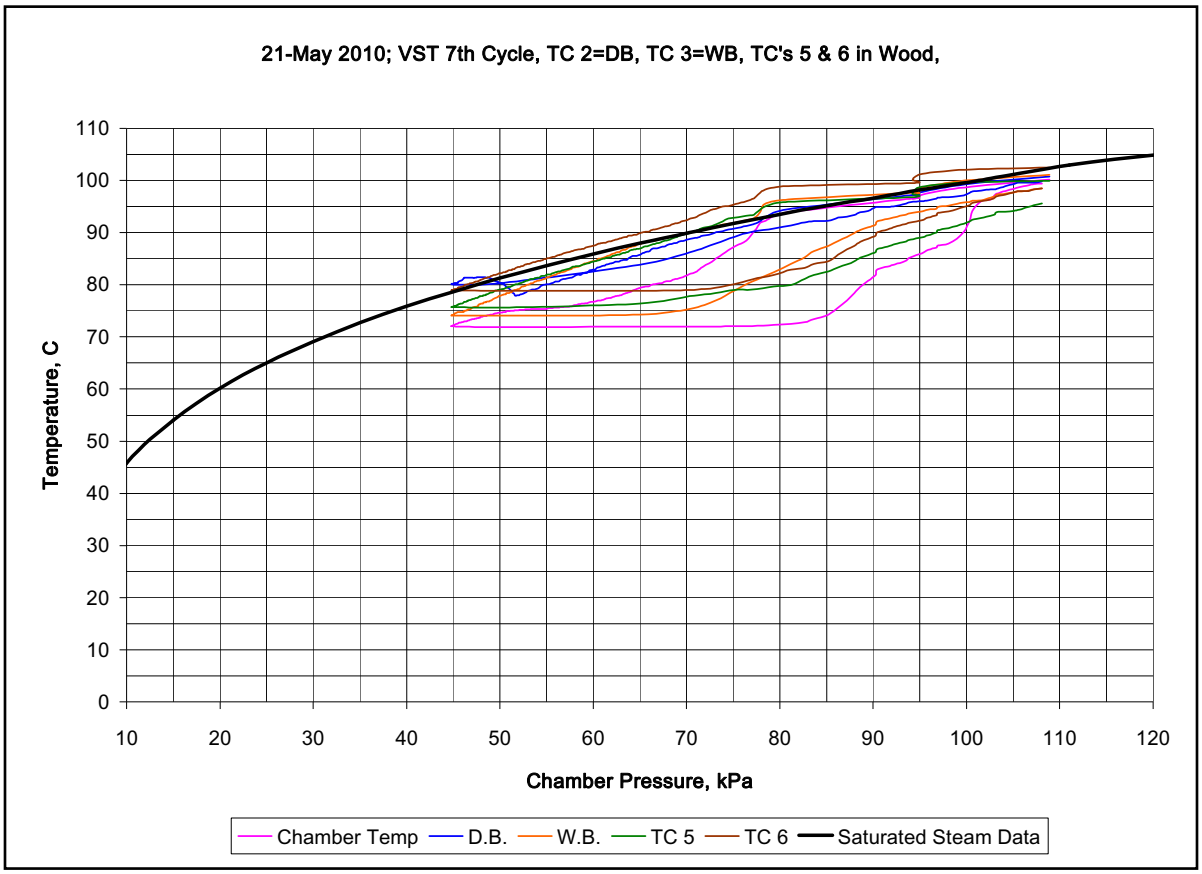

Graph 5.6 Final cycle - test with full sized wood specimens and standardized VST method

Success of the test is based on the actual moisture gain within the wood during the VST process. Table 5.2 lists four system tests of VST with maple specimens and the weights of

each specimen at appropriate points during the testing. The last row in Table 5.2 lists the percent moisture gain in each specimen due to the VST process. The position of each specimen in the chamber is listed to illustrate the performance characteristic of the specimen closest to the steam inlet gaining less moisture than the specimen closer to the chamber wall opposite the steam inlet.

Seven VST cycles, plus the initial vacuum and steam cycles resulted in an average of 35.7% moisture content gain due to the VST process; this was more moisture gain than necessary. Four VST cycles plus the initial vacuum and steam cycle resulted in an average of 16.8% moisture gain; this was on the lower edge of sufficient moisture gain. Ultimately, 6 VST cycles were chosen as the standard treatment for the specimen size used in this research. However the total treatment time also included the combination of the initial vacuum cycle and initial steam cycle, which in itself was a vacuum-steam cycle. Therefore, 6 VST cycles plus the initial cycle comprised the treatment for RA #2.

Table 5.2 Weights and moisture contents of maple following VST procedure tests

	VST 1	VST 2	VST 3	VST 4
Thermocouple #	TC 5	TC 6	TC 5	TC 6
Number of VST Cycles	7	7	4	4
Initial Weight, g	109.22 g	95.80 g	102.87 g	114.05 g
Initial Moisture Content, %	7.0 %	6.5 %	6.7 %	6.5 %
Final Weight, g	148.78 g	125.18 g	121.95 g	128.70 g
Final Moisture Content, %	45.7 %	39.2 %	26.5 %	20.2 %
Oven Dry Weight, g	102.08 g	89.95 g	96.39 g	107.10 g
Position (steam or wall)	Wall	Steam	Wall	Steam
Process Time, min: sec	45:00	45:00	27:00	27:00
% Moisture Gain from VST	38.7 %	32.7 %	19.8 %	13.7 %

5.5 Methodology: The VST Standard Operating Procedure and Notes

It was never the intent to optimize the VST process, but to develop a procedure that would produce bendable maple from kiln dried maple in a short period of time. The procedure follows:

a) Preheat chamber to a front steel temperature of: 85°C ≦ T_{Front} ≦ 90°C
b) Vent chamber to atmospheric pressure for specimen loading
c) Drain condensate from chamber, save for the wet bulb cup
d) Check that vacuum valve to chamber is closed and start vacuum pumps
e) Weigh specimens with TC's sealed in place, record initial weight
f) Open 150mm loading valve
g) Two specimens on rack @ rear, connect and secure specimens and their TC wires
h) Slide rack part-way into chamber, fill wet bulb cup, connect and secure WB/DB TC wires
i) Slide rack remainder of way into chamber, center chamber TC, check all TC signals
j) Close loading valve, record beginning steel temperatures. Ideally 82°C ≦ T_{Front} ≦ 86°C
k) Close chamber condensate drain valve, set steam trap trim valve to 45° angle w/ flange
l) Set steam trap condensate block and bleed to collect condensate from trap into cylinder
m) Open vacuum valve, observe vacuum trace on computer screen for *initial* $P_{minimum}$
n) Close vacuum valve, open steam valve, begin *initial* 3 minute steam cycle
o) Close steam valve, vent chamber to atmosphere, record trap condensate volume
p) [1] Close chamber vent, open vacuum valve, observe vacuum trace for (DB – WB) = 2°C or chamber pressure = 5.0% (52 kPa); whichever occurred first
q) Close vacuum valve, open steam valve, begin stopwatch for 3 minute steam cycle.
r) Close steam valve, vent chamber to atmosphere, record trap condensate volume
s) [2] If the steam trap condensate volume per steam cycle was below 450ml and if the front steel temperature was 80°C or less; both conditions for two consecutive steam cycles, then some condensate would have to be drained from the chamber.
t) Repeat VST steps {p, q and r} for 5 more cycles (6 total); incorporate step "s" as needed
u) Vent chamber to atmosphere
v) Drain condensate from chamber, record volume, save for the wet bulb cup
w) Open 150mm loading valve, disconnect TC's
x) Weigh specimens with TC's sealed in place, record final weight
y) Remove TC's from specimens, weigh the TC's and record for subtraction later
z) [3] Perform "over the knee" bend test, record observation

[1] Note about (P): The procedure for determination of the end of the vacuum cycle was: A maximum difference between the dry bulb temperature and the wet bulb temperature of 2°C, i.e. (DB – WB) = 2°C, or a chamber pressure of 52 kPa (5%); whichever occurred first. The technique to accomplish the control during an experiment required constant surveillance of the digital temperature readout for the DB and WB and subtracting numbers that were rapidly changing. Occasional hasty subtraction errors resulted in slightly more than a two degree differential but overall the repeatability from experiment to experiment was good.

[2] Note about (S): Monitoring the volume of condensate released from the chamber through the steam trap during the steam cycle provided evidence of the approximate amount of condensate remaining in the chamber. Earlier tests had determined that some condensate had to remain in the chamber to aid in maintaining a saturated atmosphere. However, too much condensate could result in water in contact with the wood. Wood soaking in water is not atmospheric steaming or the VST technique. The volume of condensate to be drained could not be determined because the total volume inside the chamber could not be known during an experiment. Ideally it would have been enough to leave a small pool of 50 to 200ml in the chamber. Realistically the chamber could not be opened. Practically, it was an intuitional guess in the moment of draining.

[3] Note about (Z): An “over the knee” test bend of wood specimens would be an indication of their state of plasticization immediately after the VST treatment. This ‘test’ was done by grasping the specimen at one end and at the midpoint where the thermocouple hole was located, and then trying bend across the top of the knee area. The bend was across half the specimen length because of the weakened center area from the TC hole.

5.6 Research Area #2 Results and Discussion Using VST Standard Operating Procedure

There were 27 specimens in the sample for RA #2, two per VST treatment. To maintain chamber dynamics the last VST treatment (27th specimen) reused a board from RA #1 to fill a space on the rack. Moisture content data are shown in Table 5.3.

Table 5.3 Moisture content data from RA #2

Specimen	Initial	Final	Change	Change/cycle	VST Time	Change/min
Number	% MC	% MC	Δ% MC	Δ%MC/cycle	Minutes	Δ%MC/min
77	9.1	33.7	24.6	3.5	31.23	0.79
78	9.5	26.2	16.7	2.4	31.23	0.54
79	9.0	21.1	12.1	1.7	28.13	0.43
80	9.1	19.3	10.2	1.5	28.13	0.36
81	9.7	34.8	25.0	3.6	41.42	0.60
82	9.1	41.7	32.6	4.7	41.42	0.79
83	9.3	38.2	28.9	4.1	39.08	0.74
84	9.4	39.2	29.8	4.3	39.08	0.76
85	7.8	37.3	29.5	4.2	37.37	0.79
86	8.0	55.5	47.5	6.8	37.37	1.27
87	8.0	42.9	34.9	5.0	37.72	0.92
88	8.3	29.3	21.0	3.0	37.72	0.56
89	8.2	19.5	11.3	1.6	34.15	0.33
90	8.2	31.5	23.3	3.3	34.15	0.68
91	8.1	32.0	23.8	3.4	36.38	0.65
92	8.3	38.0	29.6	4.2	36.38	0.81
93	8.6	36.8	28.2	4.0	36.55	0.77
94	8.8	39.9	31.1	4.4	36.55	0.85
95	8.7	37.9	29.2	4.2	39.08	0.75
96	8.8	46.8	38.0	5.4	39.08	0.97
97	10.1	45.7	35.6	5.1	39.40	0.90
98	10.0	57.5	47.5	6.8	39.40	1.21
99	9.1	44.5	35.4	5.1	37.72	0.94
100	9.0	53.2	44.2	6.3	37.72	1.17
101	9.5	40.8	31.3	4.5	34.80	0.90
102	8.7	53.1	44.4	6.3	34.80	1.27
103	9.5	21.8	12.3	1.8	31.70	0.39
Average	8.9	37.7	28.8	4.1	36.20	0.78
Std. Dev.	0.62	10.62	10.59	1.51	3.58	0.26

Table 5.2 contains several important results. The VST procedure in Section 5.5 successfully increased the average moisture content of kiln dried maple from 8.9% up to 37.7% for a change of 28.8%, in an average 36.2 minutes of total treatment time. The change in percent moisture content was divided by the total treatment time in minutes to produce the data in the last column; the % MC change per minute. On average the change in percent moisture content was 0.78 percentage points per minute. The maximum rate of moisture change was 1.27 percentage points per minute of treatment time. Based on the weight of the board immediately before and after the VST treatment, 1.27 percentage points is equivilent to 1.17g/min. of water absorbed by the maple due to the VST treatment.

The %MC change per cycle was calculated with the inclusion of the initial vacuum and steam cycle, therefore the total number of cycles was considered to be seven; the initial and six VST. The %MC change per cycle was 4.1% on average. Seven cycles occurred in the average total treatment time of 36.2 minutes, therefore each cycle required about 5.2 minutes. The average MC of 37.7% was more than the typical wood bending requirement of 20-25%. Consequently, to decrease the moisture content from about 38% down to 25%, a difference of 13%, might have meant three fewer cycles. Based on these research results, it is conceivable to begin with kiln dried maple and successfully plasticize it for bending in four total cycles, or about 21 minutes.

Moisture data from the specimens of RA #1 (Sp33-64) steamed at atmospheric pressure were used as an indicator of diffusion based moisture gain. The total treatment time, for either atmospheric steaming or for the VST process, was considered to begin when the chamber first left atmospheric pressure until it returned to atmospheric pressure. The change in the percent

moisture content of the specimens during the process was divided by the total treatment time so that a % MC change per minute was the resultant, normalized number. Those average values are the numbers beneath the columns of Figure 5.4. One standard deviation is indicated by the scaled error bars with the values listed above.

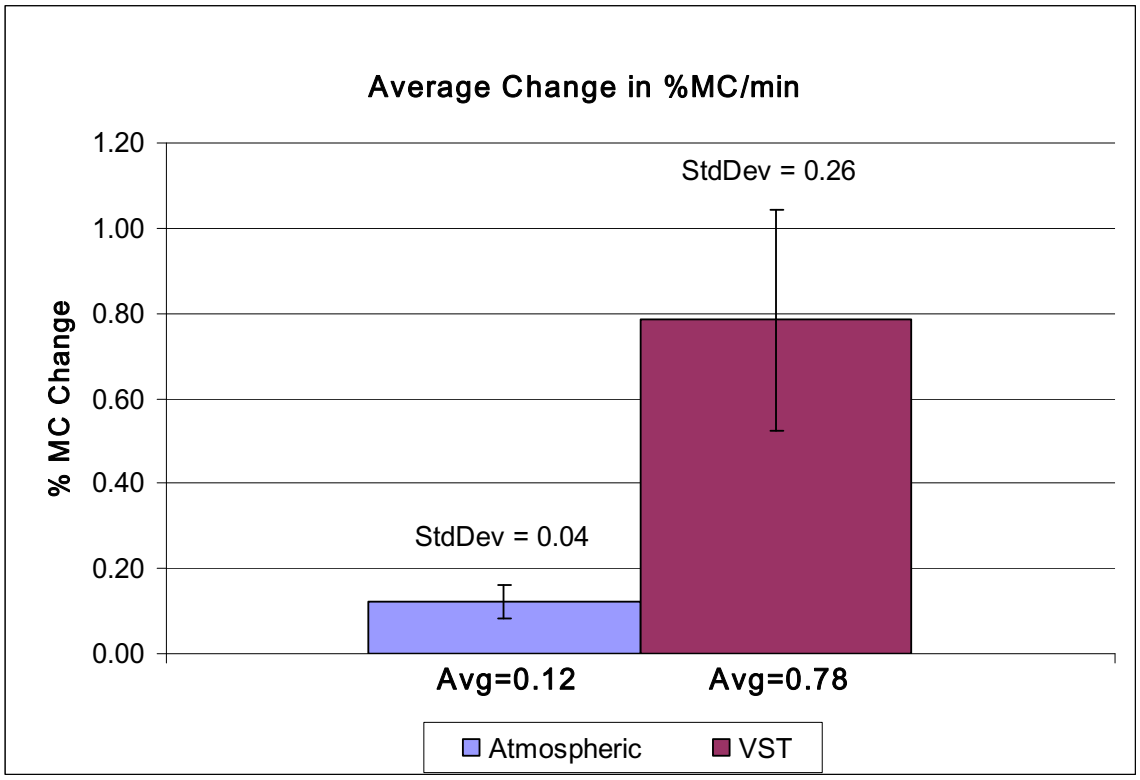

Figure 5.4 Percent moisture content change per minute for atmospheric steaming vs. VST Produced by author 2010.

The data of Figure 5.4 are vividly clear; on average the VST process resulted in a rate change of %MC/min which was 6.5 times greater than atmospheric steaming when using a sample population of similar maple specimens. Atmospheric steaming produced a maximum change of 0.14% MC per minute compared to the VST maximum change of 1.27% MC per minute; this correlates to a factor of 9 times greater with VST.

The total average treatment time was 36.2 minutes (2172s or 36min, 12s). This was important to determine because that elapsed time would become the steaming time used for the atmospheric steamed bending specimens in RA #3. This detail will be discussed in more detail in Chapter 6, Research Area #3.

5.6.1 VST – Specific Variables

Another clear trait of the VST process shown in Figure 5.4 was the variability with a standard deviation equivalent to one third of the mean. Several potential sources of the variability were investigated. Measurements of board weights after the VST treatment demonstrated a moisture content difference between the specimens based on location within the chamber. Because a specimen map had been sketched for every experiment, it was possible to split the data into two groups based on location in the chamber; the “steam” side and the “wall” side of the chamber.

Table 5.4 Variation in Δ(%MC) due to position in chamber

Steam Side			Wall Side	
Specimen #	Δ(%MC)/min		Specimen #	Δ(%MC)/min
78	0.54		77	0.79
80	0.36		79	0.43
81	0.60		82	0.79
83	0.74		84	0.76
85	0.79		86	1.27
87	0.92		88	0.56
89	0.33		90	0.68
91	0.65		92	0.81
93	0.77		94	0.85
95	0.75		96	0.97
97	0.90		98	1.21
99	0.94		100	1.17
101	0.90		102	1.27
103	0.39		n/a	n/a
AVG	**0.69**			**0.89**
STD DEV	**0.21**			**0.27**

The average values in Table 5.4 show there was a difference equal to one standard deviation in the change in percent moisture content due to the position of the board in the chamber. A Levine test for heterogeneity of variance of the data in Table 5.3 was performed: t = -1.19 for $t_{critical}$ = 2.06 and P = 0.24 and at α=0.05 two-tailed we fail to reject the null hypothesis and declare the variance are equal. A t - test with equal variance was then performed to compare the means of the data in Table 5.3. The t-statistic was -2.19 with $t_{critical}$ = 2.06 (two-tailed) and P = 0.038 so we fail to reject the null hypothesis at α=0.05 and state that the means are not significantly different; by a very slight margin. Nevertheless, a difference in means of one standard deviation is sufficient evidence to conclude there was a definite affect on the moisture gain based on chamber position and that variability most assuredly had an influence on the variability seen in Figure 5.4. Also note in Table 5.4 that the standard deviations within the segregated groups of “steam side” and “wall side” were large, at 0.21 and 0.27 respectively(one-third of the mean). This implied that within these sub-groups there were other factors affecting the variability.

The specific gravity of the maple was investigated as a source of the final moisture content variability. Figure 5.5 shows a distribution of the specimens in a plot of the percent change in moisture content due to the VST process versus the specific gravity at green moisture content. There are two groups of specific gravity, but the difference in the specific gravity does not appear to influence the amount of moisture uptake by the maple during the VST process. A Pearson’s Correlation test was done on the data and the coefficient was -0.003; confirming no correlation between specific gravity and moisture uptake due to the VST technique.

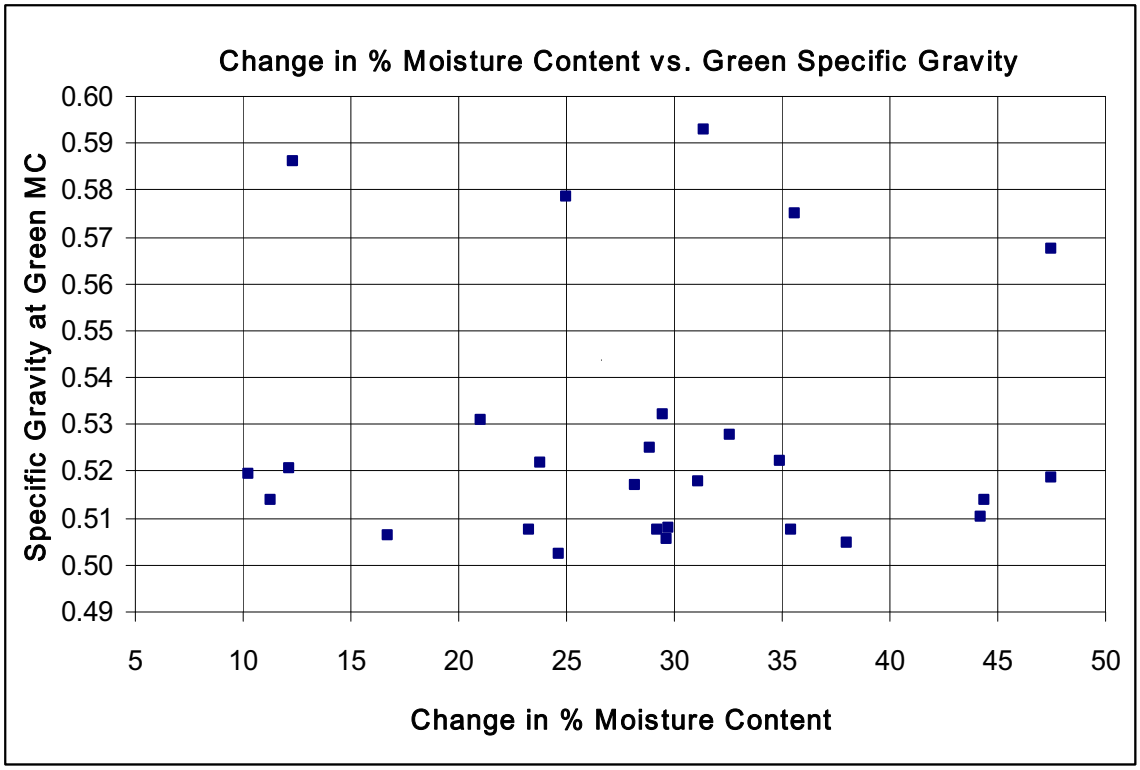

Figure 5.5 Influence of specific gravity on % moisture content change due to VST. Produced by author 2010.

A second variable was identified however, and it was actually a combination of variables resulting in a complex hydrothermal effect. The temperature of the steel chamber during the VST process was correlated to the overall steam condensate production rate, which was correlated to the steam trap flow rate, which was correlated to the chamber condensate accumulation rate. Ultimately, the percent moisture content change for the wood in the VST process was affected by the hydrothermal combination.

Complexity of the hydrothermal effect was further exacerbated by the performance of the steam trap utilized in the VST the system. The steam trap used was a Clark-Reliance model SFD-1 floating disc and that technology depends on both a minimum inlet pressure and a pressure differential (ΔP) for effective use. The VST steam system functioned with an average

maximum ΔP = 21.9kPa. This is the difference between the average maximum pressures; P_{MAX}= 116.7kPa, and the average local atmospheric pressures; P_{ATM}= 94.8kPa. The minimum *required* ΔP design value of the trap was found out to be ΔP = 25kPa for satisfactory discharge against the local atmospheric pressure. It was also later discovered the minimum pressure for proper operation was P_{MAX}= 130kPa. Therefore in two areas of applied design the steam trap was not suitable for the application and as a result probably did not perform consistently. It is reasonable to assume that some portion of the variability in percent change in moisture content observed in the VST process (Figure 5.4) was due to an incorrect hardware application.

Steel temperature average values (Figure 5.6) were in alignment with the VST operating procedure, Section 5.5, item J; 82°C ≦ T_{Front} ≦ 86°C. The front steel temperature range was 76.9°C to 91.6°C, and the rear steel temperature range was 91.6°C to 98.8°C. The rear steel temperature was not assigned a standard, nominal range.

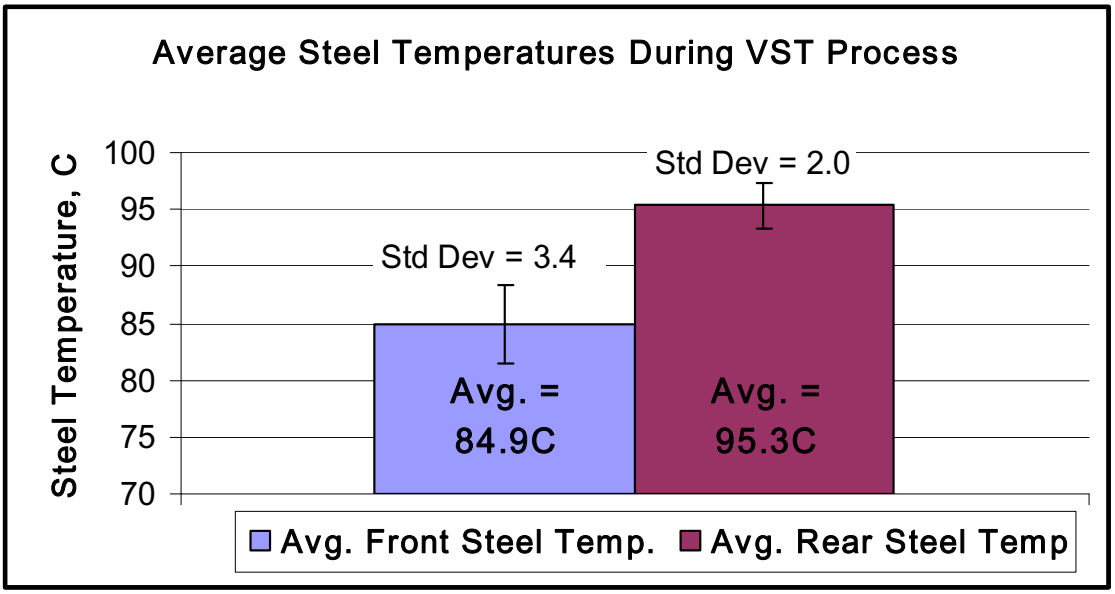

Figure 5.6 Average front and rear steel temperature for all VST treatments. Produced by author 2010.

The largest influence on steel temperatures occurred during specimen loading. During the task of specimen loading an assortment of TC wires had to be carefully fit into the chamber but not dislodge specimens from their position, or disconnect the TC mini-plugs, or spill the wet bulb cup. If an event occurred which required additional time, the steel lost heat but the experiment had to go on at that point. Therefore, despite pre-heating of the chamber occasionally the front steel temperature decreased below procedural levels.

Lower steel temperatures correlated with more condensate; Figure 5.7 below shows the effect. Total system condensate volume was calculated by summing the cumulative steam trap condensate with the chamber condensate drained at the end of the VST treatment. These values were plotted against the average front and rear steel temperatures for the corresponding VST trial. Pearson's correlation tests were performed. The front temperatures had a correlation coefficient of -0.68 and the rear temperatures had a coefficient of -0.63.

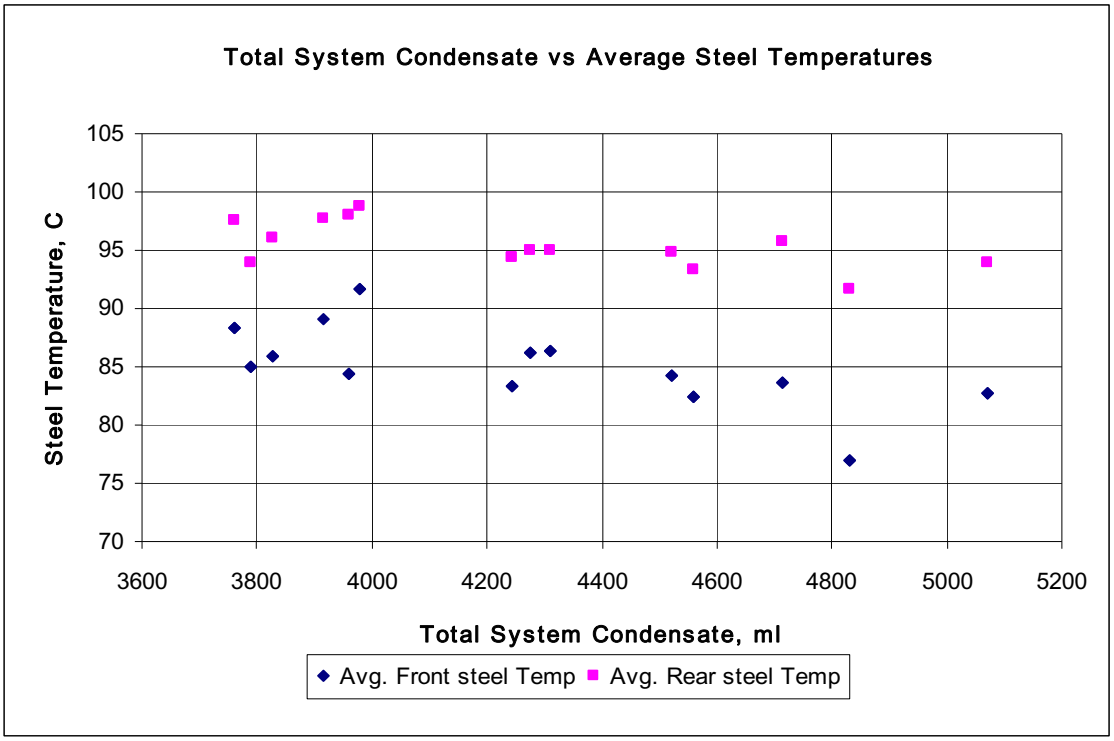

Figure 5.7 Total system condensate and average steel temperatures for VST, by author 2010

Increased condensate volumes did have a positive correlation with an increase in the change of %MC as shown in Figure 5.8. The Pearson's correlation coefficient was 0.59 for this data.

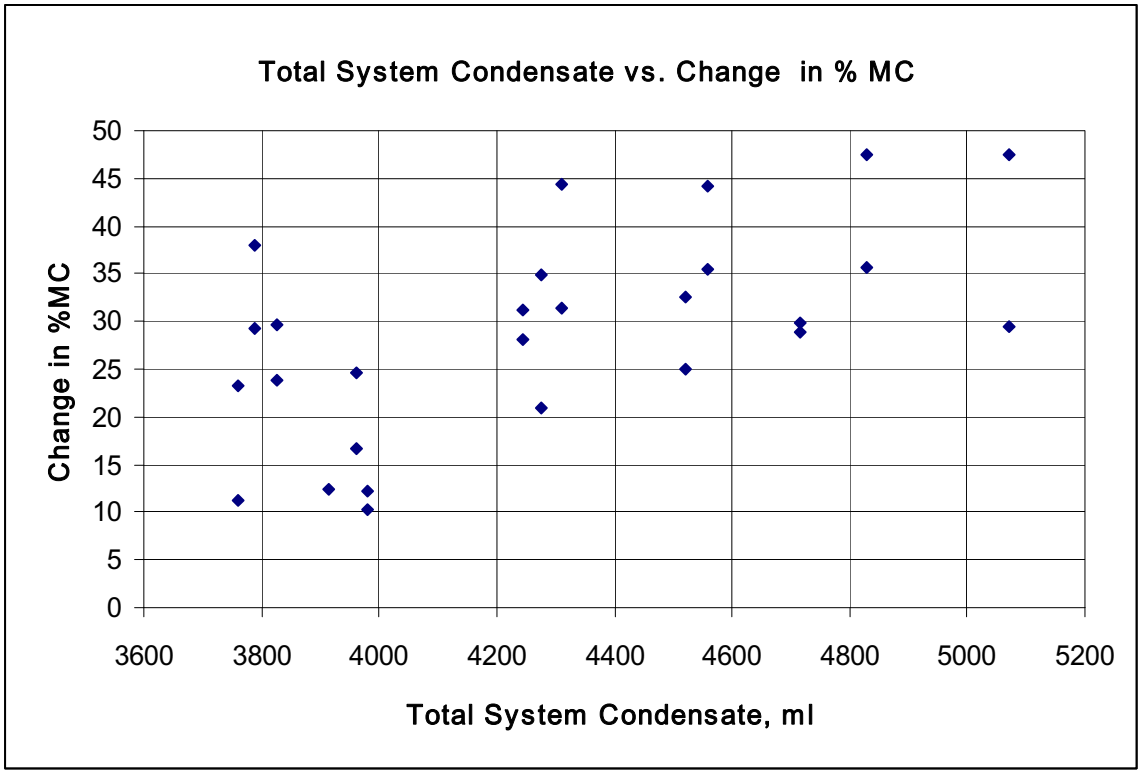

Figure 5.8 Total system condensate and the change in % MC due to VST process, by author 2010.

The data have shown that as the steel temperature decreases there was an increase in total system condensate, and as the total system condensate volume increased the percent change in moisture content due to VST also increased. Therefore it should not be a surprise that as the steel temperature decreased there was an increase in the variable of interest; the change in percent moisture content due to the VST process. A Pearson's correlation test was performed on the data and the correlation coefficients were strong. The correlation coefficient

for the front steel temperature to the change in %MC was -0.71.The correlation coefficient for the rear steel temperature to the change in %MC was -0.82. Figure 5.9 shows the relationships.

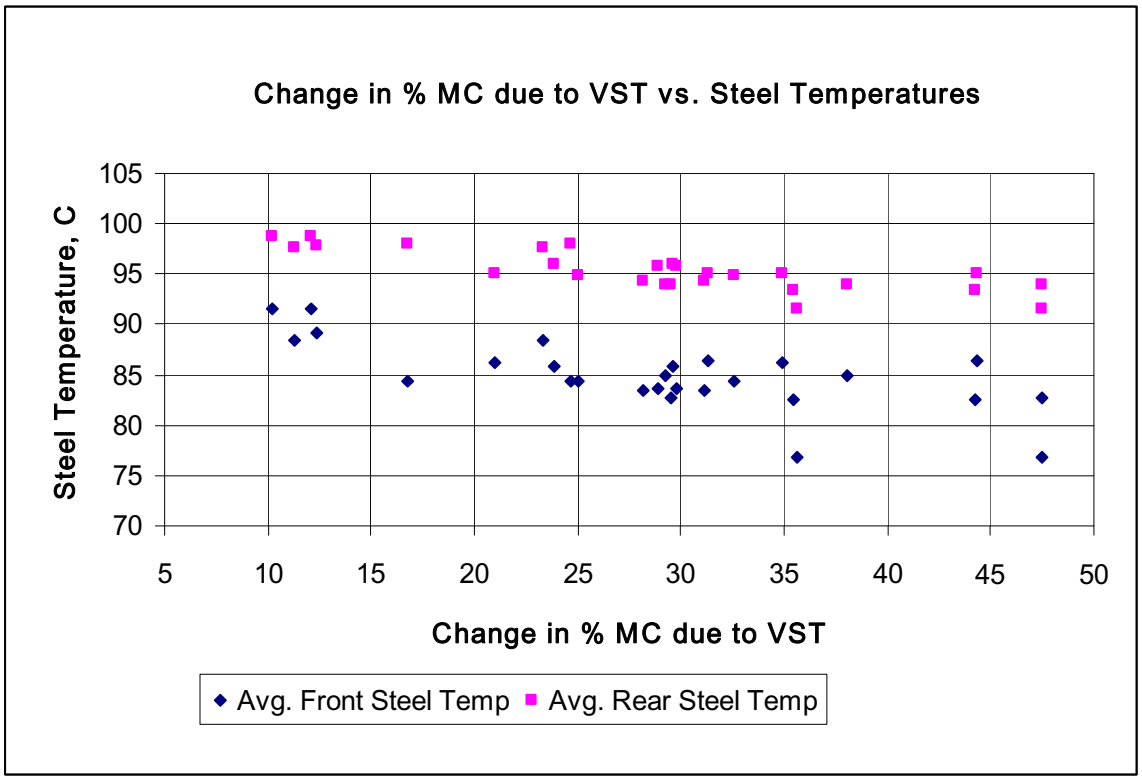

Figure 5.9 Change in the % MC of wood due to VST and temperatures of the steel, by author 2010.

5.7 Summary of Results for Research Area #2

- A VST procedure was developed which could increase the average moisture content of maple specimens from 8.9% to 37.7% in 36.2 minutes.
- The VST technique was shown to be radically faster than atmospheric steaming. On average the VST process resulted in a rate change of %MC/min which was 6.5 times greater than atmospheric steaming for similar maple specimens.
- The VST technique had quite variable performance with a standard deviation approximately one-third of the mean for change in %MC/min. The variability would have to be understood and better controlled for practical development of the technique.
- Of the variables investigated the strongest influence was the position of the boards within the chamber. Boards nearest the steam inlet were 23% less effective at moisture regain compared to the boards nearest the wall opposite of the steam inlet. This system characteristic influenced certain outcomes in Research Area #3 and will be discussed therein.
- Specific gravity of the maple specimens, variable over a range of 0.1 points differential, was found to have no correlation to moisture regain with the VST technique.
- A complex hydrothermal effect was identified which did introduce additional variability in the VST process. The strongest correlation was found to be a negative correlation (-0.82) between the temperature of the steel at the rear of the chamber and the change in % MC due to VST. That was followed by a negative correlation

(-0.71) between the steel chamber near the front and the change in % MC due to VST. A moderate positive correlation (0.59) was found to exist between the additional condensate produced as a result of cooler steel temperatures and the change in % MC due to VST. These correlations are important because they indicate areas wherein more uniform control of the variables would result in an overall improvement in system repeatability.

- The hydrothermal effect was further complicated by an inappropriate steam trap for the very low differential pressure and very low overall pressure utilized in the VST process. Careful positioning of the steam trap trim valve to a 45° angle as shown in Figure 3.7 reduced the influence.

Chapter 6: Work to Bend

6.1 Introduction to Research Area #3

The intent of this experiment was to treat two equal samples of maple specimens with two different techniques in preparation for bending and measure the load versus deflection data during a bending test in a way to facilitate the calculation of work as area under the curve of the load vs. deflection diagram. Atmospheric steaming served as the control technique and Vacuum Steam Technology (VST) was the experimental technique for preparing the specimens for bending. This experiment would address Objective (2) of this research:

> (2) Compare the work required to bend to form between VST treated maple and atmospheric steamed maple when beginning with low moisture content (<10%) specimens.

It would also answer the corresponding Research Hypothesis (2):

> (2) There is not a difference in total work required to bend wood due to the VST treatment relative to the classic process of atmospheric steaming when beginning with low moisture content (<10%) maple.
>
> Alternate Hypothesis: There is one treatment method which requires less work to bend wood than the other.

The initial concept for improving the state of the art for bending solid wood to form arose from an interest in the work of instrument luthiers and in particular banjo luthiers. To that end,

the author chose to design and build a press mould for this experiment that would simulate bending one half of a banjo hoop. Work with just one-half of the hoop, or a full 180°semi-circle, would permit use of the accurate, repeatable, and existing MTS hydraulic testing machines housed at the Virginia Tech department of Wood Science and Forest Products, Thomas M. Brooks Forest Products Research Center in Blacksburg, VA. Developing a testing procedure and a testing fixture for a full circle, 360° bend as is utilized in banjo making would have been prohibitive.

6.2 Design of the Press Mould

The author designed the press mould to simulate bending one half of a banjo hoop having an outside diameter of 304.8 mm (12 inches). The mould was comprised of two halves; a concave and a convex semi-circle that when matched together were separated by the height of the test specimens; 4.76 mm (3/16 inch). The mould halves were wider than the test specimen width to account for the possibility of slight misalignment when quickly placing specimens onto it. Small stops were attached to the finished mould to aide in rapid, repeatable placement. The convex mould was designed as the movable mould, to be attached to the MTS hydraulic ram and load cell. The concave half was located onto the test machine table and secured in place. Multiple empty tests were made to insure alignment and travel limits were properly programmed into the MTS computer. The concave half was designed with steel rollers mounted on axles with ball bearings, and the axle was supported by steel plate extending down to the MTS table. This insured a vertically rigid reaction point for the bending force but did not hinder the horizontal motion required as the wood specimen deflected during the bending test.

The mould worked very well for all tests with the exception of an oversight regarding close tolerances within the mould. The mould was not designed with any allowance for wood specimen swelling due to moisture content changes. Due to quite large amounts of moisture regain, some of the VST treated specimens had swollen enough to cause interference trouble during testing. The specimens that were swollen and cupped generally had been on the “wall” side of the chamber during the VST treatment. The “wall” side of the chamber had been shown in Table 5.4 to produce 0.2%MC/min more than the “steel” side. The interference occurred near the very end of the test when the final straight vertical section of the convex mould passed by the steel roller. The existence of artificially elevated load readings for the VST specimens due to swelling was further complicated by cupping across the width of the board due to the very high moisture uptake. In some cases the cup measured 50% of the original thickness of the board. Notes made during some bending tests recorded measurements of cup before and after the bending work. One example had 2.4mm cup (0.095 inch) before bending and 1.3mm (0.051 inch) after bending; clearly indicting the MTS machine did work in flattening the cup in addition to the work for bending. The interference manifest as an artificially high load as the maple was compressed within the tight tolerances. For this reason, all test data from the atmospheric control sample and the VST treated sample were truncated at 200 mm of deflection.

In addition to the tight tolerance issue described, another bending test artifact occurred at the beginning of the stroke during bending tests. To enable quick test set-up a 2 mm air gap between the top, movable mould half and the test specimen was programmed into the MTS control computer as its’ “return to” position. Before the beginning of each bending test the MTS ram would return to this programmed position and that left a small gap to easily fit the new

specimen into position. Due to there being zero force until the MTS ram moved enough to contact the specimen, and extremely light loads until the ram had traveled approximately 4 mm, forces were erratic and occasionally negative. These initial data points were considered noise and therefore the first 2% of deflection was removed from all data prior to calculating the load vs. deflection information from each file. The mould is shown in Figure 6.1.

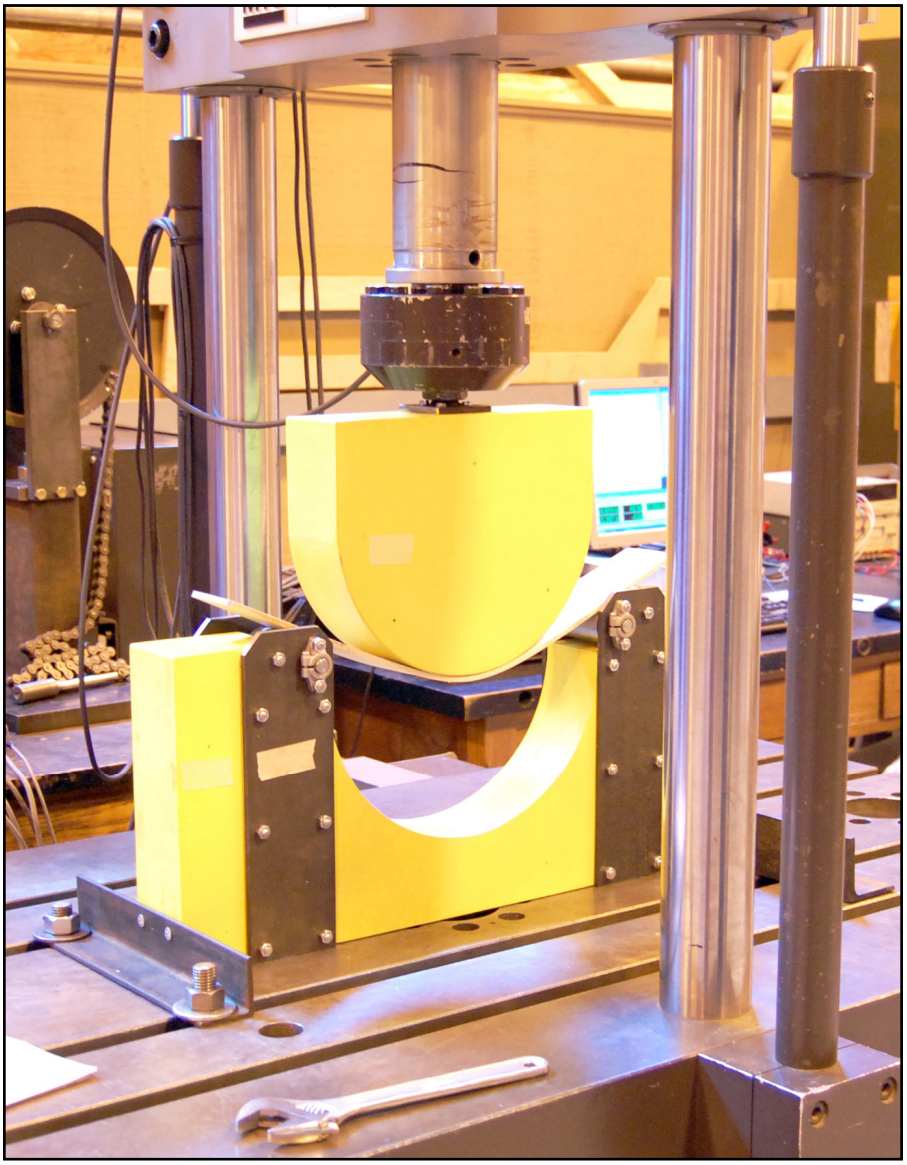

Figure 6.1 Press mould during bending test. Photograph by author, 2010.

6.3 Experimental Design

Each sample group in RA #3 was comprised of 30 specimens machined to the dimensions listed in Table 3.1 which had passed visual inspection for bending suitability as described in Section 3.3. The VST treatment sample was comprised of specimens 104 - 133. The atmospheric steam treatment (ATM) sample was comprised of specimens 134 - 163.

Since the goal of the experiment was to compare the work to bend maple based upon two different steaming techniques, the time of treatment was chosen to be the common feature between the control group and the treatment group. RA #2 had resulted in the development of a repeatable standard operating procedure for the VST treatment (Section 5.5). It was not an optimized treatment but it was successful at producing boards that had been plasticized *at least* enough for successful bending. “At least” is emphasized because several of the VST boards from RA #2 were more wet than necessary for successful bending, as 25% MC had been considered historically and empirically as the optimal moisture content for many species of wood (Section 2.2). The average total VST treatment time from RA #2 was 36 minutes, 12 seconds (2172 s). This became the treatment time for the atmospheric steamed control group. The postulation was that given the same process time and virtually identical maple specimens, the treatment technique for maple plasticization would be the variable.

Beginning with two specimens per plasticization treatment, they either underwent the atmospheric steaming treatment for 2172 s or they underwent the standard operating procedure VST treatment described in Section 5.5. Immediately before treatment and after treatment the specimens were weighed so that the moisture gain due to the treatment process could be determined. After the treatment and with absolute minimal time delay, the specimens were

placed one at a time into the bending press mould and the programmed MTS test cycle began for the load versus deflection data. The second specimen was left within the open chamber to maintain wood temperature while the first specimen was undergoing the bending test. Each bending test required about two minutes including the loading and unloading of the specimen. The actual bending test data spanned 94.5 seconds for each specimen at a strain rate of 2.12 mm/s (0.083 inch/s) which resulted in a total deflection of 200 mm (7.874 inch).

The MTS computer recorded elapsed time data, load data, and deflection data at the average rate of eight data points per second for very high resolution of the load vs. deflection data. The area underneath the load deflection curve is equivalent to the work required to perform the bending (Bodig and Jayne 1982). To calculate this area directly from the load and deflection data, an approximation to the integral of the load vs. deflection curve equation was performed. The reason for this approach was due to the fact that the precise equation describing each individual curve was not known and was not provided as a part of the data file from the MTS computer. However, with the high rate of data acquisition the integral approximation would be quite close to the actual integral. Since the data points were recorded about every $1/8^{th}$ of a second, the displacement that occurred between two data points was approximately 0.26 mm (0.010 inch).

The approximation calculated the average load between two consecutive data points and multiplied that force by the corresponding net displacement between the two points for the product of (force * distance), or work. Each incremental work product calculated throughout the test was summed for the total work to bend. An illustration and sample calculation follows.

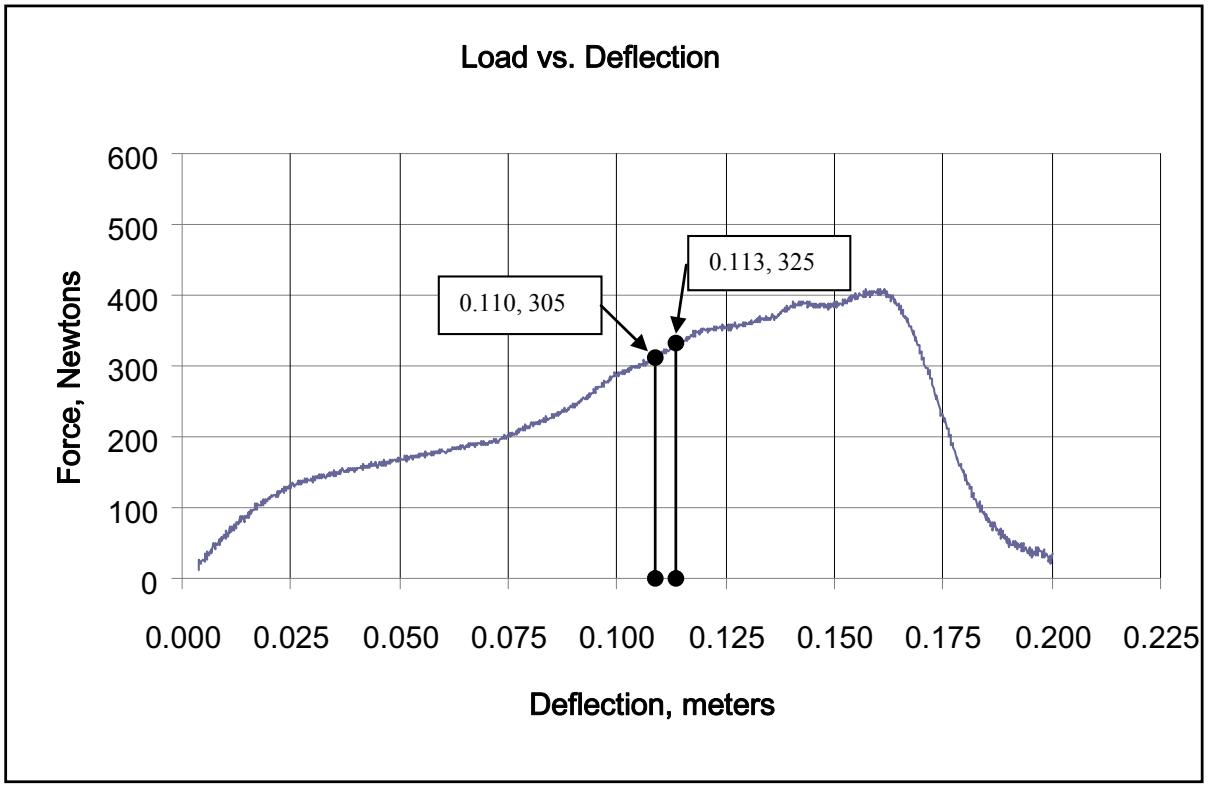

Figure 6.2 Typical load vs. deflection graph of bending test, with approximate points labeled. Produced by author 2010.

Two data points are labeled in Figure 6.2, but at a distance much further apart than the actual data. The boxes are the (X, Y) coordinates for the points. The approximation of the area under the curve and within the black vertical lines is given as follows:

$$\left(\frac{325+305}{2}\right)\times(0.113-0.110) \qquad \text{Equation 6.1}$$

In integral calculus as the distance along the X axis (ΔX) becomes smaller, approaching zero, the error due to the averaging of the change in the curve (ΔY) also approaches zero. In the data for this research ΔX = 0.26 mm (0.010 inch), therefore the error in calculating the area under the load - deflection curve with this approximation technique will be small relative to an exact integral over the total deflection range.

6.4 Results and Discussion

The plasticization step for the atmospheric control treatment was a straightforward matter of running a stop watch and stopping the steam treatment at 36 minutes, 12 seconds (2172s). The VST treatment times were derived from the data, summed and averaged. Those data are presented in Figure 6.3 below. The resultant average RA #3 VST treatment time was 2138s; therefore, RA #3 average VST treatment time was 1.6% (34s) shorter than the VST treatment time from RA #2 given the same VST standard operating procedure. Since the treatment time for the atmospheric steamed group in RA #3 was based on the average VST time from RA #2, the atmospheric steamed control group in RA #3 was actually in the plasticization process for 34s longer that the VST group of RA #3. This is important because had the overall times been reversed, the results could have been unfairly skewed in favor of the VST technique.

Due to the fact that there was only a 1.6% difference (34s) in the plasticization process time between both sample groups in RA #3 it was concluded that direct comparison of work to bend based on equal process times was appropriate and the null hypothesis could be evaluated.

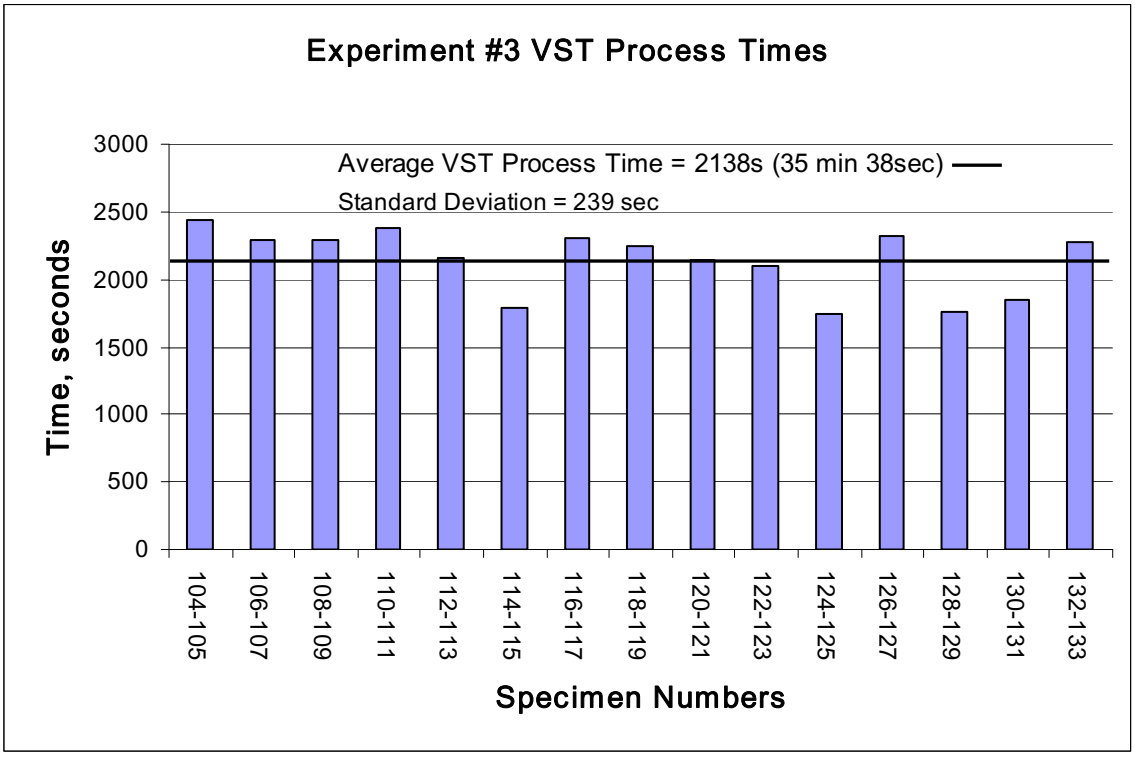

Figure 6.3 VST process times for RA #3 with average total process time, by author 2010.

The change in percent moisture content per minute of the specimens during the process was divided by the total treatment time so that a % MC change per minute was the resultant, normalized number. Those average values are the numbers beneath the columns of Figure 6.4 shown below. One standard deviation is indicated by the scaled error bars with the values listed above. The treatment of the VST data for RA#3 was identical to that done in RA #2. The change in moisture content results from RA #3 are vividly clear; on average the VST process resulted in a rate change of %MC/min which was 6 times greater than atmospheric steaming when using identical pieces of maple. VST produced a maximum change of 1.3 %MC/min, a minimum change of 0.2 %MC/min., and a large standard deviation of 0.31 %MC/min. The average total gain in %MC due to the VST process was 26.3% with a maximum gain of 47.6%. The maximum gain was equivalent to 6.8 %MC change per cycle.

For the data represented in Figure 6.4 an F-test for equality of variance resulted in an F-statistic of 89, rejecting the null hypothesis that the variances are equal. Consequently a two-tailed t-test with unequal variance and α = 0.05 was used to compare the data. In that test the t statistic was 10.5, t-critical two-tailed was 2.04 with a probability value P = 0.001 and based on that it is concluded there was a significant increase in the change in %MC/min. Given equivalent treatment times the plastic deformable state was significantly improved due to cycles of vacuum and steaming in the VST technique.

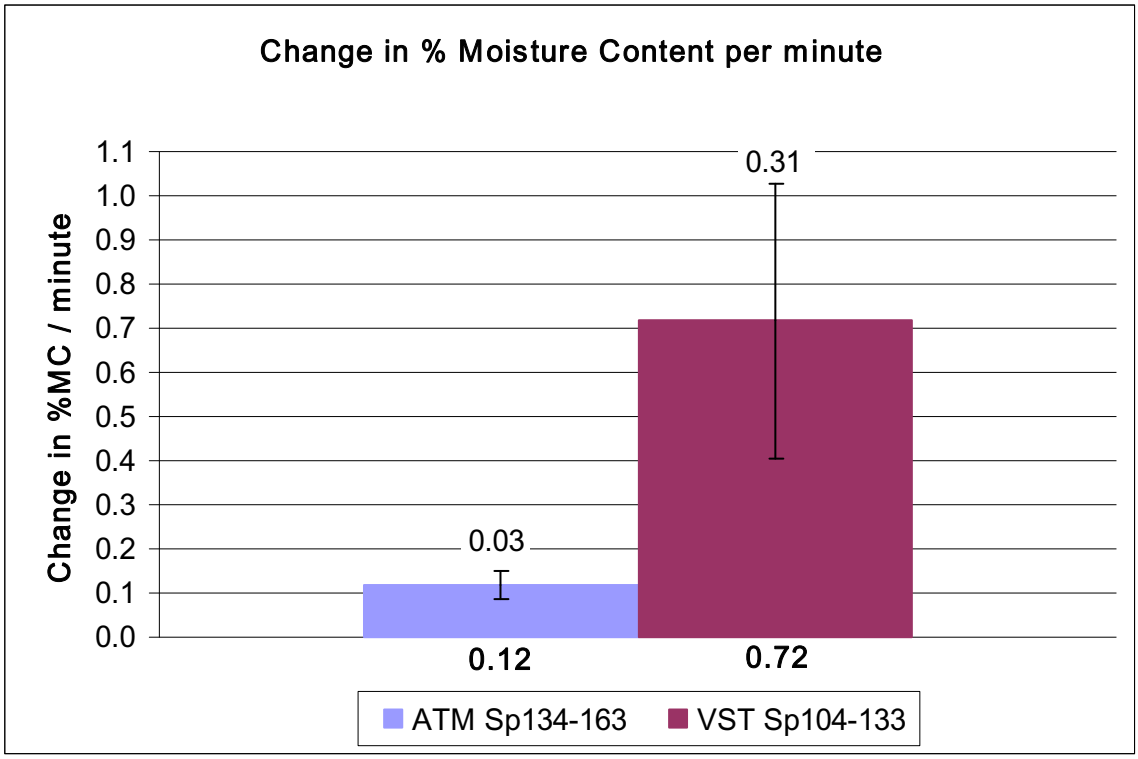

Figure 6.4 Change in % MC per minute of process time for specimens in RA #3. The numbers beneath columns are average %MC/min, by author 2010.

Two anomalous data points had been removed (156 and 157) from the atmospheric steamed control group due to excessively low steel temperatures at the beginning of an experiment (trouble loading specimens into chamber). The results showed an average total

percent moisture content gain of 4.3% with a maximum of 7.0% total gain in MC due to the atmospheric steaming treatment. The average moisture contents of the wood immediately before the plasticization treatment began were 9.7% for the VST sample and 9.6% for the atmospheric steamed sample; see Table 6.1:

Table 6.1 Average values from moisture content changes due to plasticization step

Specimen Numbers	Pre-Treatment %MC	Post-Treatment %MC	Avg. %MC Gain Due to Treatment	%MC Gain Per Minute
VST Sp 104-133	9.7	36.0	26.3	0.72
Atm. Sp 134-163	9.6	13.9	4.3	0.12

The work to bend portion of RA #3 resulted in 0 failures in the VST treated sample. Some were so well plasticized that they remained extremely flexible 2.5 hours after removal from the chamber. Such flexibility would be problematic in an actual wood bending process because the wood must re-set into the bent form in a relatively short time to enable further working of the piece. This observation hints at the need for further optimization of the VST technique to achieve optimal plasticization with slightly lower moisture gains per treatment. Fewer VST cycles to reduce the total moisture gain would beneficially further reduce the total plasticization process time.

In clear contrast, 11 of the 28 specimens in the atmospheric steamed control group fractured during the bending test, resulting in a 39% failure rate.

The difference between a 0% failure rate in bending (VST) and a 39% failure rate in bending (atmospheric) is significant. It was important to verify the result was due to the VST treatment technique. Within the atmospheric steamed sample group the data were investigated

for differences in treatment results between the specimens that did not fail and those that did fail in bending. Moisture contents were looked at and are shown in Table 6.2:

Table 6.2 Moisture data for atmospheric steamed group segregated according to broken during bending vs. not broken during bending

Moisture Content Results After Atmospheric Steaming	Broken Specimens	Not Broken Specimens
	n = 11	n = 17
Average	13.6	14.0
Standard Deviation	0.89	1.34
Maximum	15.3	16.1
Minimum	12.7	12.0

A two tailed, equal variance t-test was performed for the final atmospheric steamed moisture content data testing the null hypothesis that there is not a difference in the mean moisture contents between the two groups. The probability statistic was P = 0.39 for alpha = 0.05, the t statistic was -0.88 and t-critical was 2.06 and on this result we failed to reject the null hypothesis and there is not a significant difference between the mean moisture content values of the two groups in Table 6.2.

All specimen boards from RA #3 were visually inspected again (by the author) after the bending test, with particular attention to grain irregularities and slope of grain. This was done to confirm that from the pool of 60 boards, which had been previously inspected twice and selected into the bending specimen pool based on suitable bending quality, there was not preferential selection for which boards were to receive the atmospheric steam treatment vs. the VST treatment. The inspection segregated boards into “good grain” (GG) and “peculiar grain” (PG) for the atmospheric boards and the VST boards. A ratio of PG/GG was determined for the

atmospheric steamed boards that broke during bending, the atmospheric steamed boards that did not break during bending, and the VST boards.

For the atmospheric steamed boards that broke, the PG/GG ratio was 0.8 (5 PGs, 6 GGs). For the atmospheric steamed boards that did not break, the PG/GG ratio was 0.4 (5PGs, 12 GGs). The boards which broke had a much larger relative population of peculiar grain boards. This makes sense with every recommendation in existing literature for bending solid wood: select boards with clear, straight grain.

The inspection of the VST boards revealed a PG/GG ratio of 1.3 (17PG, 13 GG). This ratio and the fact that *none* of the VST boards broke is a strong indication of the robustness of the VST technique for plasticization of maple. The VST technique might enable the successful bending of less than optimal grade woods.

Specific gravity (G) adjusted to a green moisture content was investigated for influence on the results of the change in per cent moisture content due to the two treatments of RA #3. Correlation coefficients were calculated for the VST change in % MC vs. G and it was -0.19. The Atmospheric specimens that broke had a coefficient of -0.25 and for the atmospheric specimens that did not break the coefficient was 0.05; where 0.00 is no correlation.

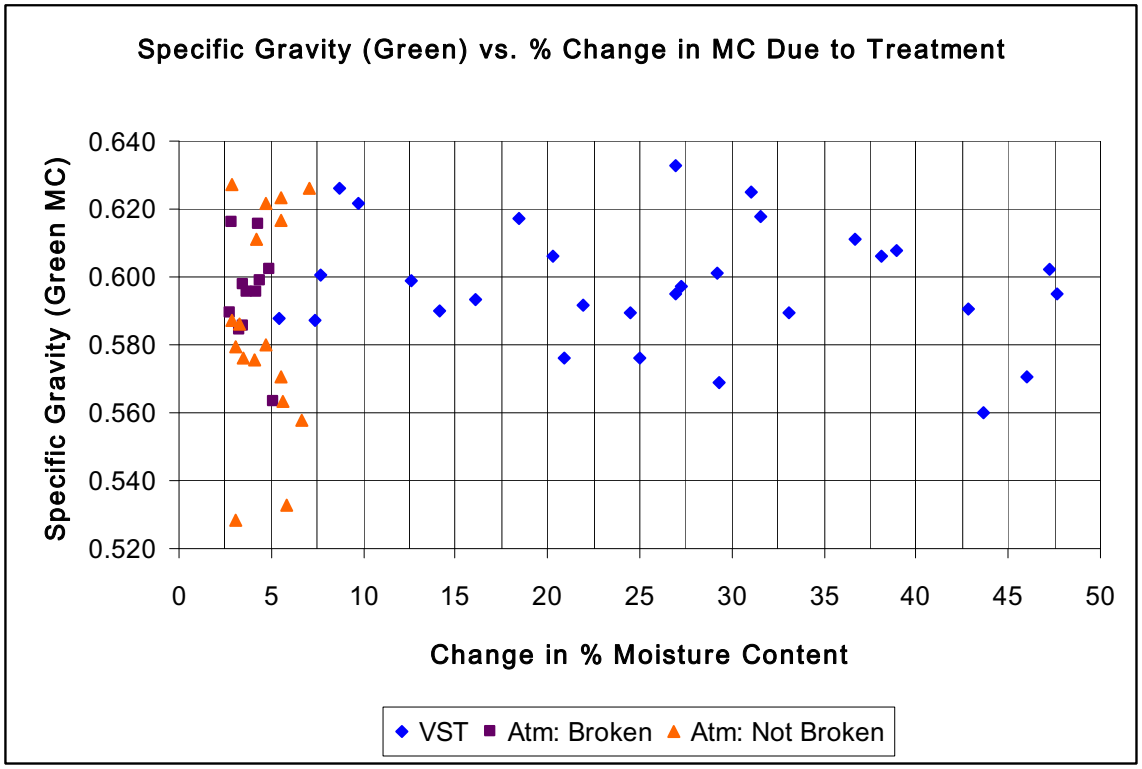

Figure 6.5 Specific gravity influence on change in %MC due to steaming treatments, by author 2010.

Figure 6.5 illustrates the spread and indicates no correlation between specific gravity and moisture regain with either technique. Figure 6.5 also serves to show there was no apparent influence due to specific gravity variations on the control group specimens that broke and those that did not.

Of the variables monitored within this experimental design there were not any significant differences between the atmospheric steamed specimens which broke during bending and the atmospheric steamed specimens which did not break. The author's post - bending examination of grain peculiarities gave indication that there was occurrence of some grain angle variability which may have contributed to bending failures but this was not statistically determined. Skaar (1976) demonstrated that damage to wood due to the combination of heat and steam occurred

quickly. Approximately 53 days at 100˚C heat was necessary to reduce the modulus of rupture of dry wood by 5% compared to only 16 hours for steaming at 100˚C; a 98% reduction in time required for damage due to the presence of steam. Finally there is a typical distribution of strength variations between boards due to the heterogeneity of wood as a material and this undoubtedly had an influence.

The atmospheric steam treatment used in RA #3 may have been on the very edge of conditions for plasticization. Beginning with kiln dried maple and steaming for roughly 36.5 minutes for 4.76mm (3/16”) gives a ratio of 7.7 min/mm (77 min/cm or 195 min/inch). This figure is 2.5 times the rough ‘rule-of-thumb’ estimate mentioned in the literature review section: 30 min./cm (75 minutes per inch) for ‘drier’ wood. However, the length of steam time also resulted in failed bends 39% of the time. This an indication of the particular demands of moisture regain in kiln dried wood for luthier and other applications.

In contrast the VST treatment as performed in RA #3 (and RA #2) resulted in excessive moisture regain and excessive plasticization during the same time period. Hence the period may be reduced and still maintain 100% successful bending of kiln dried wood. The VST treatment was divided such that steam time was roughly one-half to two-thirds of the total, the balance being vacuum time. A reduction of the time that wood is exposed to steam is beneficial for retaining the strength of the material (Skaar 1976). The VST process successfully plasticized a higher percentage of maple specimens that included less than optimal grain characteristics compared to the atmospheric steamed control group.

To achieve Objective (2) and address Research Hypothesis (2), evaluation of the total work required to bend the specimens necessitated the removal of bending data for the boards which broke during bending. Breaking is not successful bending and the data must not be compared. The evaluation was made using 17 atmospheric steamed boards that did not break compared to 30 specimens in the VST group. The data are presented in Figure 6.6:

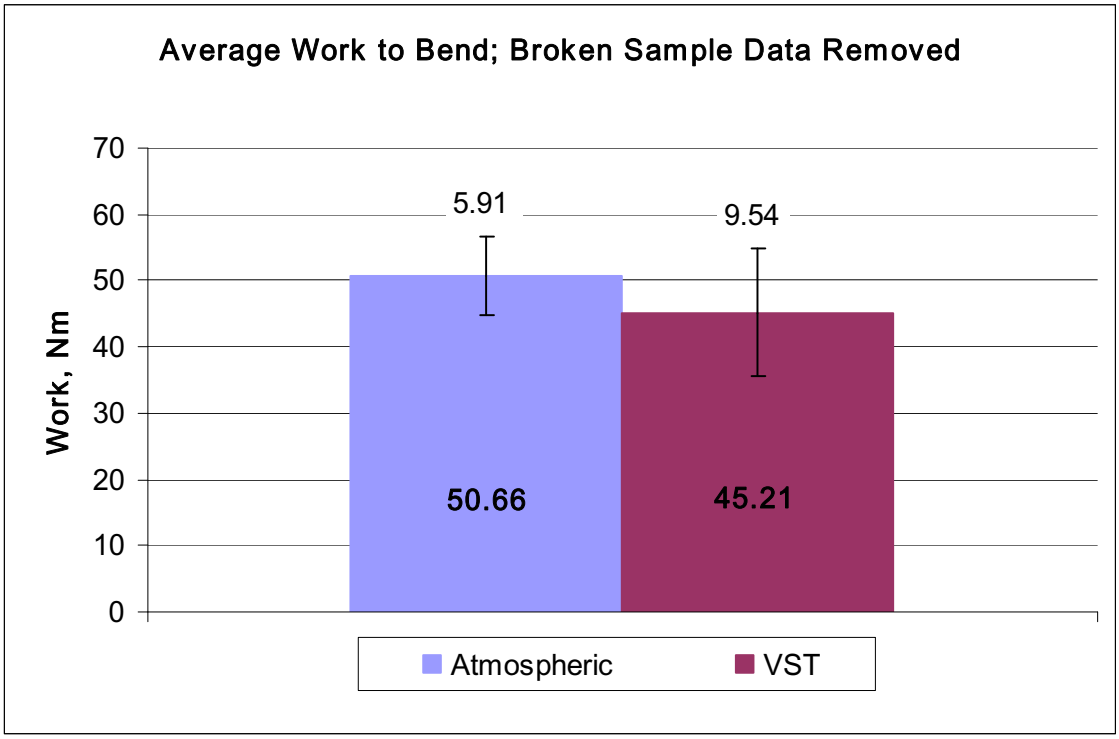

Figure 6.6 Average values of the total work (Nm) to bend. Data are in bold font in the columns, standard deviation values given above the error bars, by author 2010.

An F-test for equality of variance resulted in an F-statistic of 2.6, rejecting the null hypothesis that the variances are equal. Consequently a two-tailed t-test with unequal variance ($\alpha = 0.05$) was used to compare the data. The t statistic was -2.47, t-critical two-tailed was 2.01 with a probability value $P = 0.017$; therefore, we reject the null hypothesis and conclude that there was a significant decrease in the amount of work to bend VST treated maple compared to

the atmospheric steamed maple specimens that did not break. The average work to bend was 5.5 Nm less for the VST treated sample, significant at P = 0.017.

6.5 Summary of Results for Research Area #3

- The average moisture content of maple specimens changed from 9.7% to 36.0% due to VST in a treatment time 35.6 minutes, and for the atmospheric steamed control the average moisture content changed from 9.6% to 13.9% in a treatment time of 36.2 minutes. This was found significant at $\alpha = 0.05$ in a two-tailed t-test with unequal variance, the t-statistic was 10.5, t-critical two-tailed was 2.04 with a probability value P = 0.001.
- On average the VST process resulted in a rate change; %MC/min, which was 6 times greater than atmospheric steaming when using similar samples of maple specimens and for equivalent treatment times.
- It was determined that there was no correlation between specific gravity (green) of the maple specimens and the change in %MC/min for either treatment method.
- There were 0 (zero) boards that failed in bending from the VST treated group whereas 11 out of 28 total (39%) of the atmospheric steamed boards failed in bending due to complete fracture, clearly indicating the superior plasticization result from VST.
- The VST maple specimens were successfully bent with an average 45.2Nm work, 5.5Nm less on average compared to the atmospheric steamed maple specimens that did not fail. This was found to be significant at P= 0.017, $\alpha = 0.05$ two-tailed.

Chapter 7: Summary and Conclusions

7.1 Summary

The basic premise and theory for steam plasticization of wood for the purpose of bending solid wood to form has not significantly changed since the early 19th century when it was considered to be a well known method (Benson 2008). This classic technique requires the wood be within a relatively narrow range of starting moisture contents of approximately 18-25% (Stevens and Turner 2008); the upper range presenting some long term storage concerns for wood degrade.

The author proposes a new technique; Vacuum Steam Technology (VST) which is tantamount to the reverse process of cyclic vacuum drying of wood. As a cyclic technique VST can result in moisture regain and heat regain suitable for the needs of plasticization of wood at significantly faster rates when compared to atmospheric steaming. A complete system of hardware was conceived, designed, constructed, tested, developed and proven satisfactory to evaluate certain aspects of vacuum steam technology. A VST standard operating procedure was developed (Section 5.5, page 148) for rapid plasticization of maple specimens.

Specifically this research addressed two research objectives:

(1) Determine whether cycles of vacuum and steaming could significantly improve the plastic-deformable state relative to the classic process of atmospheric steaming given equivalent treatment times when beginning with low moisture content (<10%) maple.

(2) Compare the work required to bend to form between VST treated maple and atmospheric-steamed maple given equivalent treatment times (36 minutes) when beginning with low moisture content (<10%) specimens.

7.2 Conclusions

1) Given equivalent treatment times of 35.6 minutes (VST) and 36.2 minutes (atmospheric), cycles of vacuum and steaming (VST) significantly improved the plastic deformable state of low moisture content maple compared to atmospheric steaming as demonstrated by an increase in moisture content of 26.3% (VST) compared to 13.9% (atmospheric) beginning at 9.6%MC, and zero failed bends (VST) compared to 39% (atmospheric).

2) Given equivalent treatment times of 35.6 minutes (VST) and 36.2 minutes (atmospheric) the work required to bend maple specimens to form was significantly reduced due to the VST treatment compared to atmospheric as demonstrated by a 5.5Nm reduction in average work; significant at $\alpha = 0.05$ two-tailed, $P = 0.017$.

7.3 Significance

The positive outcome and contribution of this research is that it has been demonstrated the preparation of kiln dried maple for bending applications can be accomplished within a shorter total treatment time, a shorter period of time when wood is subjected to steam, less work is required for bending VST treated maple, and perhaps at a lower energy cost relative to the existing state of the art for steaming and bending solid wood to form.

Perhaps a very large improvement in the plastic state of the wood, due to more uniform moisture and heat redistribution within the wood, could enable the use of lower grades of wood or species currently considered ‘difficult’ to bend.

7.4 Limitations

The VST technique works, however we certainly do not understand all of the phenomena; wood temperatures greater than the steam temperature is one example. To completely elucidate every phenomenon was beyond the scope of work. Another example was the system variability in the performance of change in %MC/min. In two different samples the standard deviation was approximately one-third of the mean. Of the variables investigated the strongest influence was the position of the boards within the chamber. Boards nearest the steam inlet were 23% less effective at moisture regain compared to the boards nearest the wall opposite of the steam inlet.

A complex hydrothermal effect was identified which introduced additional variability in the VST process. The strongest correlation was found to be a negative correlation (-0.82) between the temperature of the steel at the rear of the chamber and the change in % MC due to VST. Radiant heat gain to the chamber atmosphere had a profound effect on the atmosphere entering the superheated steam state. Next was a negative correlation (-0.71) between the steel chamber near the front and the change in % MC due to VST. A moderate positive correlation (0.59) was found to exist between the additional condensate produced as a result of cooler steel temperatures and the change in % MC due to VST.

The task of manually operating the array of valves at the rear of the chamber as well as manually timing the valve changes and focused observation of the wet bulb/dry bulb temperature signals on the control computer required strict concentration for the duration of each VST treatment.

7.5 Future Work

It is conceivable that ring porous woods perform better in bending in part because there is more physical space for compression induced cell wall displacement after plasticization and not due to certain wood species plasticizing better than other species. A study of wood macro anatomy relative to steamed wood bending performance might be appropriate.

The cyclic vacuum and steam combination developed in this research may expand the number of wood species suitable for bending due to a different method of moisture movement within the wood (WVBF) relative to atmospheric steaming as the UK-FPL and the USDA-FPL studies were based upon. The WVBF moisture movement induced by VST might produce a more uniform moisture gradient and heat gradient. Both of these qualities are essential for plasticization of wood and VST appears to have a great propensity for producing significant results in both areas.

Clearly from this work the VST chamber design could be improved upon; particularly the wall thickness of the chamber. Using material already available is a pragmatic budgetary consideration, however not suitable for process optimization. Automated valves with appropriate sensors, a control algorithm and control computer would provide a huge benefit in terms of precision.

Theoretical aspects could be investigated more thoroughly than was appropriate for this work. Examples include; a comparison of the theoretical non-plasticized work required to achieve the same hemi-spherical shape as in these experiments and how long might the diffusion process require to achieve the same level of moisture regain.

Vacuum steam technology has been shown to be extremely efficient at introducing moisture back into wood from a dry state; up to 1.2 g/m water uptake. For any industry in need of introducing liquids into wood the VST approach is well worth investigating. One industry that comes to mind is the preservative treatment industry and another is the acetylated wood industry. The key to making VST work with other fluids is to begin to think of those other fluids in their vapor phase instead of liquid phase, or perhaps an atomized spray injected under pressure into a steam injection port immediately prior to the chamber.

Literature Cited

Abata D. 1982 A CP/M computer program to calculate the thermodynamic properties of water. Mechanical Engineering News.

Alexiou PN, Wilkins AP, Hartley J. 1990. Effect of pre-steaming on drying rate, wood anatomy and shrinkage of regrowth Eucalyptus pilularis. Wood Science and Technology. 24(1): 103-110.

American Institute of Steel Construction corporate author. 1961. Steel construction: a manual for architects, engineers and fabricators of buildings and other steel structures. ©1947 the Institute. New York (NY). 431 p.

Armstrong LD, Christensen GN. 1961. Influence of moisture changes on deformation of wood under stress. Nature.com [Internet]. [cited 2009 Nov 4]; 191: 869-870. Available from: http://www.nature.com/search/executeSearch?sp-q=10.1038%2F191869a0&sp-c=25&sp-m=0&sp-s=date_descending&include-collections=journals_nature%2Ccrawled_content&exclude-collections=journals_palgrave%2Clab_animal&sp-a=sp1001702d&sp-sfvl-field=subject|ujournal&sp-x-1=ujournal&sp-p-1=phrase&sp-a=sp1001702d&sp-sfvl-field=subject|ujournal&sp-x-1=ujournal&sp-p-1=phrase&sp-p=all&submit=go

Arpaci VS. 1979. Introduction to heat transfer; course notepack. Department of Mechanical Engineering-University of Michigan. Ann Arbor (MI). 442 p.

Back EL, Salmen L. 1982. Glass transitions of wood components hold implications for molding and pulping processes. TAPPI Journal. 65(7): 107-110.

Bensen J. 2008. Woodworker's guide to bending wood: techniques, projects and expert advice for fine woodworking. East Petersburg (PA): Fox Chapel Publishing Co. 182 p.

Bodig J, Jayne B. 1982. Mechanics of wood and wood composites. New York (NY): Van Nostrand Reinhold. 712 p.

Chen Z. 1997. Primary driving force in vacuum drying. etds@vt [Internet]. [cited 2009 May 12]; 185 p. Available from: http://scholar.lib.vt.edu/theses/available/etd-02198-185538/.

Chen Z, White MS. 2009. Method and apparatus of vacuum steam sanitation treatment. Virginia Tech Intellectual Properties provisional patent number VT09-086. [US patent applied for 61/446,078] [2011 Feb 24] [cited 2011 Mar 3] Available from: http://www.vtip.org/availableTech/technology.php?id=311072.

Chen Z, Mougel E, Perre´ P, Youngs R. 2009. Technical note; equilibrium moisture content of Norway spruce at low pressure. Wood and Fiber Science. 41(3): 325-328.

Chudnoff M, Wangaard F. 1950. The steam bending properties of certain tropical American woods. Technical report #6. Project N6-ori-44 task order XV, Office of Naval Research, United States Navy. New Haven (CT). Virginia Tech ILLiad interlibrary loan transaction 924081. [requested 2009 Jun 15].

Defo M, Fortin Y, Cloutier A. 2004. Modeling superheated steam vacuum drying of wood. Drying Technology. 22(10); 2231-2253.

Frazier C. 2010. Exothermic action of acetic acid in wood. Personal email communication. [cited 2010 Mar 19] [author's file].

Galbreath G. 2010. Purchase of kiln dried wood for banjo construction by local luthiers. Personal telephone communication. [cited 2010 Jan 8]. Available from: http://www.buckeyebanjos.com/

Hall J, Jr., compiler. 2000. Blues creek guitars, inc [Internet]. Hegins (PA): blues creek guitars and John J. Hall, Jr. [cited 2010 Jan 8]. Available from: http://www.bluescreekguitars.com.

Hiziroglu S. 1996. Basics of pressure treatment of wood [Internet]. Stillwater (OK): Oklahoma Cooperative Extension Service bulletin NREM-5047. [cited 2010 Feb 13]. Available from: http://osufacts.okstate.edu/docushare/dsweb/View/Collection-213.

Hollandsworth K. 2010. Instrument luthiers. Personal email communication. [cited 2010 Jul 25]. Blue Ridge Autoharps. Christiansburg (VA). [author's file]. Available from: http://www.blueridgeautoharps.com/

Ikuho I, Ishimaru Y. 2002. Stress relaxation of wood during the elevating and lowering processes of temperature and the set after relaxation;1. Journal of Wood Science. 48(1): 8-13.

Ikuho I, Ishimaru Y. 2002. Stress relaxation of wood during the elevating and lowering processes of temperature and the set after relaxation;2-consideration of the mechanism and simulation of stress relaxation behavior using a viscoelastic model. Journal of Wood Science. 48(2): 119-125.

Irvine GM. 1984. The glass transitions of lignin and hemicellulose and their measurement by differential thermal analysis. TAPPI Journal. 67(5): 118-121.

Ishimaru Y, Ikuho I. 2001. Changes in the mechanical properties of wood during a period of moisture conditioning. Journal of Wood Science. 47(4): 254-261.

Jansch H, compiler. 2009. Heather Jansch–sculptor [Internet]. Devon, UK. [cited 2010 Mar 1]. Available from: http://www.heatherjansch.com/index.php

Jones J. 2010. Bending. Personal email communication. [cited 2010 Jul 29]. author's file. James Jones Instruments. Bedford (VA). Available from: http://www.jamesjonesinstruments.com/

Kaelble DH. 1971. Physical Chemistry of Adhesion. New York (NY) Wiley-Interscience. 507 p.

Karenlampi PP, Tynjala P, Strom, P. 2003. Molecular reorganization in wood. Mechanics of Materials. Elsevier, Ltd. 35 (2003): 1149-1159

Kelley SS, Rials TG, Glasser WG. 1987. Relaxation behaviour of the amorphous components of wood. Journal of Materials Science 22 (1987) 617-624.

Mellouk, H, Khezami, L, Ressoug, SA, Capart, R. 2008. Total valorisation of red cedar (*Thuja plicata*) sawmills wastes. Isolation of extractives and production of activated carbon from the solid residue. BioResources [Internet]. [cited 2011 Mar 7]; 3(4): 1156-1172. Available from http://www.bioresourcesjournal.com/

Meyers MA, Chawla KK. 1999. Mechanical behavior of materials. Upper Saddle River (NJ): Prentice Hall. 680 p.

Miyara AJ, Costanze V. 1991. Gas flow in hardwoods. Wood Science and Technology. 25: 289-299.

Morris PI, Byrne A, Mackay JFG, McFarling SM. 1991. The effect of steaming prior to pressure treatment on the penetration of borates into western hemlock. Forest Products Journal. 47(3): 62-65.

Nandanwar A. 2006. Development of a test method alternate to water resistance test prescribed for higher grades of plywood and block-board. Journal of the Indian Academy of Wood Science [Internet]. [cited 2010 Mar 5]; 2(2): Abstract. Available from: http://www.cabdirect.org/abstracts/20073062925.html?resultNumber=6&q=author%3A%28Nandanwar+%29+AND+yr%3A[2004+TO+2008]

Narayanappa P. 2005. Effect of presteaming on the permeability of *Acacia nilotica* Willd (babul). Journal of the Timber Development Association of India [Internet]. [cited 2010 Mar 5]; 15(1/2) Abstract. Available from: http://www.cabdirect.org/abstracts/20053149239.html?resultNumber=5&q=author%3A%28Narayanappa%2C+P.%29

Onouye B, Kane K. 2007. Statics and strength of materials for architecture and building construction. Upper Saddle River (NJ): Pearson Prentice Hall. 629 p.

Ping M, WenJing Z. 2009. Effect of steaming treatment on transverse permeability of wood. Journal of Nanjing Forestry University [Internet]. [cited 2011 Mar 8]; 33(2) Abstract. Available from: http://www.cabdirect.org/abstracts/20093163716.html?resultNumber=0&q=author%3A%28Ping%29+AND+author%3A%28WenJing%29+AND+%28permeability%29+AND+yr%3A[2007+TO+2010]

Peck EC. 1957. Bending Solid Wood to Form. USDA Forest Products Laboratory [Internet]. [cited 2009 Oct 3] AH-125: 37 p. Available from: http://www.fpl.fs.fed.us/search/search_action.php?phrasesAndKeywords=%22bending+solid+wood+to+form%22&searchmode=fullpublications&sortgroup=significance&relatedinformation=yes&pubyearstart=1919&pubyearend=2011

Perry RH, Green DW, Maloney JO, editors. 1984. Fluid and particle mechanics. In: Perry's chemical engineers' handbook, sixth edition. New York (NY): McGraw-Hill. p 5.1-5.68.

Popov, EP. 1976. Mechanics of materials. Englewood Cliffs (NJ): Prentice Hall. 590 p.

Reimschuessel HK. 1978. Relationships on the effect of water on glass transition temperature and Young's modulus of Nylon 6. Journal of Polymer Science: Polymer Chemistry Edition [Internet]. [cited 2010 Apr 12]; 16(6):1229-1236. Available from: http://onlinelibrary.wiley.com/doi/10.1002/pol.1978.170160606/abstract

Remond R, Passard J, Perre´ P. 2007. The effect of temperature and moisture content on the mechanical behaviour of wood: a comprehensive model applied to drying and bending. European Journal of Mechanics - A/Solids. 26(3): 558-572.

Rezzoug SA. 2009. Optimization of steam extraction of oil from maritime pine needles. Journal of Wood Chemistry and Technology. 29(2): 87-100.

Rice RW, Lucas J. 2003. The effect of moisture content and bending rate on the work required to bend solid red oak. Forest Products Journal. 53(2): 71-77.

Richardson, NA. 1953. Wood Preservation. ICE Proceedings [Internet]. [cited 2010 Dec 10]; 2(6): 649-663. Available from: http://www.icevirtuallibrary.com/content/article/10.1680/iicep.1953.11141

Rowell RM, Lange S, McSweeny J, Davis M. 2002. Modification of wood fiber using steam. In: Humphrey P, editor. Proceedings of the 6th Pacific Rim Bio-Based Composites Symposium & Workshop on the Chemical Modification of Cellulosics [Internet]; Wood Science and Engineering Department, Oregon State University, Corvallis (OR). [cited 2011 Jan 9]; p 606-615. Available from: http://www.fpl.fs.fed.us/search/search_action.php?phrasesAndKeywords=%22modification+of+wood+fiber+using+steam%22&searchmode=fullpublications&sortgroup=title&relatedinformation=yes&pubyearstart=1919&pubyearend=2011

Sasaki K, Kawabe J, Mori M. 1987. Vacuum drying of wood with high frequency heating (II), the pressure within lumber during evacuation and drying [Internet]. Bulletin of the Kyushu University Forest. 57:245-265. [cited 2009 Sep 21]; Abstract. Available from: http://ci.nii.ac.jp/naid/110001377027/en

Siau JF. 1995. Wood: influence of moisture on physical properties. Blacksburg (VA): Department of Wood Science and Forest Products. 227 p.

Siau JF. 1984. Transport processes in wood. New York (NY): Springer-Verlag. 245 p.

Skaar C. 1988. Wood-water relations. New York (NY): Springer-Verlag. 279 p.

Skaar C. 1976. Effect of high temperature on the rate of degradation and reduction in hygroscopicity of wood. In: Gerhards CC, McMillen JM, editors. Processing Research Conference; High Temperature Drying Effects on Mechanical Properties of Softwood Lumber, USDA Forest Service, Forest Products Laboratory. 1976 Feb 25-26; Madison, WI pg113-127.

Sorz J, Hietz P. 2005. Gas diffusion through wood; implications for oxygen supply. Trees-structure and function [Internet]. [cited 2011 Jan 22]; 20(1): 34-41. Available from: http://www.springerlink.com/content/lp0421803452660h/

Stevens WC, Turner N. [1948, 1970] 2008. Wood bending handbook. East Petersburg (PA): Fox Chapel Publishing. 109 p.

TaiAn C, LianBai G, ZhaoBin S. 2003. The effects of steaming on the shrinkage coefficient and air permeability of oak. Journal of Nanjing Forestry University 27(2): 62-64. [cited 2010 Feb 9]. Abstract. Available from: http://www.cabdirect.org/abstracts/20033134141.html?resultNumber=0&q=title%3A%28The+effects+of+steaming+on+the+shrinkage+coefficient+AND+air+permeability+of+oak%29

VanWylen G, Sonntag R. 1976. Fundamentals of classical thermodynamics. New York (NY). John Wiley & Sons. 718 p.

Ward IM. 1983. Mechanical properties of solid polymers. New York (NY). Wiley-Interscience. 475 p.

Wengert EM. 1988. The wood doctor's Rx. Blacksburg (VA). Wood science and forest products. 378 p. Availabel from; special collections at Newman Library.

Wikimedia Foundation, Inc., compiler. 2010. Thermocouple [Internet]. [cited 2010 Mar 8]. Available from: http://en.wikipedia.org/wiki/Thermocouple.

Wolcott MP, Kamke FA, Dillard DA. 1990. Fundamentals of flakeboard manufacture: viscoelastic behavior of the wood component. Wood and Fiber Science. 22(4): 345-361

Wood Handbook, Wood as an Engineering Material, 2010. Published by Forest Products Laboratory, U.S. Department of Agriculture, Forest Service, General Technical Report FPL-GTR-190, Madison, WI. 508 p. Complete PDF available online at: http://www.fpl.fs.fed.us/search/search_action.php?phrasesAndKeywords=Wood+Handbook&searchmode=fullsite&sortgroup=significance&relatedinformation=no&pubyearstart=1919&pubyearend=2011

Wright RS. 1999. Superficial gas permeability in steamed wood. Unpublished research report. [author's file].

Yamsaengsung R, Sattho T. 2008. Superheated steam vacuum drying of rubberwood. Drying Technology 26(6): 798-805.

Yang D, Li Shuangyue, Li Shujan, Li Jian, Sun Molong, Jin Yan. 2009. Effect of juglone from *Juglans mandshurica* bark on the activity of wood decay fungi. Forest Products Journal 59(9): 79-82.

Yilgor N, Unsal O, Kartal SN. 2001. Physical, mechanical and chemical properties of steamed beech wood. Forest Products Journal 51(11/12): 89-94.

Marie-Lan Nguyen -Tombstone Xanthippos Permission:

File:Tombstone Xanthippos BM Sc628.jpg

From Wikipedia, the free encyclopedia

Size of this preview: 396 × 600 pixels

Full resolution (2,400 × 3,636 pixels, file size: 3.55 MB, MIME type: image/jpeg)

This is a file from the Wikimedia Commons. Information from its **description page there** is shown below.

Commons is a freely licensed media file repository. You can help.

[edit] Summary

Description	**English:** Tombstone of the shoemaker Xanthippos. Marble, Greek artwork, ca. 430-420 BC. From Athens. **Français :** Stèle funéraire du cordonnier Xanthippos. Marbre, art grec, vers 430-420 av. J.-C. Provenance : Athènes.
Date	
Dimensions	4H. 83.75 cm (32 ¾ in.), W. 50.75 cm (19 ¾ in.)
Current location	[show]British Museum Main floor, room 19: Greece: Athens
Accession number	GR 1805.7-3.183 (Cat. Sculptures 628)
Credit line	Townley Collection
Source/Photographer	Marie-Lan Nguyen (2007)
Permission (Reusing this file)	See below.

[edit] Licensing

I, the copyright holder of this work, hereby publish it under the following license:

This file is licensed under the Creative Commons Attribution 2.5 Generic license.

You are free:

- **to share** – to copy, distribute and transmit the work
- **to remix** – to adapt the work

Under the following conditions:

- **attribution** – You must attribute the work in the manner specified by the author or licensor (but not in any way that suggests that they endorse

you or your use of the work).

You are free to use this picture for any purpose as long as you credit its author, **Marie-Lan Nguyen** (**user:Jastrow**).

Example: © Marie-Lan Nguyen / Wikimedia Commons

If you use this image outside of the Wikimedia projects, I would be happy to hear from you (jastrow pip-pip DOT org).

Deutsch – Français

File history

Click on a date/time to view the file as it appeared at that time.

Date/Time	Thumbnail	Dimensions	User	Comment
current 17:41, 7 August 2007		2,400×3,636 (3.55 MB)	Jastrow	(== Summary == {{Information British Museum |artist=Unknown |description= {{en|Tombstone of the shoemaker Xanthippos. Marble, Greek artwork, ca. 430-420 BC. From Athens.}} {{fr|Stèle funéraire du cordonnier Xanthippos. Marbre, art grec, vers 430-420)

File links

The following pages on the English Wikipedia link to this file (pages on other projects are not listed):

- History of the chair
- Klismos
- Wikipedia:Did you know/Statistics/Archive 2008

Global file usage

The following other wikis use this file:

- Usage on es.wikipedia.org
  - Artesanía de la Antigua Grecia
- Usage on fr.wikipedia.org
  - Artisanat en Grèce antique

Metadata

This file contains additional information, probably added from the digital camera or scanner used to create or digitize it. If the file has been modified from its original state, some details may not fully reflect the modified file.

Camera manufacturer	NIKON CORPORATION
Camera model	NIKON D200
Exposure time	1/50 sec (0.02)
F-number	f/3.5
ISO speed rating	400
Date and time of data generation	16:04, 28 July 2007
Lens focal length	26 mm

Show extended details

Fox Chapel Permission:

From: John Kelsey [kelsey@foxchapelpublishing.com]
Sent: Monday, July 19, 2010 1:52 PM
To: Customer Service; Wright, Bob
Subject: Re: Contact Form: copyright permission

Yes permission granted. Please be sure to credit Fox Chapel as the current publisher of this material, including at minimum our web address: www.foxchapelpublishing.com

John Kelsey
editorial director
717-715-8630
kelsey@foxchapelpublishing.com

On Mon, Jul 19, 2010 at 12:42 PM, Customer Service
<customerservice@foxchapelpublishing.com> wrote:
Pretty sure this is fine, but sending to you to make sure that we let him know it's ok.

The Customer Care Team
Fox Chapel Publishing
1970 Broad Street
East Petersburg, PA 17520
USA
1-800-457-9112
www.FoxChapelPublishing.com
www.WoodcarvingIllustrated.com
www.Scrollsawer.com

---------- Forwarded message ----------
From: Bob Wright <rswright@vt.edu>
Date: Mon, Jul 19, 2010 at 12:31 PM
Subject: Contact Form: copyright permission

To: "customerservice@foxchapelpublishing.com" <customerservice@foxchapelpublishing.com>
The Contact Form Was Submitted With The Following Information:
Name: Bob Wright
Email: rswright@vt.edu
Phone: 540-231-8838
Subject: copyright permission
Message:

Hello, I am writing a MS thesis in Wood Science and Forest Products at Virginia Tech, Blacksburg, VA. I would like to include several items from: "Wood Bending Handbook", c.1970, William Cornwell Stevens and N. Turner, ISBN 978-1-56523-354-6. On page 3: Fig 1 - “Effect of steaming treatment on the position of the neutral axis in a bend”, Fig 2 - "Effect of Steaming on the stress/strain relationship in tension of home-grown ash", and Fig 3 - "Effect of steaming on the stress/strain relationship in compression of home grown ash". Also, select data from Table 1 - “Limiting Radii of Curvature of Various Species in Steam Bending” page 96, Table 2 - “Limiting Radii of Curvature of Thin Laminations” page 101, and Table 6 - “Approximate Ratio of Radius of Curvature to Lamination Thickness for Structural Laminations Bent Dry” page 106.
My deadline is 20-August, 2010.

Thank You,
Bob Wright

Zhangjing Chen Permission:

From: Chen, Zhangjing [chengo@vt.edu]
Sent: Thursday, April 28, 2011 2:00 PM
To: Wright, Bob

Robert S. Wright has permission to use several figures from my dissertation of 1997.

April, 28. 2011

Chen, Zhangjing, Ph. D.
Dept. of Wood Science and Forest Products Virginia Tech Univ.
Blacksburg, VA 24060
Phone 540-2314406
fax 5412318868

Richard Goff Permission:

From: richgoff@vt.edu
Sent: Monday, May 02, 2011 2:10 PM
To: Wright, Bob
Subject: Re: photograph permission

Hi Bob
You have my permission to use the photo for any purposes. If you become a millionaire as a result, you can send me 10 bucks:-) Thanks Richard

Quoting "Wright, Bob" <rswright@exchange.vt.edu>:
> Hi Richard,

> I am using the photograph that you took of me holding a combination
> square against the chamber to position a valve handle in a repeatable
> way.
>
> You own that photo and I need permission to use it in the form of an
> email would be fine.
>
> A copy is attached if you need that to remember what I am
> talking about.
>
> Thank You !
>
> Bob Wright
>
> Virginia Tech
> Wood Science and Forest Products department and the Biological Systems
> Engineering department Blacksburg, VA 24061
> rswright@vt.edu<mailto:rswright@vt.edu>
> 540-231-8838

Appendix B: Annotated List of Figures